5-2012

Study of VOCs Transport and Storage in Porous Media and Assemblies

Jing Xu
Syracuse University

Abstract

Indoor VOCs concentrations are influenced greatly by the transport and storage of VOCs in building and furnishing materials, majority of which belong to porous media. The transport and storage ability of a porous media for a given VOC can be characterized by its diffusion coefficient and partition coefficient, respectively, and such data are currently lacking. Besides, environmental conditions are another important factor that affects the VOCs emission. The main purposes of this dissertation are: (1) validate the similarity hypothesis between the transport of water vapor and VOCs in porous materials, and help build a database of VOC transport and storage properties with the assistance of the similarity hypothesis; (2) investigate the effect of relative humidity on the diffusion and partition coefficients; (3) develop a numerical multilayer model to simulate the VOCs' emission characteristics in both short and long term.

To better understand the similarity and difference between moisture and volatile organic compounds (VOCs) diffusion through porous media, a dynamic dual-chamber experimental system was developed. The diffusion coefficients and partition coefficients of moisture and selected VOCs in materials were compared. Based on the developed similarity theory, the diffusion behavior of each particular VOC in porous media is predictable as long as the similarity coefficient of the VOC is known.

Experimental results showed that relative humidity in the 80%RH led to a higher partition coefficient for formaldehyde compared to 50%RH. However, between 25% and 50% RH, there was no significant difference in partition coefficient. The partition coefficient of toluene decreased with the increase of humidity due to competition with water molecules for pore surface area and the non-soluble nature of toluene. The solubility of VOCs was found to correlate well with the partition coefficient of VOCs. The partition coefficient of VOCs was not simply inversely proportional to the vapor pressure of the compound, but also increased with the increase of the Henry's law constant. Experiment results also showed that a higher relative

humidity led to a larger effective diffusion coefficient for both conventional wallboard and green wallboard. The partition coefficient (K_{ma}) of formaldehyde in conventional wallboard was larger at 50% RH than at 20% RH, while the difference in partition coefficient between 50% RH and 70% RH was insignificant. For the green wallboard and green carpet, the partition coefficient increased slightly with the increase of relative humidity from 20% to 50% and 70%.

Engineered wood products such as particleboard have widely been used with wood veneer and laminate to form multilayer assembly work surfaces or panels. The multilayer model study in this dissertation comprised both numerical and experimental investigation of the VOCs emission from such an assembly. A coupled 1D multilayer model based on CHAMPS (coupled heat, air, moisture and pollutant simulations) was first described. Later, the transport properties of each material layer were determined. Several emission cases from a three-layered heterogeneous work assembly were modeled using a developed simulation model. At last, the numerical model was verified by the experimental data of both hexanal and acetaldehyde emissions in a 50L standard small scale chamber. The model is promising in predicting VOCs' emissions for multilayered porous materials in emission tests.

STUDY OF VOCS TRANSPORT AND STORAGE IN POROUS MEDIA AND ASSEMBLIES

By

Jing Xu

M.S. Tianjin University, 2005

DISSERTATION

Submitted in partial fulfillment of the requirements for the Degree of Doctor of Philosophy in Mechanical and Aerospace Engineering in the Graduate School of Syracuse University

May 2012

Acknowledgements

Pursuing Ph.D. degree is quite a long process, which costs me exactly six and half years. In those valuable years, I cannot count the days that I stayed late in school in order to finish the experiment work on that day no matter in weekdays, weekends and holidays and the sleepless nights that I had to come up with the reasons for the failures in work. However, sometimes, I have the illusion that I came to Syracuse just a few days before since I still clearly remembered the sunny day in summer 2005 that I first visited my advisor in his office and stepped into the laboratory to do BIFMA project in excitement with Ilka as a beginner. It opened the first page of my Ph.D. stage. Most of what have I contributed to indoor air science in this long period goes into this dissertation. As for how I can accomplish this, it is determined by a great amount of endeavor from many people.

First, I would like to deeply thank my Ph.D. advisor Professor Jianshun (Jensen) Zhang in Department of Mechanical and Aerospace engineering, Syracuse University. It is him who advised me in selecting the research topics in VOCs emission filed and helped me out of a lot of tough situations during the practical difficulties both in theory and in experiment details. I would like to take this unique opportunity to express my sincere gratitude to him for his wisdom, knowledge, commitment and patience through all the long way to achieve this creative work. Without him, I am definitely not able to achieve so much in the field of indoor air quality. I also wish to express my sincere appreciation and thanks to my committee members Dr. Shobha Bhatia, Dr.Shalabh C. Maroo, Dr. Jeongmin Ahn, Dr. Lawrence L. Tavlarides, and Dr. Alan Levy for their constructional suggestions and during the preparation of this dissertation.

Second, I would especially like to express my special gratitude to Dr. Hui Li for his patience and experience in the beginning of my Ph.D. He taught and also helped me in my first year regarding the use of many types of equipment; without him, I couldn't successfully finish the first phase of BIFMA project from August 2005 to May 2007. I would also like to thank Professor John

Grunewald in Dresden University of Technology in Germany. During his stay as an adjunct associate professor in Syracuse University, he taught me step by step in great patience the basic knowledge and skill in using CHAMPS-BES, which triggered my interest in the modeling of the VOCs emission. It is also for his help that the first version of modeling of chamber emission testing and dual chamber method became realistic. His humorous but positive attitude towards work and life expressed me a lot, which also broadened my narrow thinking about some points. I also like to thank my colleagues in our lab Mr. Jim Smith and Ms. Beverly Guo for their generous help in many technical issues during the work.

Thirdly, the financial support for my Ph.D. study provided by BIFMA, US Environmental Protection Agency and Department of Mechanical and Aerospace Engineering of Syracuse University is also greatly appreciated.

At the end of my long Ph.D. journey, I would like to deeply thank my dearest parents because it was their absolute encouragement that helped me get through numerous difficult times encountered in my life in U.S. and Ph.D. study. They always tried to motivate me to do good work since I entered school. I also would like to thank my younger brother who stayed with our parents after his college in my hometown because it provides me better feeling to study and work without any concern far away from our parents. I would also like to thank my beloved husband for his absolute support during my Ph.D. period. His encouragement and constant love are the basic condition for my successful completion of my degree. He was always the first one that helped me solve any problem. Five years long distance love is another happy achievement for both of us besides Ph.D. degree. Last but not the least, I am very delighted to warmly welcome the coming of our next generation my nephew Tuoyu Xu on December 31st, 2009 into our family, and I sincerely wish him grow stronger and healthier day by day.

Jing Xu

Syracuse, U.S.A. May 2012

Table of Contents

List of Figures

List of Tables

Nomenclature

a : constant

A : specimen area, m^2

b : constant

c : constant

C : concentration, kg/m^3 or mg/m^3

C_1 : VOC concentration at the steady state condition in the primary chamber, mg/m^3

C_2 : VOC concentration at the steady state condition in the secondary chamber, mg/m^3

C_{Ain} : inflow VOC concentration for chamber A, kg/m^3

C_{Bin} : inflow VOC concentration for chamber B, kg/m^3

C_{Aout} : outflow VOC concentration for chamber A, kg/m^3

C_{Bout} : outflow VOC concentration for chamber B, kg/m^3

C_A : VOC concentration in air phase of chamber A, kg/m^3

C_B : VOC concentration in air phase of chamber B, kg/m^3

C_m : VOC concentration in the material, kg/m^3

C_a : VOC concentration in the air phase outside of the material, kg/m^3

C_{pm} : sorbed phase VOC concentration in porous medium, kg/m^3 REV

C_{pa} : air phase VOC concentration, kg/m^3 REV

d : constant

D_s : diffusion coefficient in the material excluding boundary layer resistance, m^2/s

D_e : effective diffusion coefficient, m^2/s

D_p : pore diffusion coefficient, m^2/s

D : apparent diffusion coefficient, m^2/s

D_{air} : diffusion coefficient in air, m^2/s

D_m : diffusion coefficient caused by molecular diffusion only, m^2/s

D_k : diffusion coefficient caused by Knudsen diffusion only, m^2/s

e : diffusion error, %

h : convective mass transfer coefficient, m/s

h_A : convective mass transfer coefficient in chamber A, m/s

h_B : convective mass transfer coefficient in chamber B, m/s

j : mass flux across the specimen, $kg/(m^2.s)$

j_{total} : formaldehyde mass flux due to both convection and diffusion, kg/s

$j_{diffusion}$: formaldehyde mass flux due to diffusion, kg/s

$j_{convection}$: formaldehyde mass flux due to convection, kg/s

k_H : Henry's law constant, dimensionless ratio between the aqueous-phase concentration of VOC and its gas-phase concentration

K_{ma} : partition coefficient at equilibrium, $=C_m/C_a$, dimensionless

K_s : partition coefficient, $=C_{pm}/C_{pa}$, dimensionless

L : specimen thickness, m

$\dot{m}$: mass flow rate through the material, mg/s

M : total VOC mass in the material, kg

M_{REV} : total VOC mass in the REV, kg

M_{pm} : sorbed phase VOC mass in the matrix, kg

M_{pa} : VOC mass in the pore air, kg

MW : molecular weight, kg/mol

P : pressure, Pa

Q_A : flow rate into chamber A, m^3/s

Q_B : flow rate into chamber B, m^3/s

r : mean pore radius, m

Re : Reynolds number

REV : representative elemental volume

RH : relative humidity, %

RH_{Ain} : relative humidity of inflow for chamber A, %

RH_{Aout} : relative humidity of outflow for chamber A, %

RH_{Bin} : relative humidity of inflow for chamber B, %

RH_{Bout} : relative humidity of outflow for chamber B, %

R : universal gas constant, 8.31 J/(mol.K)

R_v : gas constant for water vapor, 462 J/ (.kg.K)

Sc : Schmidt number

Sh : Sherwood number

T : temperature, Kelvin

T_i : end time of the diffusion test, hours

t : time, s

U : overall mass transfer coefficient, m/s

v_A : molecular volume of dry air, mL/gmol

v_B : molecular volume of formaldehyde, mL/gmol

V : ventilation rate, m^3/s

V_{mat} : volume of material, m^3

V_{mat} : volume of material, m^3

V_{REV} : volume of REV, m^3

WVT : rate of water vapor transmission, kg/ ($s.m^2$)

x : depth in the direction of specimen thickness, m

Greek symbols

ε : porosity, m^3 (of air) /m^3(of REV)

τ : tortuosity, dimensionless

λ : mean free path of the molecule, m

δ : permeability of the carpet in kg/msPa

ϱ : specimen density, kg/m^3

ϱ_{Ain} : density of inflow air for chamber A, kg/m^3

ϱ_{Aout} : density of outflow air for chamber A, kg/m^3

ϱ_{Bin} : density of inflow air for chamber B, kg/m^3

ϱ_{Bout} : density of outflow for chamber B, kg/m^3

μ' : dynamic viscosity, $P_a.s$

μ_{vapor} : Mew value of water vapor, = D_{air} (of Water vapor)/D_e, dimensionless

μ_{voc} : Mew value of VOC, = D_{air} (of VOC)/D_e, dimensionless

k_{voc} : similarity coefficient, = μ_{voc} / μ_{vapor} , dimensionless

Chapter 1 Introduction

1.1 Background and problem definition

Indoor air quality (IAQ) continues to be one of the major environmental issues due to the presence of many pollutants indoors and their health risks, irritation and discomfort to building occupants. Due to the growing cost of energy in recent years, in order to reduce energy consumption for heating, cooling and ventilation, more air-tight building construction has been commonly adopted. In the meantime, a large number of building materials that emit volatile organic compounds (VOCs) continue to be used including carpet, ceiling tile, paints, furniture. These materials emit a large variety of indoor pollutants in their service life time. New and secondary emissions as a result of indoor chemistry have also been identified (Weschler and Shields 1999, Destaillats et al. 2006, Weschler 2009). Sick building syndrome (SBS) due to indoor emission sources has been widely reported (U.S. EPA 1989, Baechler et al. 1993). As a result, indoor air pollution has been identified by the U.S. Environmental Protection Agency and the World Health Organization (WHO) as one of the top environmental risks to the nation's health (WHO, 1989; U.S. EPA 1990).

Indoor air pollutant includes odor, inorganic compound (CO, CO_2, SO_2, NO_x, O_3, etc.), organic compounds, radioactive gases, particles and bioaerosols (derived from virus, bacteria, fungi, dust mites etc.). Based on their boiling points, WHO defines organic compounds as further divided into very volatile organic compounds (VVOC), volatile organic compounds (VOC), semi-volatile organic compounds (SVOC) and particulate organic matter (POM) respectively, as shown in Table 1.1. Volatile organic compounds or VOCs are organic chemical compounds whose composition makes it possible for them to evaporate under normal indoor atmospheric conditions of temperature and pressure, and hence accounts for a significant dose in occupants' exposure to airborne indoor pollutants.

Table 1.1 Category of organic compounds (WHO, 1989)

Description	Abbr.	Boiling point range (°C)
Very volatile	VVOC	<0 to 50-100
Volatile	VOC	50-100 to 240-260
Semi-volatile	SVOC	240-260 to 380
Particulate organic matter	POM	380-400

VOCs include a variety of chemicals, some of which may have short- and long-term adverse health effects. The ability of organic chemicals to cause health effects varies greatly, from those that are highly toxic to those with no known health effect. As with other pollutants, the extent and nature of the health effect will depend on many factors including the level of exposure and the length of time exposed. Eye and respiratory tract irritation, headaches, dizziness, visual disorders and memory impairment are among the immediate symptoms that some people have experienced soon after exposure to some organics. Many organic compounds are known to cause cancer in animals; some are suspected of causing or are known to cause cancer in humans. California 1350 (2010) lists the inhalation reference exposure level for each specific compound, and the hazardous index target organs are also provided. Each compound has different target values.

The research on VOCs' emission characteristics, control and removal has received much attention in the last two decades because of their health risk to the health of building occupants. This dissertation focuses on VOCs' emission characterization via experiments and modeling. Emission characteristics of a given VOC are primarily determined by its initial concentration level and distribution, internal diffusion and sorption within the material. The objective of this research was to improve the understanding of how they affect the VOC emission rate over time and develop experimental methods to determine the critical parameters needed to model VOC emissions from dry materials and material assemblies.

VOCs are emitted by a wide array of products numbering in the thousands. Examples include: paints and lacquers, paint strippers, cleaning supplies, pesticides, building materials and furnishings, office equipment such as copiers and printers, correction fluids and carbonless copy paper, graphics and craft materials including glues and adhesives, permanent markers, and photographic solutions. All of these products can release organic compounds while you are using them and, to some degree, when they are stored.

It is necessary to identify those indoor contaminants and their sources within the building as well as to establish acceptable concentrations in indoor air. Since more than 8000 chemical species have been identified in the indoor environment, this would appear a daunting task. Furthermore, very little scientific data exist on the potential health effect of most of these chemicals either on an individual basis or as aggregates (Hazim Awbi, 2002). ASHRAE Standard 189.1-2009 provides comprehensive lists of chemicals which are known to be present in domestic, commercial and industrial environments and give information on acceptable contaminant levels for both long- and short-term exposures. Building materials as VOC emission sources fall into dry materials or wet materials. "Dry" building materials are defined as products employed in either commercial or residential building construction that does not typically require any curing period following installation. Internal diffusion and storage processes generally control VOC emissions from these materials. Air velocity and turbulence over the material surface have little effect on their VOC emission rates. Such "dry" products include solid woods (spruce, pine, maple, oak), engineered wood materials (plywood, particleboard, oriented strand board), gypsum wallboard (standard, water- or fire- resistant), flooring materials (carpet, underpad /cushion, vinyl flooring), and acoustical ceiling tile (Magee et al., 1999). "Wet" building materials are defined as products employed in either commercial or residential building construction that typically requires a curing period following installation. They include products such as wood stain, paint, floor wax, polyurethane, adhesive and calking materials (Zhu et al., 1999). The VOC emission rates of dry materials are primarily determined by the internal transport and storage process while

those of wet materials are also strongly affected by mass transfer through the boundary layer over the material surface.

Furniture as delivered products can be considered dry materials. Many VOCs may emit from furniture, including aldehydes, acids, alcohols, glycol esters, ketones, terpenes, etc. The amount of emissions varies from only several $\mu g/m^2s$ to hundreds of $\mu g/m^2s$. Some compounds fluctuate; however, the trend is still down in the long run. Many factors may affect emission properties for furniture, such as temperature, relative humidity, air change rate, texture of the material, manufacture date, and paint type. The conventional experimental method to determine the VOC rate and its contribution to indoor concentration is through a dynamic chamber test. Either small scale (ASTM D5116), mid scale and full scale chamber (ASTM D6670) may be used. ASTM standards describe in detail the dimension and the steps in doing a chamber test for VOC concentrations. Generally, in the test, temperature and relative humidity of the chamber are kept constant. Fresh air is supplied to the chamber at a specific air change rate and is let out of the chamber as exhaust outflow. Positive pressure is maintained inside the chamber to prevent contamination from the ambient environment. The air samples in the exhaust flow are taken at specified times and then they are analyzed by appropriate analysis instruments for compound identification of VOCs and concentration quantification. The emission rate or emission factor of a VOC from the material is then determined by applying the mass balance principle to the chamber's air volume.

There are also some established influential standards that can be used to quantify the VOCs concentration at specified days after the materials are put into the chamber like (EPA/ETV 1999, California 2000, California 2004 and BIFMA M7.1 2005). In these test protocols, environmental chambers are used to determine the emission rates or emission factors of a workstation system or its components, which are in turn used to estimate the impact of the workstation system on the VOC concentration levels in a prescribed typical office environment.

However, the obtained VOCs concentration by any test method only provides information on specific VOCs from prescribed materials for the period of testing or shortly after that. It is difficult to extrapolate the emission data from test period to long term. Such prediction requires understanding of the emission mechanisms and fundamental mass transfer, sorption models to describe the internal transport and storage processes, and knowledge of the critical model parameters.

Although experimental methods are available to measure the VOC concentrations for the studied materials, they are costly and time consuming, and limited to only short-term emission characterization. If the VOCs' rates and their impact on indoor concentrations can be obtained by modeling, then it would be much more efficient and less costly. The model-based testing and evaluation method requires necessary model parameters to complete successful modeling. Mechanistic model development and experiment validations have been studied extensively previously: Guo and Tichenor (1992) developed the mass transfer model for "wet" coating material. Bodalal (1999) developed the double chamber method to measure diffusion/partition coefficient; Zhang et al. (1999) developed the diffusion model for multi-layer and complex materials; and Yang et al. (2001) developed the mass transfer model for "wet" coating materials applied to absorptive materials. However, each study often covers a few selected materials and VOCs, so it is impossible to predict most of the VOCs detected in indoor air and in most of the widely used materials.

To fill this gap, a complete VOCs database of model parameters is needed in order to cover the typical VOCs and widely used materials. In addition, the effect of environmental conditions on emissions is not well understood yet. In terms of VOCs database development and environment effect, the previous studies still lack:

1. Sufficient measurement of the diffusion and partition coefficients of typical VOCs in common building/furniture materials.

2. A general VOC database needed for the modeling of VOCs' emissions from porous building/furniture materials.
3. A possible method to reduce conventional chamber testing.
4. Accurate measurement of changes of the diffusion/partition coefficient within indoor humidity range.
5. Understanding of the physical mechanism of the effect of humidity conditions on the emission rate of VOCs and partition/diffusion coefficients.

In reality, most building/furniture materials are made of many layers instead of one single layer, so it is better that the VOCs emission from those multilayer materials can be simulated in both short term and long term. Relevant emission issues can be analyzed by the simulation as well. However, a convenient simulation tool for this purpose is not available yet. In terms of numerical model development for multilayered materials, the previous work still lacks:

1. A numerical model to simulate VOC emission from multilayer materials.
2. Prediction of long term VOC emission effects on indoor air quality based on the input of critical parameters.
3. Emission characteristics of VOCs within and from the multilayer materials.
4. Possible control methods to reduce emission concentrations.

1.2 Research objectives

To fill the gaps in the areas mentioned above, the research objectives of this dissertation are defined as follows:

1) Validate the similarity hypothesis between the transport of water vapor and VOCs in porous materials, and build a VOCs database of model parameters with the assistance of the similarity hypothesis;
2) Investigate the relative humidity effect on the diffusion and partition coefficient;

3) Develop a numerical multilayer model to simulate the VOCs' emission characteristics in both short and long term.

1.3 Research scope

This study included three major components.

First was the development of the laboratory test method and dynamic dual chamber system which was used to validate the proposed similarity hypothesis between water vapor and VOCs transport. The important relevant theory regarding the determination of diffusion coefficient and partition coefficient was first reviewed and discussed. A reference material, calcium silicate, was adopted for the experimental validation of the similarity between water vapor and VOCs transport. Both measurement for water vapor transport and VOCs transport were conducted. In order to confirm the test method, repeat tests for water vapor and several selected VOCs (formaldehyde, acetaldehyde and toluene) were conducted. The conventional dry cup test method was used to validate the water vapor measurement. The mercury intrusion porosimetry method was also used to determine the pore size distribution and used to estimate the diffusion coefficients of VOCs and water vapor for comparison with dynamic dual chamber test results. The uncertainty of the dual chamber test method was analyzed. The similarity theory was also confirmed by the VOCs emission test data for particleboard by comparing the emission rate estimated from the similarity theory with the actual measurements.

Second was the experimental investigation of the relative humidity effect on the partition and diffusion coefficients. VOC transport and sorption in a porous medium in the building materials (calcium silicate) were measured under three levels of relative humidity (25%, 50% and 80%) by using the same dynamic dual chamber method. Tests were conducted for a water-soluble compound (formaldehyde) and a non-soluble compound (toluene). In addition, the transport of acetaldehyde, hexanal, benzaldehyde, butanol and decane through the calcium silicate were also tested at 50% RH to study the relationship between the effective diffusion coefficient (D_e),

partition coefficient (K_{ma}) and the VOCs' physical properties (molecular weight, vapor pressure, and Henry's law constant). Furthermore, the partition and diffusion coefficients of formaldehyde were measured for three other widely used materials (conventional gypsum wallboard, "green" gypsum wallboard, and "green" carpet) under three relative humidity (RH) conditions (20%, 50% and 70% RH). The main purpose was to generate enough accurate test results for a conclusion of humidity effect.

Third was the development of a numerical model to simulate VOC emission from a multilayered worksurface. This study comprises both numerical and experimental investigation of the VOCs emission from such an assembly composed of painted veneer, particleboard and veneer. A coupled 2D multilayer model based on CHAMPS-BES (coupled heat, air, moisture and pollutant simulations) was first described physically and mathematically. Parametric studies were used to help determine the input parameters for the model. Simulations regarding the emission characteristics of VOCs emission and the effect of additional layers on the particleboard and veneer were also conducted. At last, the numerical model was verified by experimental data on hexanal emission from both individual layers and multilayers in a 50L standard small scale chamber.

1.4 Dissertation organization

Chapter 1 introduces the background for the indoor air quality and VOCs, and identifies research needs in the fields of VOCs emission. Also, the specific objectives and scope of this dissertation are outlined.

Chapter 2 gives literature reviews of related work previously performed by other researchers. First, the fundamentals of transport and sorption are reviewed. Later, the existing experimental methods to determine partition and diffusion coefficients are also summarized. Both advantages and disadvantages of those methods are given. There is also a detailed introduction to previous studies on the relative humidity effect on VOCs emission and diffusion/partition coefficients.

Finally, the state-of-the-art of both the theoretical and numerical models development for multilayer assembly is reviewed.

The focus of Chapter 3 is the validation of the similarity theory between water vapor and VOCs transport in porous media. It begins with a description of the developed dual chamber experiment facility to measure the diffusion and partition coefficient. Theoretically, the definitions of three diffusion coefficients are clarified. The experiment results of VOCs (formaldehyde, toluene, acetaldehyde, butanol, hexanal, benzaldehyde, decane) in a reference material, calcium silicate, are presented and analyzed in detail; in the meantime, a validation of the dual chamber method is also presented. Finally, the validation of similarity theory in particleboard is also given.

Chapter 4 presents the experimental data on relative humidity's effect on diffusion and partition coefficients. The results of diffusion and partition coefficients of four common materials: calcium silicate, conventional gypsum wallboard, "green" gypsum wallboard and "green" carpet under different humidity conditions are given. The possible reasons for the phenomenon are also discussed in detail.

Chapter 5 introduces the numerical model that is used to simulate VOCs emission from multilayered worksurfaces. The model is first described in detail in terms of its mathematical development. Then parametric studies of the effects of the diffusion coefficient, the partition coefficient and the initial VOC concentration on the emission rate are presented. Later, the simulations of CHAMPS-BES which were designed to evaluate multilayer models by comparing the simulation results against the experimental measurements are presented. Several simulations regarding real scenarios, such as the emission characteristics of VOCs from worksurface and an investigation of the possibility of reducing VOC concentration by adding additional layers on top of the major VOCs source, are also presented.

Chapter 6 summarizes the work in this study. The limitations and possible applications of similarity theory and the multilayer model are discussed. The findings of the experiment and

simulations in this dissertation are concluded. The recommendations for future research in these fields are also given.

Additional work regarding 1) the VOCs database, 2) the material characterization of calcium silicate and particleboard, 3) the individual test results of conventional gypsum wallboard, "green" wallboard and "green" carpet, and 4) the cited standards of procedures used in the lab measurement are documented in the Appendices.

Chapter 2 Literature Review

2.1 Introduction

This chapter reviews previous research on: 1) fundamentals of VOC transport and sorption in porous media, 2) the methods to determine the diffusion and partition coefficients of VOCs, 3) the effect of relative humidity condition on VOC transport and storage, and 4) the development of a multilayer model to predict the VOC emission from the furniture/building materials. The objective was to understand the state of art in these subjects, and identify knowledge gaps and areas for further research.

2.2 Fundamentals of VOCs transport and sorption in porous media

2.2.1 Microscopic view of porous media

Most building and furniture materials are considered as porous media which in the microscale, consist of a solid material matrix and void space (pores). The pore size and shape depend on the nature of the material itself. By use of sophisticated optical and electron microscopy, the microstructure of porous materials can be observed. These methods are widely used in soil science, petroleum engineering and the paper making industry. Out of all of these technologies, one - scanning electron microscopy (SEM) – has been introduced into indoor air science to study the microscopic details of building materials of interest (Xiong et al. 2008). Representative 2D cross images from the scanning electron microscopy (SEM) of two materials of interest in this dissertation (particle board and veneer) are shown in Fig. 2.1. A 3D SEM image of hardwood is also shown in Fig. 2.2.

The SEM images help gain insight into the micro structure of the studied porous media and also serve as the basis for the development of a mechanistic model for the transport of the pollutants like VOCs and moisture.

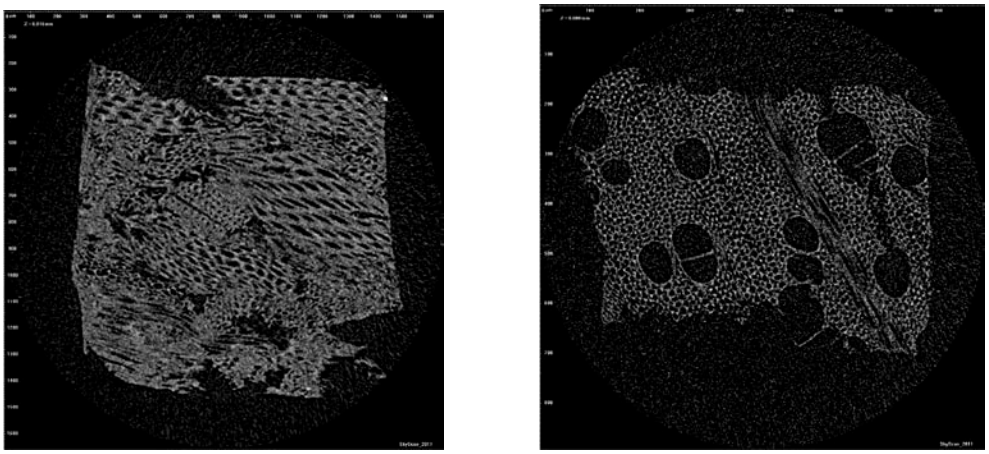

Figure 2.1 Representative side face image of (a) particleboard and (b) veneer (Tests conducted in College of Environmental Science and Forestry, State University of New York as part of this research)

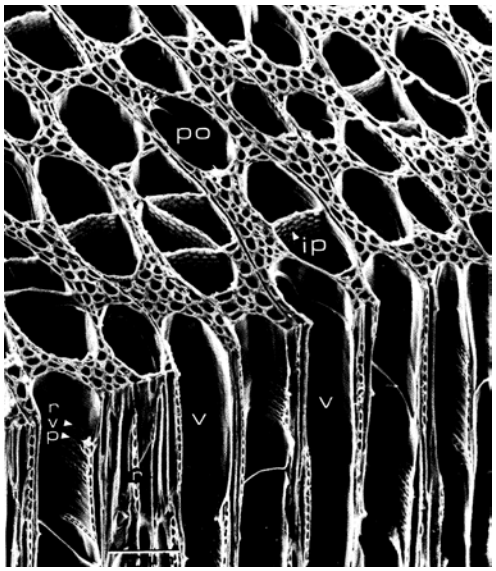

Figure 2.2 3D scanning electron micrograph of a hardwood, Populus deltoids, showing vessels (v), and the characteristic structural features of the wood of broad-leaved species. Note also the inter-vessel pitting (ip), ray-vessel pitting (rvp), and the pores (po) which are vessels as seen on the transverse surface. r=ray. (Core et al. 1979)

To quantify the pore size distribution and structure, mercury intrusion porosimetry (MIP) or the BET method have been used to provide the pore volume distribution. The total porosity of several common building/furniture materials are provided in Table 2.1. It can be seen that even

for the same type of materials like calcium silicate and ceiling tile, their porosity may vary significantly. The pore volume distributions of four porous materials of high density calcium silicate, low density calcium silicate, particleboard and veneer are provided in Fig. 2.3. The pore size of calcium silicate is relatively uniform compared to particleboard and veneer, which is in the range of 0.3μm-2.0μm for high density and 0.8μm-3.0μm for low density. For particleboard, the majority of pores are in the range of 1.6μm-105μm, while some pores are also in the range of 0.003μm-0.07μm. For veneer, pore sizes cover 0.003μm-100μm. By comparison, we can see that each material has different distribution characteristics, which may be governed by the raw materials and the manufacturing process. Pore size distribution helps determine the types of VOCs diffusions that take place in the porous media.

Table 2.1 Porosity of materials measured by MIP

Materials	Porosity (%)
Calcium silicate_Low density(LD)	26.67
Calcium silicate_High density(HD)	16.97
Particleboard	37.00
Veneer	51.89
Ceiling tile 1	28.67
Ceiling tile 2	55.48

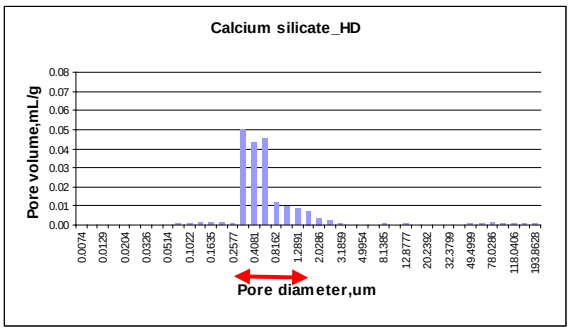

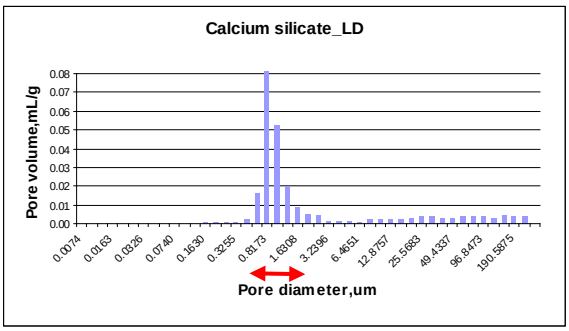

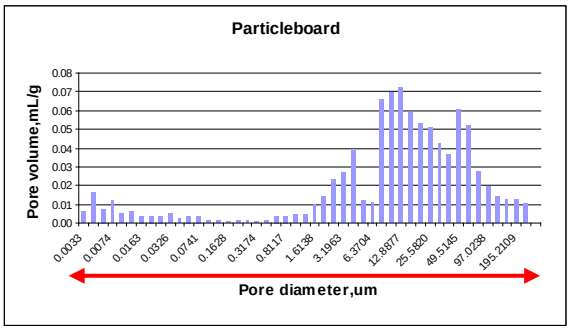

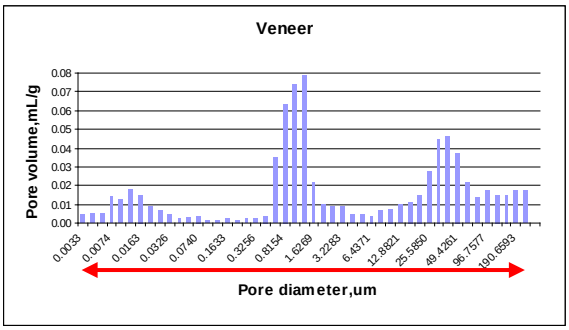

Figure 2.3 Pore volume distribution of high density (HD) calcium silicate, low density (LD) calcium silicate, particleboard, and veneer (tests conducted in LABTEB, University of La Roche, France as part of this research)

2.2.2 The representative elemental volume (REV)

In order to model transport and storage processes at the microscopic level using the continuum approach, the concept of a representative elementary volume has been introduced (Whitaker 1969, Bear and Bachmat 1991).

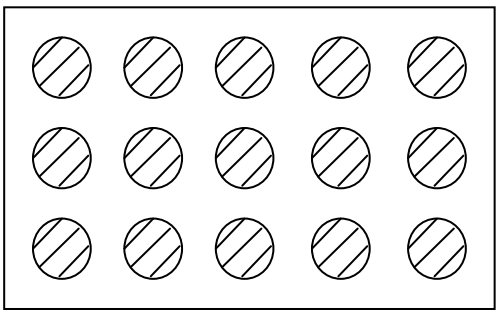

Figure 2.4 Schematic of a Representative Elementary Volume (REV)

The size of the REV (refer to Fig. 2.4) is very important: the obtained properties have to be independent of the size and continuous in space and time. Therefore, it has to be small enough to be considered as infinitesimal and large enough to account for the microscopic heterogeneity of the material. To obtain meaningful macroscopic values, Whitaker (1969) states that the characteristic length (l) of the REV must satisfy:

$$d << l << L \tag{2.1}$$

where d is a typical microscopic distance, L is a typical macroscopic length and l is the characteristic length of the REV. The left part of the inequality states that the characteristic length of the REV must be sufficiently larger than the size of a single pore so that the REV includes a sufficient number of pores. The right part of the inequality states that the characteristic

length of the REV must be sufficiently smaller than the length over which macroscopic variations in material properties occur.

This characteristic length l of the REV is not a feature of the material but is determined by the property investigated. The properties include the transport and storage properties in the porous media. As a consequence, the concept of an REV implies the existence of a scale at which a common characteristic length of the REV can be found for the properties of interest.

2.2.3 Sorption and sorption isotherms

Sorption usually refers to two processes, adsorption and desorption. Adsorption is the process by which the gas molecules (namely VOCs molecules in this dissertation) are adsorbed to the surface of porous material by physical or chemical means. Only physical adsorption is covered in this dissertation. Physisorption (or physical adsorption) is adsorption in which the forces involved are intermolecular forces (van der Waals forces) of the same kind as those responsible for the imperfection of real gases and the condensation of vapours, and which do not involve a significant change in the electronic orbital patterns of the species involved. Desorption is the opposite process from adsorption, in which the adsorbed molecules are released back into gas phase from the adsorbed sites. When the concentration (or pressure) of substance in the gas phase is lowered, some of the sorbed substance changes to the gas state. Heat gain or release may be involved in those two phenomena, depending on the specific substance and material as adsorbent. Heat of adsorption is that latent heat given off by a material as it is adsorbed onto another substance. One example would be the release of significant heat by water vapor adsorbing on dry silica gel. Heat of desorption would be the heat associated with desorbing a material, such as in the baking out of silica gel to dry it.

Sorption isotherm describes the adsorbed VOCs in the material versus the gas phase at a series of consecutive concentration levels, i.e., the relationship between the concentrations of adsorbed VOCs and the gas phase VOCs. Several well-known adsorption isotherm theories have been

developed to describe the adsorption/desorption behavior of gas molecules with solid surfaces such as Langmuir, Freundlich, and Brunauer-Emmett (Ruthven 1984, Do 1998). A sorption isotherm can be measured by using the VOC extraction method (James, et al. 2009). For low concentration levels as in most indoor VOC emission problems, a linear sorption isotherm has been found to be applicable, and has been widely adopted. In this case, the partition coefficient, defined as the ratio between the sorbed phase and gas phase concentration at equilibrium conditions is the only parameter needed to describe the sorption isotherm.

2.2.4 Transport mechanisms and governing equations

Four distinct mechanisms of transport inside a porous media may be identified: molecular diffusion, Knudsen diffusion, Poiseuille flow and surface diffusion. Molecular diffusion is the dominant transport mechanism when the mean free pass of the gas (i.e. the average distance traveled between molecular collisions) is small relative to the pore diameter. However, in small pores and at low pressure the mean free path can be greater than the pore diameter and collisions of molecules with the pore walls occur more frequently than collisions between diffusing molecules. Under these conditions the collisions between molecules and pore walls provide the main driving force for transport, known as Knudsen diffusion. Both the Knudsen and molecular diffusion mechanisms involve flow through the gas phase within the pore. There is in addition the possibility of a direct contribution to the flux from transport through the physically adsorbed layer on the surface of the pores, and this is referred to as surface diffusion. If there is a difference in total pressure across a porous medium, then there will be a direct contribution to the total flux of VOCs from forced laminar flow through the pore, which is called Poiseuille flow.

The diffusion process can be expressed by the Fick's first equation:

$$J = -D\frac{\partial C}{\partial x} \tag{2.2}$$

where, J is the mass flux in kg/m^{2}s, D is the diffusion coefficient in m^2/s, C is the concentration in kg/m^3, and x is the distance in the direction of transport.

For molecular diffusion, the diffusion coefficient of VOC in the material can be obtained by:

$$D_m = \frac{D^{air}\varepsilon}{\tau} \tag{2.3}$$

where D_m is the diffusion coefficient caused by molecular diffusion only in m^2/s, D^{air} is the diffusion coefficient of VOC in air in m^2/s, ε is the porosity of the material, τ is the tortuosity of the material, which is typically determined by experiment. For Knudsen diffusion, the diffusion coefficient is obtained by:

$$D_k = 97r\left(\frac{T}{M}\right)^{1/2} \tag{2.4}$$

where, D_k is the diffusion coefficient caused by Knudsen diffusion only in m^2/s, r is the mean pore radius in m, T is the temperature in Kelvin and M is the molecular weight of the diffusing species in g/mol. Typically, for VOC emissions from the dry materials, both molecular and Knudsen diffusion are significant transport mechanisms, and in this case, the combined diffusion coefficient due to both of these two modes becomes:

$$\frac{1}{D} = \frac{1}{D_m} + \frac{1}{D_k} \tag{2.5}$$

The conditions under which either Knudsen or molecular diffusion becomes the dominant transport mechanism follow $D_k >> D_m$ or $D_m >> D_k$ (Ruthven 1984, pp137), respectively. The procedure to obtain the diffusion coefficient due to surface diffusion is described in detail in the literature (Ruthven, 1984, pp137). According to the findings of Blondeau (2008), surface diffusion might also be significant even in the indoor VOC application. For Poiseuille flow, the corresponding diffusion coefficient is:

$$D = \frac{\mathrm{Pr}^2}{8\mu} \tag{2.6}$$

Where P is the absolute pressure in p_a, μ is the dynamic viscosity in p_a.s, and r is the mean pore radius in m. This effect is negligible if the pressure drop across the material is small.

2.3 Methods for Determination of Diffusion and Partition Coefficients

The diffusion and partition coefficients depend on the properties of VOCs, the microstructure of the materials, and environmental conditions. The diffusion coefficient has been found to be linearly correlated with the reciprocal of VOCs' molecular weight, and the partition coefficient to be inversely proportional to VOCs' vapor pressure (An et al. 1999, Bodalal 2000 and 2001, Cox et al. 2001). Additionally, the partition coefficient is found to be linearly proportional to the octanol-air partition coefficient (m^3 air/m^3 octanol) for some VOCs (Won et al. 2001). The octanol-air partition coefficient is the ratio of a chemical's concentration in liquid octanol ($C_7H_{15}CH_2OH$) to its concentration in air at equilibrium.

In order to mechanistically simulate VOC emissions from materials by using the diffusion model, three critical parameters need to be known: the initial VOC concentration, the partition coefficient and the diffusion coefficient. However, experimental data are still very limited for these parameters. Four major categories of measuring methods have been proposed in the past: the cup method, the twin chamber method, the porosity test method, and the microbalance test method. They are discussed in detail in this section.

2.3.1 Cup method

The cup method is the simplest way to measure the diffusion coefficient. Only one VOC can be applied in the apparatus since it measures the weight change of the specimen In the wet cup method, a material specimen covers the top of a cup containing a liquid VOC, placed in a controlled atmosphere, and the specimen-cup assembly is weighed periodically by microbalance until a steady state is approached for a period of time. The diffusion coefficient is calculated from the steady-state rate of VOC weight loss:

$$D_S = \frac{\dot{m}}{A}\frac{d}{C} \tag{2.7}$$

where D is the diffusion coefficient of tested material in m^2/s, $\dot{m}$ is the mass flow rate through the material (calculated from the slope of the weight loss curve) in mg/s, A is the material area in m^2, d is the material thickness in m, and C is the mass concentration of the diffusing substance in mg/m^3 in the cup. The schematic of the wet cup method is as following:

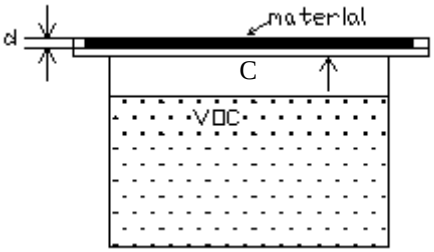

Figure 2.5 Wet cup method

The defect of the wet cup method is that the liquid VOC placed in the cup creates saturation concentration, which is unrealistically high for indoor air quality application; e.g., at 23°C, the saturation concentration for n-octane is $97.36g/m^3$ and that for ethyl acetate is $473.45\ g/m^3$. These values are not realistic compared to tens of $\mu g/m^3$ (or less) or hundreds of ug/m^3 in room air. From the studies on water vapor diffusion through building materials, it was found that the difference in the concentration level could lead to a significant difference in diffusion coefficients (ASHRAE 1997). The strong point of the wet cup method is the simplicity of the apparatus and the theory itself.

The dry cup method evolved from the wet cup method to overcome the preceding disadvantages. The liquid VOC is replaced by a much lower injected VOC inflow concentration, which maybe closer to the reality. Desiccants (for water vapor) or strong sorbents (for VOCs) are placed inside the cup to guarantee zero vapor pressure and the vapor is introduced into a control

chamber. However, it takes more time to obtain the diffusion coefficient due to the relatively small VOCs.

2.3.2 Microbalance test method

Cox et al. utilized the high resolution dynamic microbalance to measure and record changes in a vinyl flooring (VF) sample weight during sorption and desorption tests. Using this method, the diffusion and partition coefficients of water, n-butane, toluene, phenol, n-decane, n-dodecane, n-tetradecane, n-pentadecane in vinyl flooring were determined individually. A VF sample was placed on the microbalance in the sample chamber. The sample weight was first stabilized by passing clean air through the sample chamber until equilibrium was reached. Influent air was then switched to clean air and the desorption process was monitored until equilibrium was re-established. Equilibrium was assumed when a five-point moving average rate of mass change reached ~1% of the maximum rate of change of the mass.

For a particular VOC, the sorption equilibrium was described using a partition coefficient, or

$$K = \frac{C}{y} \tag{2.8}$$

where C was the equilibrium concentration in the material phase, and y was the corresponding concentration of the species in the gas phase. The diffusion coefficient D was determined by fitting a diffusion model to experimental sorption and desorption data. Under the experimental conditions, the rate of change in mass due to Fickian diffusion was given (Crank, 1975) by

$$\frac{M_t}{M_\infty} = 1 - \sum_{n=0}^{\infty} \frac{8}{(2n+1)^2 \pi^2} \exp\left\{ \frac{-D(2n+1)^2 \pi^2 t}{4L^2} \right\} \tag{2.9}$$

where M was the total mass of a VOC that had entered or left the slab in time t, M_∞ was the corresponding quantity at saturation reached, and 2L was the thickness of the VF sample.

The experiment (Cox et al 2001) proved that the derived diffusion coefficient is independent of the initial inflow concentration in the range of 11500-65000 $\mu g/m^3$ during the adsorption period, and the sorption profile was not actually affected by the appearance of the other compound. This agreed with the traditional belief that the diffusion coefficient and the partition coefficient were independent of concentration at the lower concentrations typically associated with gas and material-phases in the indoor environment. However, the adsorbed VOCs (phenol and n-dodecane) had a slight increase due to the elevation of the water vapor at 50%RH compared to single compound tests.

Under given environmental conditions, diffusion coefficient and partition coefficient were determined not only by VOC physical properties, but also by the material itself. Evidence showed that the logarithm of the partition coefficient of n-dodecane in vinyl flooring correlated well with the logarithm of vapor pressure (R^2=0.998) and that diffusion coefficients of n-decane, n-dodecane, n-tetradecane, and n-pentadecane correlated well with their molecular weights (R^2=0.983)(Cox et al. 2001).

This method avoids taking many samples to quantify air concentrations and reduces the relevant errors induced by air sampling, thermal desorption and GC/MS analysis. A demanding requirement for this method is that the microbalance is supposed to be highly sensitive and the concentrations of interest must be within the measurement ranges.

2.3.3 Twin chamber method

Just as the name implies, the twin chamber method uses two identical chambers with the material specimen placed between them. VOCs are injected into one of the chambers. Air samples in both chambers are taken periodically until the system reaches a steady state. Unlike above methods, several VOCs can be tested at the same time.

2.3.3.1 CLIMPAQ method

Meininghaus et al. (1998) used two CLIMPAQ type small-scale chambers (Gunnarsen et al. 1994) to measure the diffusion coefficients for n-octane and ethyl acetate in eight building materials. They were wallpaper with paste, PVC floor covering, carpet, acrylic paint on woodchip paper, gypsum board, and aerated concrete, solid concrete, and brick wall. The test chamber CLIMPAQ was made of panes of window glass. Other main surface materials were stainless steel and eloxated aluminum. The volume of each chamber was 50.9 L and the experiment was carried out at 24±0.5ºC and relative humidity of 45±3%. VOC concentrations in the supply and the exhaust air of each chamber were measured. The modified Fick's law was used to calculate the diffusion coefficient:

$$D_s = -\frac{m}{A}\frac{\Delta x}{\Delta C} = -\frac{Vd}{A}\frac{C_2}{C_2 - C_1} \tag{2.10}$$

where V was the ventilation rate in m^3/s, d was the material thickness in m, A was the area of specimen in m^2, and C_1, C_2 were the VOC concentrations at the steady-state condition in the primary (contaminated air supplied) and secondary (clean air supplied) chambers, respectively in mg/m^3.

The concentration difference given in the Fick's Law equation was the concentration difference of the specimen surfaces; it is, however, impossible to directly measure the surfaces concentrations of a specimen. To minimize error, they placed a fan in each chamber to mix the chamber air (air velocity 0.08m/s). They assumed the chamber air was perfectly mixed, and the surface concentration was the same as the chamber air concentration.

2.3.3.4 Diffusionmetric method

Bodalal et al (2000) developed the method to measure diffusion coefficients and equilibrium partition coefficients. In the test, two identical chambers were connected with the targeted material in the middle of the two chambers, among which one was a high concentration chamber;

the other was a low concentration chamber. They kept the pressure difference between the two chambers at zero and no convection occurred. In this way, both partition coefficients and diffusion coefficients could be computed.

The governing equation within the material was

$$\frac{\partial C}{\partial t} = D.\frac{\partial^2 C}{\partial x^2} \tag{2.11}$$

Boundary conditions

At x=0, $C=k_e.c_1$ (2.12)

At x=l, $C=k_e.c_2$ (2.13)

Initial condition

At t=0, $0 \le x \le l$ $C=0$ (2.14)

where C(x, t) was the concentration of the diffusing substance at time t in the test specimen at a point whose distance was x from the surface. A was the total area of the sample and D was the diffusion coefficient of the specific compound under study. K_e was the equilibrium partition coefficient. The diffusion coefficient and partition coefficient could be solved by means of the least-square regression method and Laplace-Carson Transformation. The obvious disadvantage of this method is that multiple solutions may be derived because of the least-square regression method.

2.3.4 Porosity test method

Tiffonnet et al. (2000) obtained diffusion coefficients from mercury intrusion porosimetry (MIP) tests. In assessing the diffusion coefficients, they applied Carniglia's mathematical model which considers the pore interconnections, the pore constriction, and the pore random orientation. In obtaining the effective diffusion coefficient, the connected-pore volume fraction was measured, and the mean diffusion coefficient in the pores of the material and the tortuosity

factor of the porous network were computed from the MIP tests. They tested seven building materials: solid concrete, aerated concrete, gypsum board, brick, mortar, gypsum, and chipboard. The diffusion coefficients were obtained for methane, ethyl acetate, n-octane, and n-dodecane. They compared their results with those of the cup method and the CLIMPAQ method. The results were in the same order of magnitude, but the diffusion coefficients obtained by the porosity test were generally larger than the others. Haghighat et al. (2002) and Blondeau (2008) presented tables that summarized the diffusion and partition coefficients measured in all previous research including the literature mentioned in this dissertation.

2.4 Effects of humidity Conditions on VOC Transport and Sorption

The primary environmental conditions that may affect VOC transport and sorption are temperature and relative humidity. As a critical environmental factor, the influence of relative humidity on VOC diffusion is still not well understood.

Relative humidity can affect the emission rate depending on the types of emission materials and types of VOCs emitted. Wolkoff (1998) tested five common building products under 0% and 50%RH. The materials studied were nylon carpet with latex backing, PVC flooring, floor varnish on pretreated beechwood parquet, sealant and water-borne wall paint on gypsum board. An increase from 0% to 50%RH led to a higher concentration of 2-ethylhexanol from carpet during the first week and an obvious concentration elevation of 1, 2-propandiol from wall paint during the whole test period of 25 days. The concentration of dimethyloctanols from sealant was higher at 50% than 0% during the first couple of days, but the trend reversed later. The explanations given by the paper was that the low humidity might result in a different film structure due to a faster dry out process, or that water vapor carried out polar substances from the surface.

Fang et al. (1999) measured the chemical emissions from five building materials (carpet, polyvinyl chloride (PVC) flooring, sealant, floor varnish and wall paint) in the relative humidity range of 30%-70% in modified CLIMPAQ chamber. For floor varnish and wall paint, the

measured TVOC increased very significantly when humidity increased from 30% to 70%; however, for carpet, PVC flooring and sealant, the influence of relative humidity was not obvious. Relative humidity affected only the waterborne materials-floor varnish and wall paint.

Zhang et al. (2002) tested the sorption characteristics at 25%, 50% and 80%RH, respectively. The tested VOCs included ethylbenzene, benzaldehyde, decane, 1, 4-dichlorobenzene, undecane and dodecane. For painted drywall, the increase of RH from 25% to 80% significantly increased the adsorbed amount of decane, 1, 4-diclorobenzene, undecane and dodecane. For ceiling tile, the sink effect of benzaldehyde was increased when RH increased from 50% to 80%, but the amount of dodecane adsorbed decreased with the increase of relative humidity. The results did not show obvious influence for the other compounds. For carpet, only the amount of 1, 4-dichlorobenzene increased slightly with the increase of relative humidity. The difference of solubility of VOCs might be one factor that influenced the sink effect, and the water retention curve for those materials also needed to be known in order to analyze if significant condensed water existed in higher RH level conducted in these tests.

The above results indicate that a higher humidity may lead to increase in some VOC emissions from some materials, but the mechanism for the humidity effects is not clear. Broadly speaking, possible causes of enhanced emission at a higher humidity may include enhanced diffusion, smaller sorption capacity or increased generation of VOCs due to hydrolysis.

Very limited experimental research has been done on the effect of humidity on the diffusion coefficient and partition coefficient. Huang et al. (2006) tested the partition coefficient of five VOCs (cyclohexane, toluene, ethyl acetate, isopropyl alcohol and methanol) in ceiling tile at 0%, 35% and 75% RH conditions. They did not observe any influence of relative humidity except on methanol. The partition coefficient of methanol in ceiling tile decreased linearly with the increase of relative humidity. The explanation of the phenomenon given by the paper was the high polarity of methanol. The attraction between water molecules and methanol molecules may

weaken the interaction force between solid surface and the methanol molecule. In more recent literature (Farajollah et al. 2009), five VOCs (octane, isopropanol, cyclohexane, ethyl acetate, and hexane) were measured for ceiling tile. Three relative humidity conditions (0%, 20%, and 40%RH) were investigated. Only minor humidity effects on the diffusion coefficient were observed. One possible reason for this phenomenon was that only isopropanol had relative high solubility, and the other four compounds had insignificant solubility in liquid water. That was why no obvious VOC was observed at higher RH level.

Bouilly et al. (2006) proposed a physically based model regarding the relationship between relative humidity and VOCs in porous media. They considered three kinds of interactions: competition for adsorption at the pore surfaces of the material, change in the diffusion properties, and possible absorption/desorption of VOCs due to capillary condensation of water vapour in the small pores of the materials. The proposed model analyzed the underlying principles of the relative humidity influence in the microstructure and could be used to predict the humidity effect on the diffusion and partition coefficient in theory. The detailed calculation procedure for absorption into condensed water is discussed below.

For a uniform pore air-phase concentration C' (g/g_{air}), the unit mass of a VOC contained in the porous volume, M_{air}(kg/m^3_{mat}) is given by:

$$M_{air} = \rho_{air} \varepsilon C' \tag{2.15}$$

where ϱ($kg.m^{-3}$) is the air density and ε (m^3_{air}/m^3_{mat}) is the total porosity of the material. The unit mass of VOC which is adsorbed at the pore surface, M_{ads}(kg/m^3_{mat}), depends on the sorbed-phase concentration of the chemical, C_s (kg/kg_{mat}), and the material density ϱ_{mat} (kg/m^3):

$$M_{ads} = \rho_{mat} C_s \tag{2.16}$$

Assuming a linear adsorption isotherm, the above equation transforms into:

$$M_{ads} = \rho_{mat} K C' \tag{2.17}$$

where K (kg_{air}/kg_{mat}) is the partition coefficient of the VOC and material system.

Finally, the unit mass of VOC which accumulates in the pores due to absorption in condensed water, M_{abs} (kg/m^3 mat) is given by:

$$M_{abs} = \varepsilon_{liq} C_{liq} \tag{2.18}$$

where ε_{liq} (m^3_{water}/m^3_{mat}) is the moisture content of the material for a uniform relative humidity RH in the material, and C_{liq} (kg/m^3_{liq}) is the VOC aqueous-phase concentration. For a dilute solution, Henry's law applies, and the above equation transforms into:

$$M_{abs} = \varepsilon_{liq} HC' \tag{2.19}$$

where H ($kg_{air}/m3_{water}$) is the Henry's constant (solubility in water) of the VOC.

They concluded that, for the influence of humidity on VOC absorption to condensed water, humidity might tremendously increase the water soluble-species mass capacity of any kind polydispersed material due to water condensation when relative humidity was higher than 60%.

For the influence of humidity on the VOC effective diffusivity in materials, take acetone for example, humidity showed no influence on particleboard and gypsum, but a significant decrease in acetone diffusivity in mortar occurred when humidity increased from 50%RH to 80% RH.

For the influence of humidity on competition with VOC adsorption, they found that the sorbed phase concentrations of adsorbed benzene, o-xylene and styrene in plywood at 80%RH could be up to 30% lower than in dry conditions.

2.5 Multilayer model development of VOCs emission

VOCs concentration is a big concern in assessing indoor air quality with the increasing use of chemical-related building and furniture materials in modern residential homes and offices. There are a large number of indoor VOC emission sources, such as paint, adhesive, carpet, wood, and

printer. Meanwhile, a large number of experimental measurements of the VOCs emissions have been done in the last twenty years (Zhang et al. 1996; Guo, Murray and Lee 2002; Guo et al. 2004; Virta et al. 2005; Koivula et al. 2005; Järnström et al. 2007; Shinohara et al. 2009). However, since the experiments only give information on the specific concentration level of that particular object, it is impossible to extrapolate the data from one condition to another condition, and experiments also usually take a long preparation time and test duration, not to mention the high cost associated with it.

Thus, modeling (both theoretical and numerical modeling) is necessary to overcome the disadvantages of experiment and serves as an excellent tool in providing the in-depth understanding of the mechanism of VOCs emission.

2.5.1 Theoretical model development

Little, Hodgson and Gadgil (1994) first established a simple but effective diffusion model for emissions from carpet. They assumed that all VOCs are from a thin layer of uniform polymer backing material (the main component of the carpet). The model also assumed that 1) the initial VOC concentration in the material was uniform, 2) the boundary layer resistance was negligible compared to the diffusion resistance of the material, and 3) the sink effect of the chamber wall was neglected. Therefore, the VOC concentration with respect to time in either air phase or material was calculated by the model if the diffusion coefficient, partition coefficient and initial VOCs concentration were measured. Based on this model, there are a few further improved physically-based analytical solutions to single layer material, even considering the sink effect of the surface, the mass transfer resistance in the air phase boundary layer and the distribution of initial VOC concentration et al., published in literature (Haghighat and Zhang 1999; Cox, Little and Hodgson 2002; Xu and Zhang 2003; Xu and Zhang 2004; Deng and Kim 2004).

Kumar and Little (2003) developed a single layer model to predict the source/sink behavior of diffusion-controlled building materials. The models allowed an uneven initial material-phase

concentration and a transient influent gas-phase concentration to be simultaneously considered. One of the premises for this model was that the chamber air was well mixed. The model to describe the emission from vinyl flooring was defined as following:

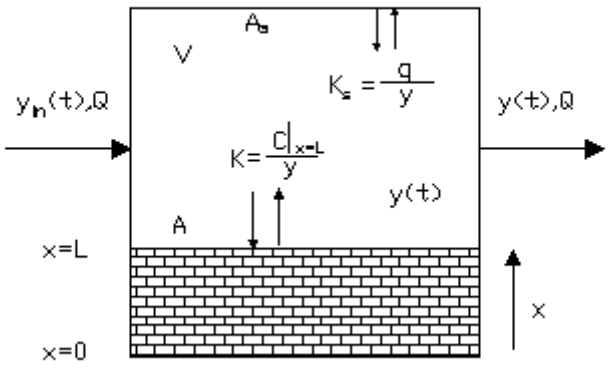

Figure 2.6 Single layer model

The model described emissions from a homogeneous, diffusion controlled source. The sink effect of a chamber wall could be included in the model in terms of K_s. Within the material, the diffusion equation was as follows:

$$\frac{\partial C}{\partial t} = D.\frac{\partial^2 C}{\partial x^2} \tag{2.20}$$

where C was the VOC concentration in the slab of material, t was time, x was distance from the base of the slab, and D was a factor of proportionality representing the amount of substance diffusing across a unit area through a unit concentration gradient in unit time, often termed diffusion coefficient. The initial condition was given by an arbitrary function describing the nonuniform material–phase concentration profile or

$$C(x,0) = f(x)$$

The VOC concentration within the chamber air was governed by the subsequent equation:

$$V\frac{dy}{dt} = Qy_{in} - AD\frac{\partial C}{\partial x} - Qy \tag{2.21}$$

where y_{in} indicated the VOC concentration in the chamber air. The solution to VOC concentration in the material was offered as

C(x, t)=

$$2\sum_{m=1}^{\infty}\left[\frac{q_m^2\{hDR(t)\cos(q_mL)+kf(L)\cos(q_mL)+I_c\}\cos(q_mx)\exp(-Dq_m^x)\exp(-Dq_m^2t)}{\cos^2(q_mL)\{L(h-kq_m^2)^2+q_m^2(k+L)+h\}}\right] \quad (2.22)$$

where

$$R(t)=\int_0^t Ky_{in}(\tau)\exp(Dq_m^2\tau)d\tau \quad (2.23)$$

$$I_c=\int_0^L\cos(q_mx)f(x)dx \quad (2.24)$$

and the q_m values are the positive, nonzero roots of

$$q_m\tan(q_mL)=h-kq_m^2 \quad (2.25)$$

and h and k were given by

$$h=\frac{Q}{AKD} \quad (2.26)$$

$$k=\frac{V}{AK} \quad (2.27)$$

Another partition coefficient K_s was introduced to indicate the chamber wall sink effect. It indicated that the order of magnitude of wall sink effect was insignificant relative to the adsorption of the material. This model was confined to homogeneous vinyl flooring material. In fact, there are more heterogeneous and nonuniform materials than homogeneous materials in rooms.

Nearly all the physically-based models in the literature assumed that the convective mass transfer coefficient h_m was infinite, i.e., $C_s(t) = C_\infty(t)$ (Dunn, 1987; Clausen et al., 1991; Little et al., 1994). On the contrary, Xu and Zhang (2003) improved the above models by considering the convective mass transfer coefficient. The term was written as

$$-D\frac{\partial C(x,t)}{\partial x} = h_m(C_s(t) - C_\infty(t)) \tag{2.28}$$

where h_m was the convective mass transfer coefficient in m/s, C_s (t) was the concentration of VOC in the air adjacent to the interface; $C_\infty(t)$ was the VOC concentration in atmosphere. At last, the solution to the model was provided as well:

$$C(x,t) = KC_\infty(t) + \sum_{m=1}^{\infty} \frac{\sin(\beta_m L)}{\beta_m} \frac{2(\beta_m^2 + H^2)}{L(\beta_m^2 + H^2) + H} \cos(\beta_m x)$$
$$\times \left[(C_0 - KC_\infty(0))e^{-D\beta_m^2 t} + \int_0^t e^{-D\beta_m^2 (t-\tau)} KdC_\infty(\tau) \right] \tag{2.29}$$

where $H=h_m/K$, $\beta_m(m=1,2,\ldots)$ were the positive roots of

$$\beta_\infty \tan(\beta_m L) = H \tag{2.30}$$

Xu and Zhang (2004) also defined the initial concentration of VOCs of interest in the building material as an equation but not with constant and uniform distribution, i.e.

$$C(x,0) = C_0(x) \tag{2.31}$$

where, C_0 was the distribution of initial contaminant concentration.

Based on the above research, it was found that the model is being improved and that assumptions are going to be replaced by the real situations gradually. At first, the chamber air and compounds are assumed to be well mixed, and the initial contaminant distribution is considered as uniform. Afterwards, two kinds of premises (uniform initial VOC distribution and negligible

boundary layers) are being corrected. What is more, the solutions to a series of equations is solved and presented. In a sense, the model can serve as a tool to predict emission characteristics. The limitation to this model is that it can only predict emission from single layer materials, but it is not applicable to more complicated building materials, which is always the case in residential or commercial rooms. Additionally, the parameters in the model (such as diffusion coefficient, partition coefficient, mass transfer coefficient and initial compound distribution in the material) are often unknown in reality. Therefore, these factors combine to prevent the accuracy and convenience of the model.

Most building wall and furniture material is composed of different layers instead of an ideal single uniform layer: for example, a typical wall is made of, from exterior to interior surface, façade/wind barrier/OSB (oriented strand board)/insulation/gypsum, and a typical desk panel(or called worksurface) is a combination of adhesive/veneer/particleboard/veneer. Obviously, it is of more significance to study emissions from multilayered structures in the prediction and evaluation of indoor VOC concentrations. To solve this problem, a complicated analytical solution was finally put forward in detail to compute VOC emissions from the general composite assembly (Hu et al. 2007).

Though the analytical multilayer model has been developed, the solution is very complicated for people to use. In order to calculate the VOC concentrations in a room or chamber, complex equations need to be solved and errors may be encountered in the calculation process.

2.5.2 Numerical model development

On one side, more and more general analytical solutions have been gradually developed; on the other side, because of the mathematical complexity involved in solving the equations, there is also increased interest in developing a numerical solution. Bodalal Awad (1999) put forward a general multilayer numerical model by splitting 3D problem into three 1D sub-problems, taken into account both the material sink effect and the air phase boundary layer resistance. Another

complicated multilayer model using a CFD (computational fluid dynamics) model was proposed by Xudong Yang (Yang et al. 2001). They developed a more comprehensive numerical model that considered VOC transport in the air, surface sorption, and diffusion in the material. The model could be used for simulating VOC sorption and desorption rates of homogenous building materials with constant diffusion coefficients and material-air partition coefficients. Particularly, Yang developed this model based on more general and non-uniform mixing conditions for indoor air, which was different from other models. The model is able to predict the VOCs emission from dry materials in relatively short terms. Thereafter an integrated IAQ model was established in studying the vinyl floor tile/glue/plywood (Haghighat and Huang 2003). More recently, a multilayer model using the fugacity has been proposed for predicting VOC emissions from SIPs (structure insulated panels) (Yuan et al. 2007).

However, there is no numerical simulation regarding multilayer worksurfaces published in the literature so far. As a further development, in this dissertation, a general 2D multilayer model based on CHAMPS (coupled heat, air, moisture and pollutant simulations) is being described (Li 2007, Grunewald et al. 2007). The model is capable of predicting both VOC emission and moisture transport from the composite materials. The model is validated by the experimental data from the standard small scale emission test for non uniform three layered particleboard. The model has the advantage of quick use by researchers because of its interactive user interface and could be extended to other multilayer materials very easily as long as the material characteristics are known.

2.6 Summary and Conclusions

This chapter reviews the fundamentals of VOC diffusion and sorption, the method to determine the partition coefficient and diffusion coefficient, the humidity effect, and the multilayer model development. It can be concluded that:

1. It is important to know the detailed pore structure of the porous media because it helps determine the mode of transport of VOCs in a specific porous material. SEM imaging provides visual insight into the microstructures of the porous media, and the MIP or BET method can be used to measure the pore volume distribution of the media.

2. There are many previously developed methods available for the measurement of partition and diffusion coefficients, and each method has its own advantages and disadvantages. However, experimental data for diffusion and partition coefficients are still very limited considering the large number of VOCs and materials of interest to indoor air quality. This is largely due to the time and cost involved in such experiments. The similarity theory developed in chapter 3 is an attempt to investigate the possibility that much of the water vapor transport data can be utilized to estimate diffusion coefficients for VOCs.

3. Though there are some previous studies about the humidity effect on VOC emission, but there is not a consistent conclusion about the phenomenon. The mechanism of the humidity effect is also not well understood.

4. Most building or furniture materials are multilayered. There is a need to develop numerical simulation models for predicting the emissions from multilayer material assemblies such as the composite wood assemblies that are widely used in desks, cabinets, floors etc. In Chapter 5, we will present a CHAMPS-BES model for simulating multilayer assemblies and investigate how the different model parameters and initial concentration distributions in different layers affect the overall emissions from the assemblies.

Chapter 3 Analogy between Water Vapour and VOCs Diffusions in Porous Media

3.1 Introduction

The majority of building and furnishing materials are porous media. In-materials, diffusion and storage play a predominant role in determining the rates of VOC emissions from these materials. Knowledge and data on the diffusion and partition coefficients are necessary in applying mass transfer models to predict the emission rates, but such data are very limited. Four major categories of measuring methods have been proposed in the past few years: the cup method, the twin chamber method, the porosity test method, and microbalance test method. In the wet cup method, tested material was covered over the top of a cup containing a liquid VOC, placed in a controlled atmosphere, and then weighed periodically by microbalance (Haghighat et al. 2002). The diffusion coefficient was calculated from the rate of VOC weight loss. The twin chamber test method (Bodaldal et al. 2000) was capable of measuring several compounds simultaneously, but multiple solutions might be derived due to the estimation of the diffusion coefficient and partition coefficient in the same least-square regression method. A porosity test method had been applied to homogenous and single layer material. Tiffonnet et al. (2000) obtained diffusion coefficients from mercury intrusion porosimetry (MIP) tests. In this method, the connected-pore volume distribution was measured by MIP; the mean diffusion coefficient in the pores of the material and the tortuosity factor of the porous network were computed from the pore volume distribution. The method relied on physical mechanisms at the microscopic scale to describe the kinetics of sorption. In the microbalance test method, Cox et al. (2001) made use of the high resolution dynamic microbalance to measure and record changes in vinyl flooring (VF) sample weight during sorption and desorption tests, which were then used to fit a 1-D diffusion model to determine the diffusion coefficient. However, the comparison among different studies is difficult because different materials were tested.

Salonvaara et al. (2006) used a dynamic dual-chamber system to compare the diffusion of decane and water vapor (Table 3.1). Similar orders of magnitude of diffusion coefficients were found between the water vapor and decane for the same material, while the two materials tested (gypsum wallboard and OSB) differed by an order of magnitude. The results suggested that there might be a similarity relationship between water vapor and VOCs in diffusion through porous media. The objective of this study was to further validate the similarity hypothesis and investigate the feasibility of determining VOC transport properties based on water vapor diffusion characteristics of building materials.

Table 3.1 Effective diffusion coefficients of water vapor and decane

Material	Compounds	Effective diffusion coefficients in m^2/s, (T=23°C, RH =50%)
Gypsum board	Water vapor	4.1×10^{-6}
	Decane	2.8×10^{-6}
Oriented strand board	Water vapor	1.5×10^{-7}
	Decane	1.1×10^{-7}

3.2 Theory

Consider two identical chambers that are separated by a material (with a cross section area of A) whose diffusion coefficients for a VOC and water vapor are to be determined (Fig. 3.1). With constant Q_A, Q_B and C_{Ain}, and $C_{Bin}=0$, the VOC or water vapor flux through the material at steady state can be calculated by:

$$j = \frac{C_{Bout} Q_B}{A} \tag{3.1a}$$

3.2.1 Diffusion coefficients

Three different definitions of the diffusion coefficient have been used in the literature and sometime cause confusion. Their relationships and how they can be calculated from the diffusion flux in Equation (3.1a) are elucidated below:

1) Effective diffusion coefficient D_e:

At steady state,

$$j = D_e \frac{C_A - C_B}{L} = \frac{C_{Bout} Q_B}{A} \tag{3.1b}$$

hence, D_e can be obtained by

$$D_e = \frac{C_B}{C_A - C_B} \frac{L}{A} Q_B \tag{3.2}$$

where D_e is the effective diffusion coefficient in m^2/s. C_A and C_B are the VOC concentrations in the air phase of chambers A and B in kg/m^3, respectively (Note: $C_A=C_{Aout}$ and $C_B=C_{Bout}$ assuming perfect mixing in both chambers). L is the thickness of the material in m (Fig. 3.1). A is the material area exposed to the air in m^2. j is the mass flux in kg/ (m^2.s). This definition was used in the wet cup method (Haghighat et al. 2002), CLIMPAQ method (Meininghaus et al. 2000) and dual chamber method (Salonvaara et al. 2006) and was directly determined from the experimental data in this study. This definition also included the effects of convective mass transfer resistance through the air film on either surface of the material, which are usually negligible as compared to the in-material diffusion resistance except for very permeable materials.

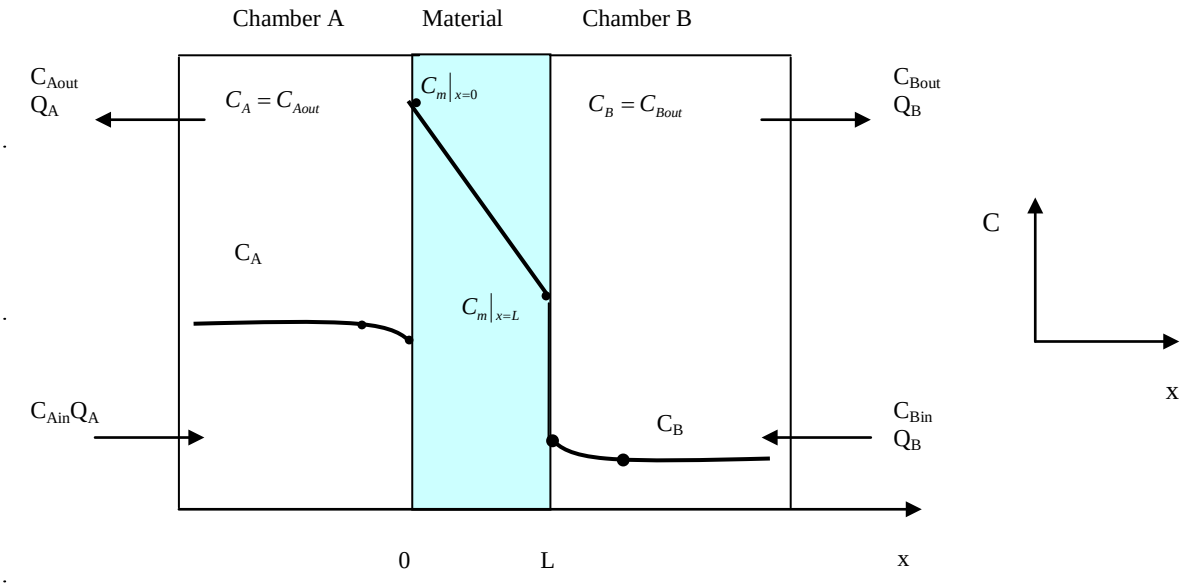

Figure 3.1 Schematic of a dual-chamber setup and expected concentration profile at steady state

2) Apparent diffusion coefficient: Assuming a homogeneous material, the VOC diffusion mass flux inside the material can be described by the one dimensional Fick's law as:

$$j = -D\frac{\partial C_m}{\partial x}, \quad 0 \le x \le L \tag{3.3}$$

at steady state,

$$j = D\frac{C_m\big|_{x=0} - C_m\big|_{x=L}}{L} \tag{3.4}$$

where D is the apparent diffusion coefficient in m^2/s; $C_m\big|_{x=0}, C_m\big|_{x=L}$ are the VOC concentrations in the material at the interfaces in kg/ (m^3 material). This definition was used, for example, by Bodalal et al. (2000) and Cox et al. (2001) (termed "diffusion coefficient" in their papers). The difference between D_e and D is that the driving force adopted for D_e is the VOC concentration gradient in the air phase instead of that in the material as in D. The relationship between apparent diffusion coefficient and effective diffusion coefficient is deduced as follows,

$$j = D\frac{C_m\big|_{x=0} - C_m\big|_{x=L}}{L} = D\frac{C_A K_{ma} - C_B K_{ma}}{L} = DK_{ma}\frac{C_A - C_B}{L} = D_e\frac{C_A - C_B}{L} \tag{3.5}$$

That is,

$$D = \frac{D_e}{K_{ma}} \tag{3.6}$$

where K_{ma} is the partition coefficient defined as $K_{ma} = C_m / C_a$ at equilibrium, C_m is the concentration inside the material and C_a is the concentration outside the material. The same partition coefficient is assumed to represent the material-air phase partition of the VOC at both interfaces considering that the resistance in the boundary layer is very small and hence negligible as compared to the resistance of in-material diffusion for dry material. It also has the assumption that equilibrium establishes instantaneously at the interfaces, which is justified since it is a much faster process than the in-material diffusion process.

3) Pore diffusion coefficient: The aforementioned two definitions regard the material as solid and homogeneous without considering its internal porous structure. Consider that a porous material consists of inter-connected air pores and a solid matrix, and assume that VOC transports only through the pore air which can be stored (adsorbed) on the surfaces of the solid matrix (e.g. represented by a partition coefficient K_s) in a Representative Elementary Volume (REV, Fig. 3.2).

K_s, the partition coefficient, is defined as

$$K_s = \frac{C_{pm}}{C_{pa}} \tag{3.7}$$

where C_{pm} is the sorbed phase concentration in kg/m^3 REV and C_{pa} is the gas phase concentration in the porous air in kg/m^3 REV.

$$C_{pa} = \frac{M_{pa}}{V_{REV}} \tag{3.8a}$$

$$C_{pm} = \frac{M_{pm}}{V_{REV}} \tag{3.8b}$$

$$C_m = \frac{M_{REV}}{V_{REV}} \tag{3.8c}$$

$$M_{REV} = M_{pm} + M_{pa} \tag{3.9}$$

where M_{REV} is the total VOC mass in the REV in kg, M_{pm} is the sorbed phase VOC mass in the matrix in kg and M_{pa} is the VOC mass in the pore air in kg.

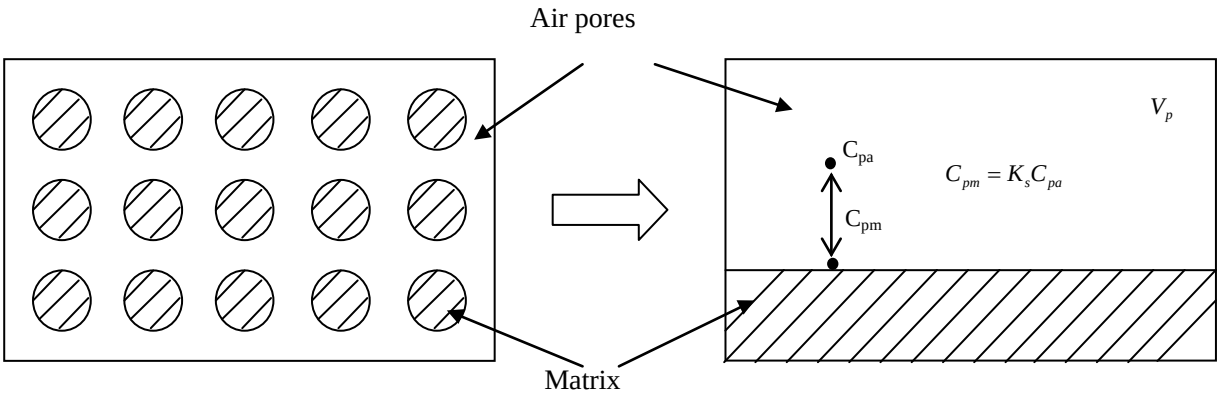

(a) Physically (b) Conceptually

Figure 3.2 Schematic of a Representative Elementary Volume (REV)

Dividing both sides of Eq. (3.9) by V_{REV}, the relationship between the three concentrations can be obtained:

$$\frac{M_{REV}}{V_{REV}} = \frac{M_{pa}}{V_{REV}} + \frac{M_{pm}}{V_{REV}} \qquad i.e. \quad C_m = C_{pa} + C_{pm} \tag{3.10}$$

When the concentration in the material is in equilibrium with that in air outside the material, the relationship between C_{pa} and C_a can be derived from:

$$C_{pa}.V_{REV} = C_a.V_{REV}.\varepsilon \qquad \text{i.e.} \quad C_{pa} = \varepsilon C_a \tag{3.11}$$

where porosity $\varepsilon = V_p/V_{REV}$ and V_p is volume of pore air in m^3. The relationship of K_{ma} and K_s is:

$$K_{ma} = \frac{C_m}{C_a} = \frac{C_{pa} + C_{pm}}{C_{pa}/\varepsilon} = \varepsilon\left(\frac{C_{pa} + C_{pm}}{C_{pa}}\right) = \varepsilon(1 + K_s) \tag{3.12}$$

$$K_s = \frac{K_{ma}}{\varepsilon} - 1 \tag{3.13}$$

Note that K_{ma} is typically measured in the experiment, such as in a headspace test and analysis (Little et al. 1994), while K_s is typically used in a numerical simulation models for vapor transport in a porous media such as the CHAMPS-BES (Grunewald et al. 2007). The local in-material diffusion flux can be described as

$$j = -D_p \frac{\partial C_{pa}}{\partial x} \tag{3.14}$$

at steady state,

$$j = -D_p \frac{\partial C_{pa}}{\partial x} = D_p \frac{C_{pa}\big|_{x=0} - C_{pa}\big|_{x=L}}{L} \tag{3.15}$$

where D_p is the pore diffusion coefficient in m^2/s. If the diffusion inside the pores is governed by molecular diffusion only (if $d/\lambda \geq 10$; d is mean pore diameter; λ is mean free path of the VOC molecules), D_p can be calculated by

$$D_p = D_{air} \frac{\varepsilon}{\tau} = \frac{D_{air}}{\frac{\tau}{\varepsilon}} = \frac{D_{air}}{\mu} \tag{3.16}$$

where D_{air} is the diffusivity in free air in m^2/s; μ is a factor that accounts for both porosity and tortuosity of the material. In CHAMPS (Grunewald et al. 2007, Li 2007, Xu et al. 2007&2008), it is termed the diffusion resistance factor and is represented by μ_{voc} and μ_{vapor} for VOC and water vapor respectively. Tortuosity represents the geometric constraints which result in a longer diffusion path compared to the free path in the air. In Blondeau et al. (2003), the porosity ε and tortuosity τ were measured individually and used to calculate the pore diffusion coefficient. Since $C_m = C_{pa} + C_{pm} = C_{pa}(1 + K_s)$, we have,

$$C_{pa} = \frac{C_m}{1 + K_s} \tag{3.17}$$

plug Eq. (3.17) in Eq. (3.15), we have,

$$j = D_p \frac{C_{pa}\big|_{x=0} - C_{pa}\big|_{x=L}}{L} = D_p \frac{1}{1 + K_s} \frac{C_m\big|_{x=0} - C_m\big|_{x=L}}{L} \tag{3.18}$$

comparing Eq. (3.18) and (3.4), the relationship between D and D_p is obtained:

$$D = \frac{D_p}{1 + K_s} \tag{3.19}$$

That is, the "apparent" diffusion coefficient, D, includes the effect of sorption on the net transport of VOC in the porous material as well as diffusion through pore air. From Eq. (3.6) and (3.12), we have $D = \frac{D_e}{\varepsilon(1+K_s)}$, insert this in Eq. (3.19), thus, the relationship between D_p and D_e can be described as

$$D_e = \varepsilon D_p \tag{3.20}$$

3.2.2 Similarity coefficient

In the field of Building Physics, μ_{vapor} factor (water vapor diffusion resistance factor) is attributed to the combined effect of both porosity and tortuosity. i.e., $\mu_{vapor} = tortuosity / porosity$, and

$$D_e^{vapor} = \frac{D_{air}^{vapor}}{\mu_{vapor}} \tag{3.21a}$$

Similarly we introduced a μ_{voc} factor for VOC diffusion in a porous material, which is calculated as:

$$\mu_{voc} = \frac{D_{air}}{D_e} \tag{3.21b}$$

D_{air} is the VOC diffusion coefficient in the free air in m^2/s. However, the difference in physical properties (molar mass, polarity, and boiling point, et al.) between VOCs and water vapor, and the difference in concentration level inside the material would lead to different magnitude between water vapor and VOC diffusion coefficient in the pore air. For example, when the Knudsen diffusion or surface diffusion becomes important in porous media, the diffusion resistance will no longer only depend on the porosity and tortuosity. Therefore, it seems justifiable to relate the water vapor diffusion resistance factor and the VOC diffusion resistance factor by a similarity coefficient. We define the ratio between μ_{voc} and μ_{vapor} as a similarity coefficient: That is,

$$\kappa_{voc} = \frac{\mu_{voc}}{\mu_{vapor}} = \frac{D_{air}}{D_e \mu_{vapor}} \tag{3.21c}$$

where κ_{voc} is a dimensionless similarity coefficient, which is likely to be dependent on both VOCs and the material properties; μ_{vapor} is a dimensionless water vapor diffusion resistance factor, which can be obtained either by the dry cup or wet cup test method in hygrothermal experiments or by the dual chamber test method. If the similarity coefficients can be determined for VOCs and a reference material, the data on μ_{vapor} from previous hygrothermal research can be applied to estimate the diffusion coefficients for VOCs in the materials, and thus reduce the amount of testing needed for establishing a database of VOC diffusion coefficients in building materials and furnishings. To be useful, the ability to extrapolate from a reference VOC or material to other VOCs or materials is needed.

3.3 Experimental

3.3.1 Setup

In this study, two stainless steel chambers (0.35m x 0.35m x 0.15m each) were partitioned by a test specimen (Fig. 3.3). Each chamber was supplied with inflows under controlled temperature and relative humidity. Both chambers were supplied with the same airflow rate and the exhaust flow resistance was adjusted to achieve near zero pressure difference (<2 Pa) across the specimen so that air convection through the specimen was negligible for the material tested. The dual chamber system was placed in a laboratory with constant temperature 23 °C. The relative humidity of the inflow for both chambers was maintained at 50% by bubbling the liquid water via a PID (proportional-integral- derivative) control. The temperature and relative humidity of the inflow and outflow for both chambers were recorded continuously by a computer-based data acquisition system. Chamber A had a constant VOC injection in the inflow while Chamber B had no VOC injection. VOC was supplied by a Dynacalibrator containing a VOC permeation tube maintained at a specific temperature. The pressure drop between the two chambers was negligible

as verified by pressure measurements, since the same amount of air flow rate was supplied to both chambers and the same piping configuration was used for both chambers. An axial fan was mounted inside each chamber to ensure a good mixing condition. The VOC concentration in the inflow of chamber A was set at constant, and the concentration in chambers A and B were continuously monitored until they reached a steady state. The expected VOC concentration change within chambers A and B in the diffusion period were shown in Fig. 3.4(a). Concentrations in the outlets of chamber A and B were monitored as C_{Aout} and C_{Bout}. Under well-mixed condition, $C_A=C_{Aout}$ and $C_B=C_{Bout}$. At steady state, C_{Aout} and C_{Bout} were constant. The measured concentrations were considered to reach steady state when the moving average of C_{Aout} and C_{Bout} did not change more than 1% between two adjacent data points. Constant VOC concentration into chamber A (C_{Ain}) was provided by the permeation tube within a dynacalibrator. VOC concentrations (formaldehyde, acetaldehyde, toluene, benzaldehyde, butanol) of the outflows of both chambers were measured by proton transfer reaction mass spectrometry (PTRMS), which was pre-calibrated by the permeation tube under each RH condition because PTRMS measurement might be influenced by RH depending on the property of the specific VOC. Hexanal and decane concentrations were measured by gas chromatography mass spectrometry (GCMS) because they could not be measured by PTRMS. The sampling flow rate by PTRMS was $85.6 \times 10^{-6} m^3/min$. As indicated by the dotted line in Fig. 3.3, the PTRMS sampling line switched among C_{Aout}, C_{Bout} and C_{Ain} during the test.

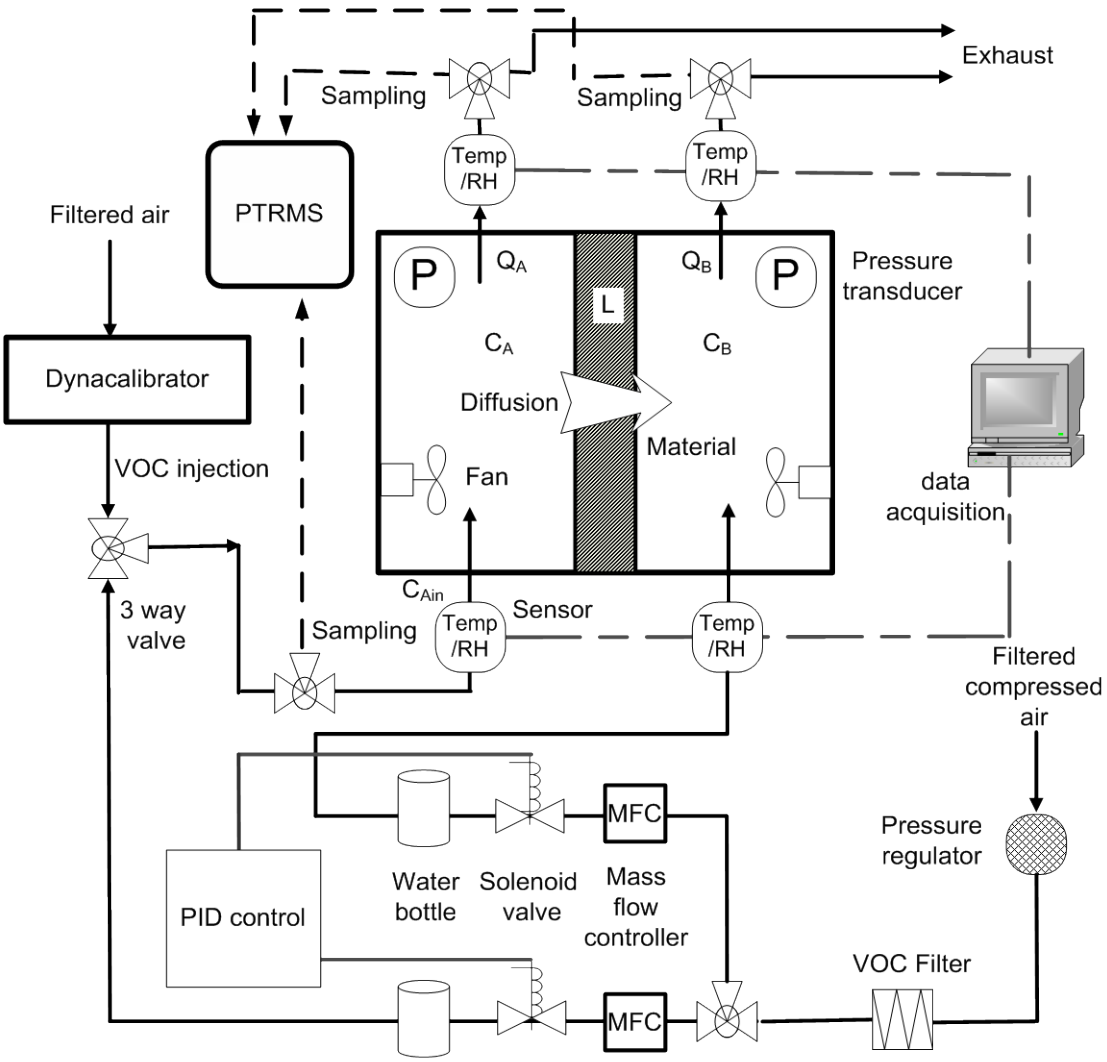

(a) Schematic

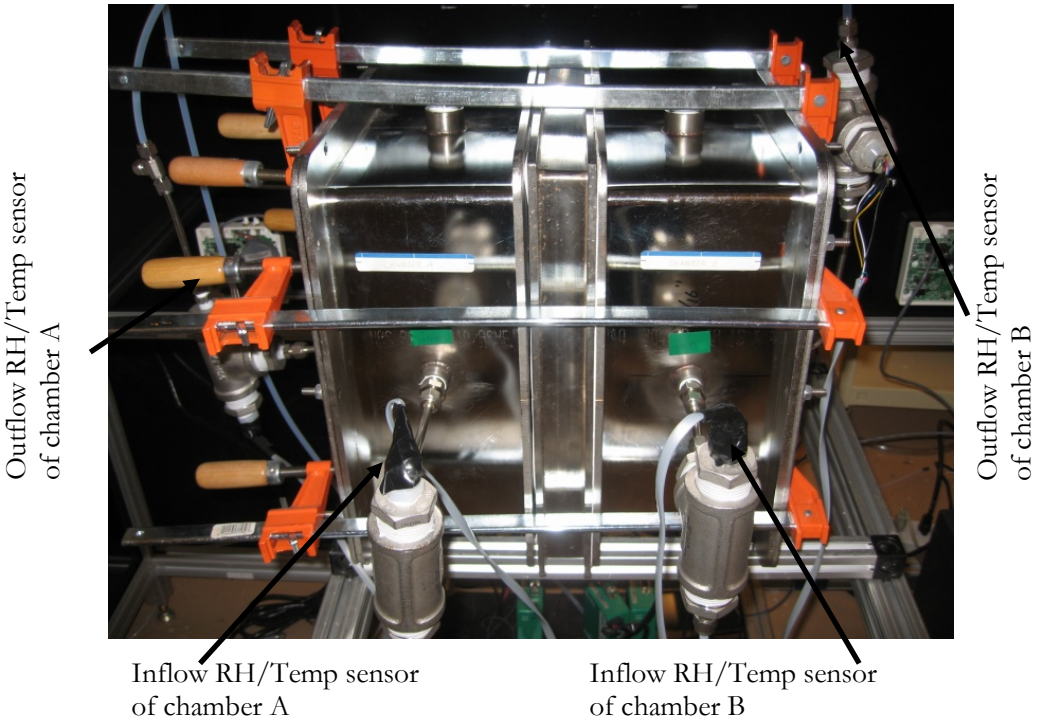

(b)Photograph

Figure 3.3 Dual chamber system

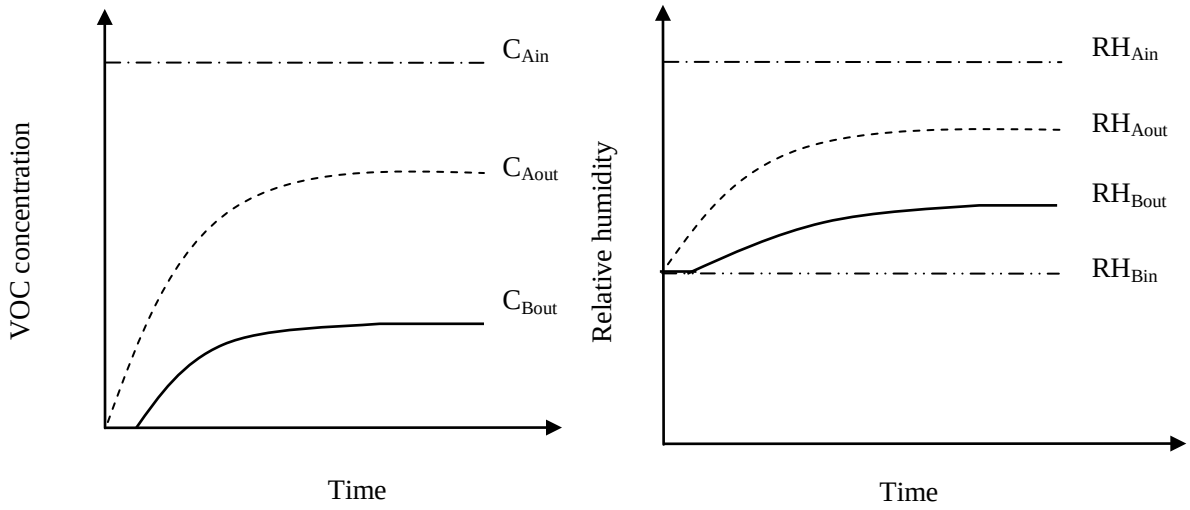

(a) VOC test

(b) Water vapor test

Figure 3.4 Expected VOC concentrations and RHs

For VOCs, the chambers were flushed in the beginning, which meant that initial VOC concentrations for both chambers were zero. In contrast to the VOCs test, for the water vapor

test both chambers were initially kept at a specific relative humidity. When test began, a higher level of relative humidity was supplied into chamber A while the same relative humidity was maintained for the supply flow of chamber B. The change in relative humidity was recorded continuously until a steady state was reached. RH_A and RH_B were the relative humidity of chambers A and B. the relative humidity in the outlets of chambers A and B were monitored as RH_{Aout} and RH_{Bout}. Under well-mixed condition, RH_A=RH_{Aout} and RH_B=RH_{Bout}. At steady state, RH_{Aout} and RH_{Bout} were constant. The measured relative humidity was considered to reach a steady state when the moving average of RH_{Aout} and RH_{Bout} did not change more than 1% between two adjacent data points. The expected RHs in chambers are shown in Fig. 3.4(b).

3.3.2 Test procedures

For each VOC test, the following steps were followed:

a) To make sure the sealing of the material is tight enough, a plastic board is installed in the specimen holder. Pressure test is conducted to check the tightness of the chambers. After the check, remove the plastic board from the specimen holder.

b) Install the specimen in the specimen holder and assemble it air-tight with the dual chambers. The leakage of the two chambers should be less than 3% of the total supply air flow rate as determined by the difference between the inlet and outlet flow rates of the two chambers.

c) Precondition the dual chamber facility by supplying the desired flow rates under the specified RH into both chambers.

d) Measure the pressure drop between two chambers and verify that it is negligible (less than 2 Pa).

e) When the airflow rate, temperature and relative humidity are stable, take VOC background sample for chamber A and B, respectively.

f) Start the test by injecting constant VOC concentration into chamber A. In the meantime, record the VOC concentration change continuously.

g) Stop the test once the VOC concentrations in two chambers reach steady state---i.e., the difference between two adjacent sampling time points is less than 1%.

h) Flush the specimen until the VOC concentration approaches the background concentration in step d) and then go back to step b).

For each water vapor test, the following steps were followed:

a) Install the specimen in the specimen holder and assemble it air-tight with the dual chambers. The leakage of the two chambers should be less than 3% of the total supply air flow rate as determined by the difference between the inlet and outlet flow rates of the two chambers.

b) Precondition the dual chamber facility by supplying the desired flow rates under the specified RH into both chambers.

c) Measure the pressure drop between two chambers and verify that it is negligible (less than 2 Pa).

d) When the airflow rate, temperature and relative humidity are stable, take relative humidity background samples for chamber A and B, respectively.

e) Start the test by injecting a higher relative humidity into chamber A. In the meantime, record the relative humidity change continuously.

f) Stop the test once the relative humidity in the two chambers reaches a steady state---i.e., the difference between two adjacent sampling time points is less than 1%.

3.3.3 Experimental design

To validate the proposed similarity hypothesis, both water vapor and VOCs diffusion tests were conducted and compared. Two different levels of relative humidity testing were conducted. In the first water vapor diffusion test, the initial RHs in chamber A and B were both 25%. When

the test began, the RH of inflow for chamber A was increased to 50%RH while maintaining a constant 25%RH inflow for chamber B, and then the changes of RHs in chamber A and B were monitored over time. In the second water vapor diffusion test, the initial RHs in chamber A and B were both 50%. When the test began, the RH of inflow for chamber A was increased to 80%RH while maintaining a constant 50%RH inflow for chamber B. Table 3.2 summarizes the experiment design and the conditions for water vapor. Repeat tests were also done to evaluate the accuracy of the dual chamber method in measuring water vapor diffusion.

Table 3.2 Experimental design and the conditions for water vapor

No.	Compounds	Initial RH_A (%)	Initial RH_B (%)	RH_{Ain} (%)	RH_{Bin} (%)	$Q_A=Q_B$ (m^3/h)	Test purpose
1	WV	25	25	50	25	0.0658	Obtain μ_{vapor}
2	WV	50	50	80	50		
3	WV^R	25	25	50	25		Assess repeatability
4	WV^R	50	50	80	50		

Seven common VOCs in indoor air were selected as target VOCs: formaldehyde, toluene, acetaldehyde, hexanal, benzaldehyde, butanol and decane. Repeat tests for formaldehyde, toluene and acetaldehyde were also conducted to evaluate the accuracy of the dual chamber method in measuring the VOCs' diffusion. The physicochemical properties of the selected VOCs and water vapor are presented in Table 3.3. Among all the compounds, formaldehyde has the largest vapor pressure.

Table 3.3 Physicochemical properties of the selected VOCs and water vapor

Compound	Chemical Class	CAS #	Formula	MW (g/mol)	Density(23 °C,kg/m³)	Vapor Pressure (23°C,mm Hg)	Polarity (debye)	Henry's law constant((mol/L)/atm),23°C
WV			H_2O	18	1.00			
FOR	Aldehyde	50-00-0	CH_2O	30	1.09×10^{-3}	3643.8	2.3	2743
ACE	Aldehyde	75-07-0	C_2H_4O	44	0.79×10^{-3}	837.5	2.5	12
HEX	Aldehyde	66-25-1	$C_6H_{12}O$	100	0.83×10^{-3}	10.00	na[a]	4.2
BZD	Aldehyde	100-52-7	C_7H_6O	106	0.98×10^{-3}	1.06	2.8	35
BUT	Alcohol	71-36-3	C_4H_9OH	74	0.81×10^{-3}	6.5	1.8	110
TOL	Aromatic	108-88-3	C_7H_8	92	0.86×10^{-3}	25.8	0.4	0.14
DEC	Alkane	124-18-5	$C_{10}H_{22}$	142	0.73×10^{-3}	1.18	0.0	$1.4x10^{-4}$ [b]

[a] Not available in the literature

[b] The value provided here is at 25°C. The conversion from 25°C to 23°C is not possible because of the lack of the necessary data

In the test of VOCs diffusion through a calcium silicate, the inlet concentration of chamber A was set as 372μg/m^3 except haxanal (128μg/m^3). The flow rates of both chambers were 6.58×10^{-2} m^3/h except hexanal (3.52×10^{-2} m^3/h). Before the test, calcium silicate was dried in the oven under 30ºC for 3 days and then preconditioned under a relative humidity of 50% to ensure a constant relative humidity for the calcium silicate. During the test, the relative humidity of both inflows of the chamber was maintained unchanged at 50% as well. The same procedure was applied for all the tests. All eleven test conditions are summarized in Table 3.4.

Table 3.4 Experimental design and the conditions for VOCs

No.	Compounds	RH	C_{Ain} (μg/m^3)	$Q_A=Q_B$ (m^3/h)	Test purpose
1	FOR	50	372	0.0658	Obtain effective diffusion coefficient, partition coefficient
2	TOL	50	383		
3	FOR^R	50	372	0.0658	Evaluate the accuracy and reliability of dynamic dual chamber method in measuring effective diffusion coefficient and partition coefficient for VOCs
4	TOL^R		383		
5	ACE^{R1}		374		
6	ACE^{R2}		374		
7	ACE	50	374	0.0658	Obtain effective diffusion coefficient, partition coefficient
8	HEX		128	0.0352	
9	BZD		401	0.0658	
10	BUT		383	0.0658	
11	DEC		372	0.0658	

Abbreviation: FOR-- formaldehyde; TOL-- toluene; ACE-- acetaldehyde; HEX-- hexanal; BZD-- benzaldehyde; BUT-- butanol; DEC-- decane;

R-- repeat test; R1-- repeat test 1; R2-- repeat test 2.

3.3.4 Test Specimen

Calcium silicate (Fig. 3.5) was selected as a reference material in this study due to its well-characterized moisture diffusion properties and wide usage as a building insulation material. Prior to the test, the calcium silicate was cut into a 50.8cm ×50.8cm ×1.0cm block, and sealed on each side by VOC free tape to prevent VOC diffusion through the edges. The specimen was then placed in a specially prepared steel specimen holder between two chambers, and clamped tightly together.

Figure 3.5 Picture of calcium silicate

The pore volume distribution of calcium silicate measured by mercury intrusion porosimetry is provided in Fig.3.5 (a). Its pore surface area is 1722 m^2/kg and the measured porosity is $\varepsilon=0.1697 m^3/ (m^3$ REV). Ten times the Knudsen number (i.e.$10\lambda/d$) is used to divide the pore size ranges in which molecular diffusion or Knudsen diffusion is significant in porous media (Do 1998, Ruthven 1984, Xiong et al. 2008). At 760 Torr, the calculated mean free paths by Eq.(3.22) for formaldehyde and toluene are 35.3 and 14.3 nm, respectively. Thus the corresponding pore diameters for formaldehyde and toluene need to be less than 353 nm (0.353 μm) and 143nm(0.143 μm) respectively for the Knudsen mechanism to be significant.

$$\lambda = \frac{3.2\mu'}{P}\left(\frac{RT}{2\pi MW}\right)^{0.5} \tag{3.22}$$

where λ is the mean free path of the molecule (m); R is universal gas constant in J/ (mol. K); T is temperature in Kelvin; P is the pressure in Pa; MW is the molecular weight of the diffusing molecule (kg/mol); and μ' is the dynamic viscosity of the free air (P_a.s). From the analysis in Fig. 3.6(a), we can see that the pore diameter in calcium silicate ranges from 0.326 μm to 0.589 μm; hence molecular diffusion dominates in the mechanism for formaldehyde and toluene in calcium silicate, while a meaningful amount of Knudsen diffusion can be expected for formaldehyde.

The moisture sorption isotherm of the calcium silicate was obtained previously, and is shown in Fig 3.6(b). It is noted that for the range of relative humidity conditions (25% to 80% RH)

investigated, the moisture content has a weak dependence on the relative humidity. Therefore, it may be assumed that the variation in open pore porosity in the RH range is small and its impact on gas phase diffusion may be negligible.

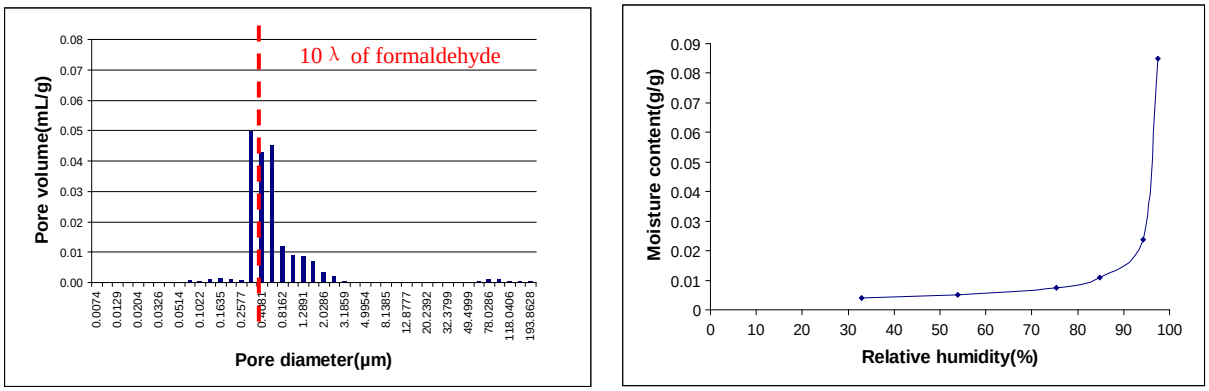

(a) Pore volume distribution (b) Moisture sorption isotherm

Figure 3.6 Characterization of the test specimens---calcium silicate (density: ρ = 843.38 kg/m^3. porosity: ε =16.97%. The diffusion resistance factor of water vapor: μ_{vapor}= 8.75. Thickness: L=0.01m. Area: A=0.093m^2)

3.3.5 The calculation of the effective diffusion coefficient and the partition coefficient

A. Diffusion coefficients

The effective diffusion coefficient, apparent diffusion coefficient and pore diffusion coefficient of VOCs are determined by Eq. (3.2), (3.6) and (3.20), respectively.

B. Partition Coefficient: The VOC mass adsorbed by the material at the steady state is:

$$M = \int_0^T [Q_A(C_{Ain} - C_{Aout}) - Q_B C_{Bout}]dt \tag{3.23}$$

where M is the total VOC mass in the material in kg; T is the end time of the diffusion test in hours. Using $K_{ma} = C_m\big|_{x=0} / C_A = C_m\big|_{x=L} / C_B$ and Eq. (3.23), the partition coefficient can be obtained by

$$K_{ma} = \frac{2M / V_{mat}}{C_{Aout} + C_{Bout}} = \frac{2\int_0^T [Q_A(C_{Ain} - C_{Aout}) - Q_B C_{Bout}]dt}{(C_{Aout} + C_{Bout})V_{mat}} \tag{3.24}$$

Where V_{mat} is the volume of calcium silicate in m^3.

The concept of the partition coefficient can also be applied to water vapor, and the only difference from VOC diffusion in the calculation procedure is the consideration of the initial moisture content before the test, which can be obtained by the sorption isotherm of water vapor (ASTM 2001).

$$M = \int_0^T [Q_A(\rho_{Ain} + \rho_{Bin} - \rho_{Aout} - \rho_{Bout})]dt \tag{3.25}$$

where ϱ_{Ain}, ϱ_{Aout}, ϱ_{Bin}, ϱ_{Bout} are water vapor density in the inflow and outflow of chamber A and B in kg/m^3. The partition coefficient of water vapor can be obtained by:

$$K_{ma} = \frac{2M/V_{mat}}{RH_{Aout} + RH_{Bout}} = \frac{2\int_0^T [Q_A(\rho_{Ain} + \rho_{Bin} - \rho_{Aout} - \rho_{Bout})]dt}{(RH_{Aout} + RH_{Bout})V_{mat}} \tag{3.26}$$

3.3.6 Sampling intervals

For VOCs testing, each diffusion test was estimated to take 5 days or longer to complete depending on the materials. An air sample was taken at least every 8 hours for C_{Aout} and C_{Bout}, which resulted in a total of 2x15=30 data points for a 5 day test. For each of these data points, the PTRMS was used to take an air sample every 10 seconds for 5 minutes, and the average value was used to determine the concentration. In addition, the background concentration of chamber A and B was taken before the injection of VOCs, and the constant injection rate was verified by measuring C_{Ain} daily. For the water vapor test, the relative humidity of both chambers was automatically recorded every minute.

3.3.7 Data analysis

In Eq. (3.23), M is the integration of the continuous concentration profile of C_A and C_B. Since C_A and C_B were obtained as discrete data points, a curve fitting was first applied to the measured C_A and C_B data by using the combination of the CHAMPS model (Zhang 2005, Grunewald et al. 2007 and Li 2007) and empirical equations. The effective diffusion coefficient was obtained

directly from the experimental data by Eq. (3.2) leaving the partition coefficient as the only unknown to be determined by the Least-Square curve fitting in CHAMPS. However, in one test result, there was a test duration in which the CHAMPS model did not fit the experimental data very well, and an empirical model was used instead to match the experimental data points. Fig. 3.7 illustrates the simulated concentration against measured concentration for toluene by CHAMPS. For the test duration from zero to one hour for C_{Bout}, the simulated result of CHAMPS was lower than the experimental data points, so the empirical equation was used to match the data points. Later, a time interval of 1 minute was used to do the numerical integration for the calculation of total mass in the material. The calculation equation was as follows:

$$M = \sum [Q_A(C_{Ain} - C_A) - Q_B C_B]\Delta t \tag{3.27}$$

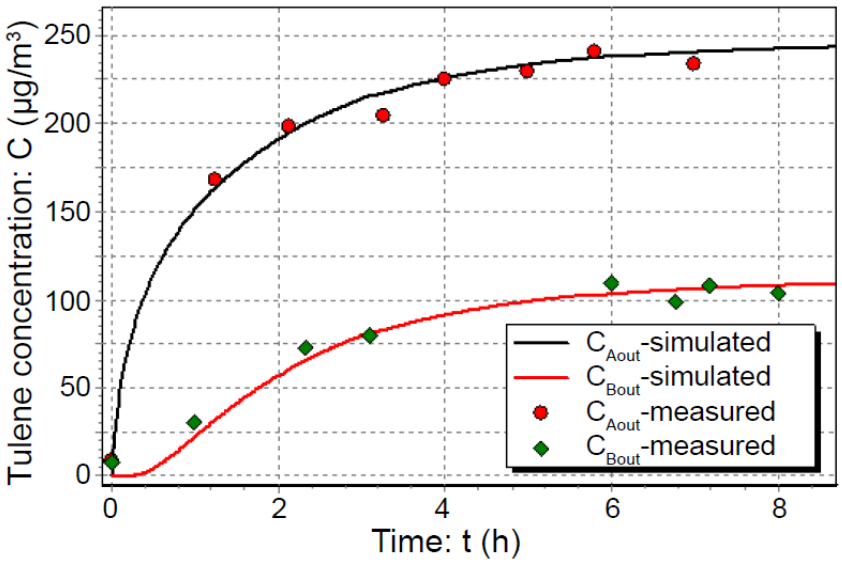

Figure 3.7 Example of measured and simulated concentration for toluene

3.3.8 Calibration of PTRMS and GCMS

PTRMS was used in the measurement of formaldehyde, toluene, acetaldehyde, benzaldehyde and butanol. The VOCs concentrations measured by PTRMS were calibrated against the permeation tube from VICI Corporation. The emission rates of the permeation tube for formaldehyde, toluene, acetaldehyde, benzaldehyde and butanol were 408ng/min, 420ng/min, 410ng/min, 440ng/min and 414ng/min, respectively. PTRMS calibration was completed by

adjusting the dilution flow from a special RH controlled system other than the dilution flow from Dynacalibrator. The operation temperature was maintained at 23 ºC for all the calibration experiments. Figure 3.8 (a~e) displays the calibration results of PTRMS for these compounds at 50%RH. The linearity coefficient was around 0.99 for all the cases, which indicated a good linearity of PTRMS measurement for these five compounds.

GC/MS was used in the measurement of decane and hexanal. The standard solution of different levels of concentrations was prepared for each test. In the calibration result of GC/MS (Fig. 3.9), the abscissa is the VOC mass adsorbed by the Tenax-TA sorbent tube, and the ordinate is the area integrated from the generated chromatograph peak for the compound.

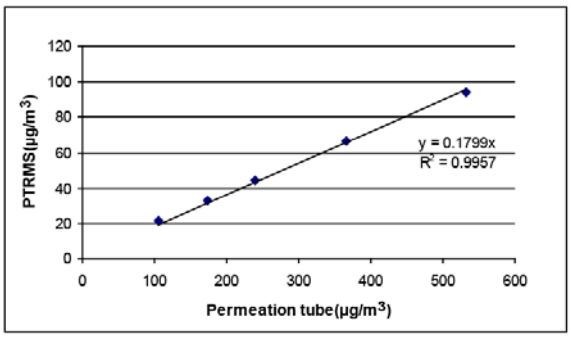

(a) formaldehyde

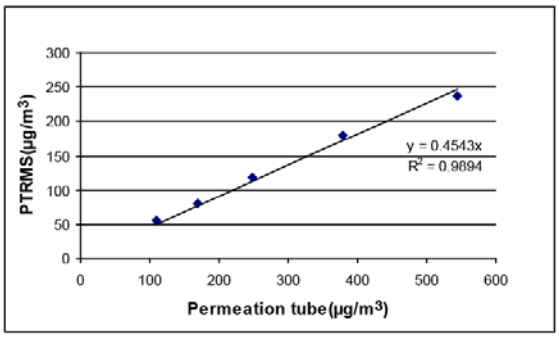

(b) toluene

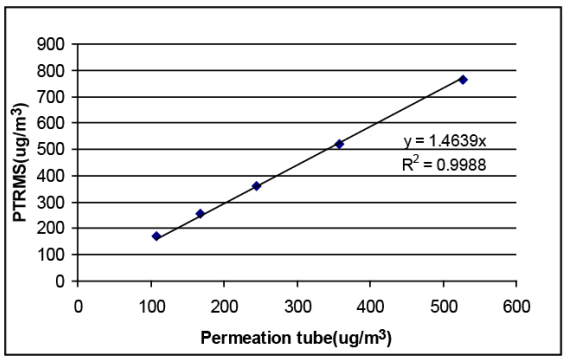

(c) acetaldehyde

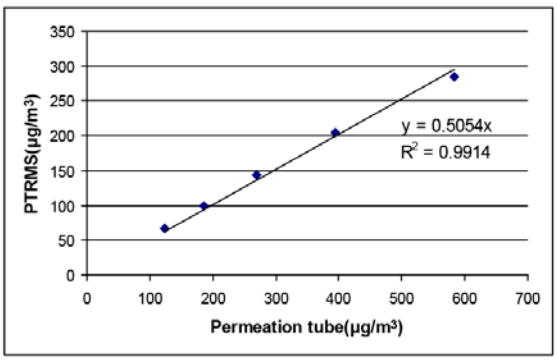

(d) benzaldehyde

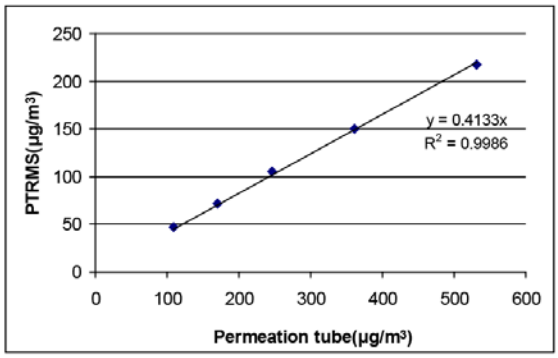

(e) butanol

Figure 3.8 Calibration results of PTRMS

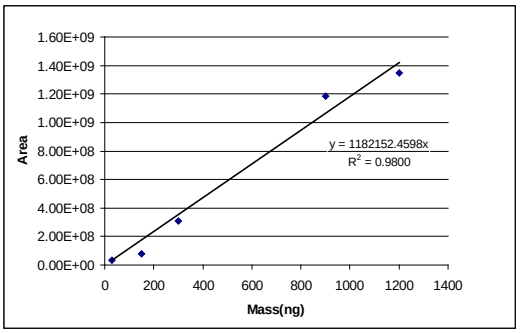

(a) decane

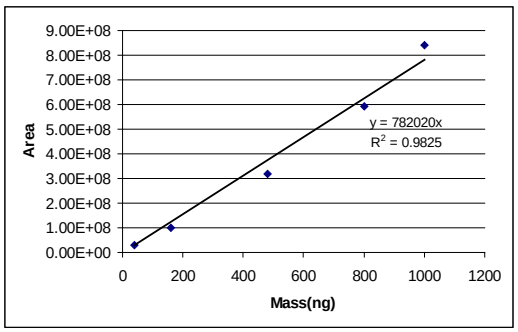

(b) hexanal

Figure 3.9 Calibration results of GC/MS

3.4 Results and discussion for calcium silicate

3.4.1 Water vapor

It took 10 hours for water vapor to reach a steady state. The experimental results for water vapor are given in Figure 3.10. The calculated diffusion coefficients and partition coefficients are presented in Table 3.5. The results of repeated tests were also presented and compared with the first tests. The data were recorded every minute, and fewer data points were drawn in the figures in order to have a better readability for the overlapped curves. The good repeatability showed that the dual chamber method was able to measure water vapor diffusion very well.

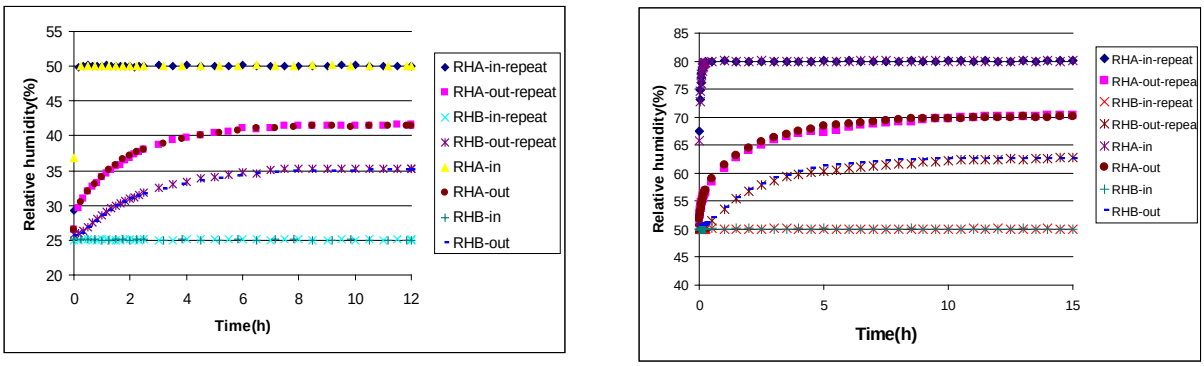

Figure 3.10 Experimental results of water vapor in calcium silicate

Table 3.5 Diffusion & partition coefficients of water vapor in calcium silicate

No.		RH_{Ain} %	RH_{Bin} %	RH_{Aout} %	RH_{Bout} %	D_{air} m^2/s	D_e m^2/s	D m^2/s	D_p m^2/s	K_{ma}	μ_{vapor}
1	WV	50.1	25.1	41.7	35.5	2.66×10^{-5}	3.04×10^{-6}	7.58×10^{-9}	1.79×10^{-5}	401	8.75
2	WV	80.0	50.0	70.0	62.8	2.66×10^{-5}	3.06×10^{-6}	9.05×10^{-9}	1.80×10^{-5}	338	8.71
3	WV^R	50.1	25.1	41.4	35.1	2.66×10^{-5}	2.89×10^{-6}	7.15×10^{-9}	1.70×10^{-5}	404	9.19
4	WV^R	80.0	50.0	70.0	62.7	2.66×10^{-5}	2.97×10^{-6}	8.51×10^{-9}	1.75×10^{-5}	349	8.97

3.4.2 VOCs

The experimental results of formaldehyde, toluene and acetaldehyde are summarized in Fig. 3.11 and Table 3.6. Repeat tests of formaldehyde, toluene and acetaldehyde under 50%RH were conducted, and the results are also given in Fig. 3.11 (a, b and c). The repeated test of each VOC agreed well with the first test. The time for formaldehyde, toluene and acetaldehyde to reach

equilibrium was 120, 8, and 8 hours, respectively. It took the longest time for formaldehyde to reach steady state because of the large sink effect of formaldehyde in calcium silicate. The results presented in Table 3.6 include the VOCs concentration at equilibrium, effective diffusion coefficients, apparent diffusion coefficient, pore diffusion coefficient, partition coefficient, and μ_{voc} for VOCs (μ_{voc} is the diffusion resistance factor for VOC in the material, which is calculated as D_{air}/D_e) and similarity coefficient k_{voc}. The similarity coefficient is the ratio of the diffusion resistance factor of VOC (μ_{voc}) to that of water vapor, which is calculated as μ_{voc}/μ_{vapor}. The diffusion coefficient in air is obtained from the literature (Nelson 1982). μ_{voc} and k_{voc} in Table 3.6 are also needed input parameters for the VOC database of CHAMPS-BES (Grunewald et al. 2007), a coupled heat, air, moisture and pollutant simulation program for porous media and building envelope systems. For the effective diffusion coefficients of all measured VOCs at 50% RH, the descending order is BZD>FOR>BUT>ACE>TOL>HEX>DEC. For the partition coefficient of tested VOCs at 50°C, the descending order is BUT>BZD>HEX>FOR>ACE>TOL.

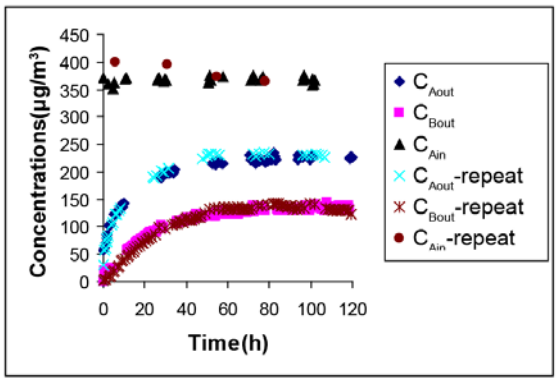

(a) Formaldehyde

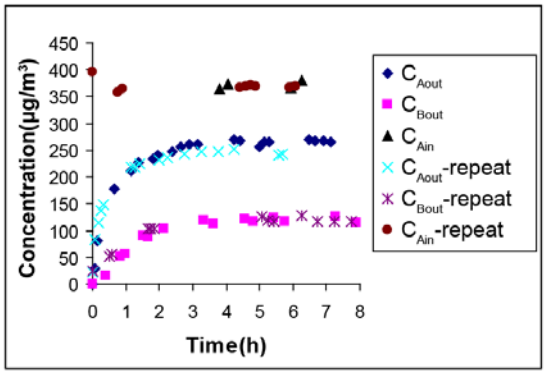

(b) Toluene

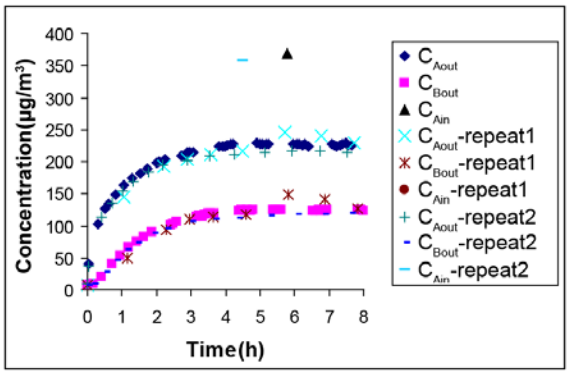

(c) Acetaldehyde

Figure 3.11 Repeat test of formaldehyde, toluene and acetaldehyde in calcium silicate

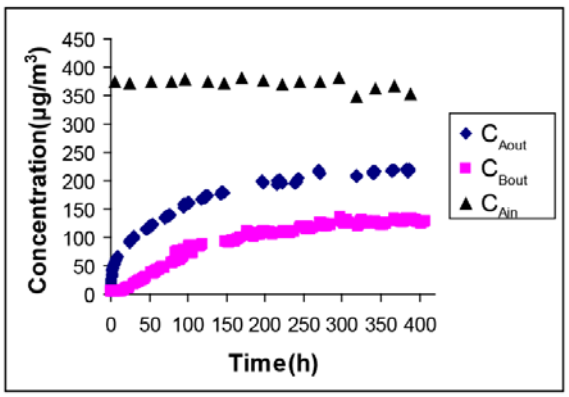

(a) Butanol

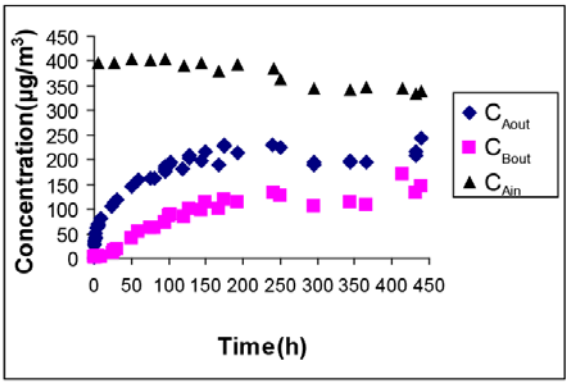

(b) Benzaldehyde

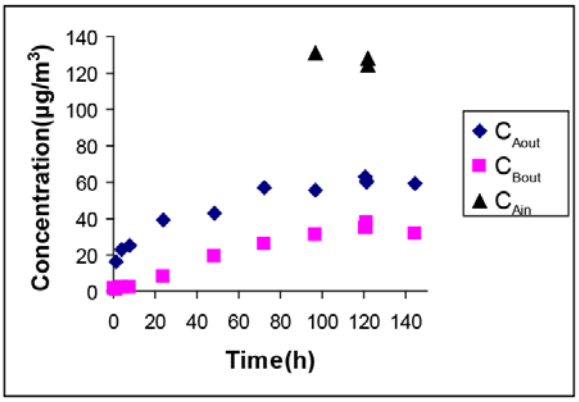

(c) Hexanal

Figure 3.12 Test of butanol, benzaldehyde and hexanal

Table 3.6 Diffusion & partition coefficients of VOCs in calcium silicate

No.	Compound	RH %	C_{Ain} μg/m³	C_{Ass} μg/m³	C_{Bss} μg/m³	D_{air}(23°C) m²/s	D_e m²/s	D m²/s	D_p m²/s	K_{ma}	μ_{voc}	k_{voc}
1	FOR	50	366.4	226.1	136.1	1.49×10^{-5}	3.28×10^{-6}	1.26×10^{-9}	1.93×10^{-5}	2597	4.54	0.52
2	TOL	50	372.7	267.4	118.2	8.40×10^{-6}	1.72×10^{-6}	1.29×10^{-8}	1.01×10^{-5}	133	4.88	0.56
3	ACE	50	367.9	227.6	125.6	1.12×10^{-5}	2.67×10^{-6}	1.21×10^{-8}	1.57×10^{-5}	221	4.19	0.48
4	HEX*	50	128.1	60.8	34.8	6.71×10^{-6}	1.55×10^{-6}	1.98×10^{-10}	9.13×10^{-6}	7809	4.32	0.49
5	BZD	50	390.9	227.5	149.6	6.99×10^{-6}	4.17×10^{-6}	2.59×10^{-10}	2.46×10^{-5}	16111	1.68	0.19
6	BUT	50	370.5	218.7	128.4	8.52×10^{-6}	3.09×10^{-6}	1.71×10^{-10}	1.82×10^{-5}	18100	2.76	0.32
7	DEC	50	356.8	218.5	76.7	5.25×10^{-6}	1.17×10^{-6}		6.89×10^{-6}	/	4.47	0.51
8	FOR^R	50	385.6	231.4	138.1	1.49×10^{-5}	3.21×10^{-6}	1.25×10^{-9}	1.89×10^{-5}	2568	4.64	0.53
9	TOL^R	50	379.6	253.6	124.7	8.40×10^{-6}	2.10×10^{-6}	1.71×10^{-8}	1.24×10^{-5}	123	4.00	0.46
10	ACE^{R1}	50	359.2	222.2	121.3	1.12×10^{-5}	2.61×10^{-6}	1.13×10^{-8}	1.54×10^{-5}	232	4.29	0.49
11	ACE^{R2}	50	357.5	217.9	119.6	1.12×10^{-5}	2.64×10^{-6}	9.33×10^{-9}	1.56×10^{-5}	283	4.24	0.48

- The standard deviation of the mean for measured concentrations is +/- 1.8%
- The volume of the specimen $V_{mat}=8.53\times10^{-4}$ m³
- * means the flowrate for this test is different from other tests

3.4.3 Sensitivity study of surface diffusion

It was found that most of the similarity coefficients of the tested VOCs are close to 0.5, except for benzladehyde and butanol, which have relatively larger partition coefficients than the rest of VOCs tested. A larger partition coefficient means more VOC molecules adsorbed onto

the internal surfaces of porous media. Surface diffusion may play a role under relatively high sorbed phase VOC concentrations. To quantify the relative importance of surface diffusion, an order of magnitude analysis of surface diffusion to the diffusion coefficient caused by molecular diffusion and Knudsen diffusion was conducted. According to Blondeau et al. (2003 and 2008), the importance of surface diffusion can be indicated by the ratio of $D_{sf}K_{ma}$ and D_{mk}, where D_{sf} is the coefficient of surface diffusion, which is in the order of 10^{-9} m^2/s; D_{mk} is the diffusion coefficient caused by both molecular diffusion and Knudsen diffusion. The pore volume distribution of the material can be obtained by mercury intrusion porosimetry. D_{mk} can be calculated by:

$$D_{mk} = \frac{D^0 \varepsilon \sigma_p}{\tau} \tag{3.28}$$

where ε is the porosity of the material, τ is the tortuosity of the material. σ_p is the constriction factor, which stands for the effect of varying cross-sectional areas within a pore. It is often omitted, either because it is close to unity or because these effects are included in the tortuosity factor. D^0 is the mean diffusion coefficient, which is calculated by:

$$D^0 = \frac{\sum_{i=1}^{m} D(r)\Delta V_i}{\sum_{i=1}^{m} \Delta V_i} \tag{3.29}$$

where ΔV_i is the volume of mercury penetrating the pores. i=1 refers to the smallest group present which contributes a detectible non-zero ΔV_i and i=m refers to the maximum size group present which contributes a detectible non-zero ΔV_i. D(r) describes the way the diffusion coefficient varies as a function of the pore radius r. In most cases, it may be defined as:

$$D(r) = \frac{D_{air}}{1 + (\lambda / 2r)} \tag{3.30}$$

where D_{air} is the VOC diffusion coefficient in air; λ is the mean free path of species; and r is the pore radius. Table 3.7 lists the comparison between the surface diffusion coefficient and diffusion

coefficient caused by molecular diffusion and Knudsen diffusion. Porosity and tortuosity are fixed properties for one specific material, so they are not involved in the calculation.

Table 3.7 Sensitivity study for surface diffusion in calcium silicate

Compound	D_{sf} m^2/s	K_{ma}	D^0	$\frac{D_{sf}K_{ma}}{D_{mk}} = \frac{D_{sf}K_{ma}}{D^0\frac{\varepsilon}{\tau}}$
Formaldehyde	10^{-9}	2597	1.39×10^{-5}	$0.19(\tau/\varepsilon)$
Toluene	10^{-9}	133	8.07×10^{-6}	$0.02(\tau/\varepsilon)$
Acetaldehyde	10^{-9}	141	1.06×10^{-5}	$0.01(\tau/\varepsilon)$
Hexanal	10^{-9}	7809	6.46×10^{-6}	$1.21(\tau/\varepsilon)$
Benzaldehyde	10^{-9}	16111	6.73×10^{-6}	$2.39(\tau/\varepsilon)$
Butanol	10^{-9}	18100	8.15×10^{-6}	$2.22(\tau/\varepsilon)$
Decane	10^{-9}		5.08×10^{-6}	

It is seen from the above table that the ratio of surface diffusion to molecular and Knudsen diffusion of benzaldehyde and butanol is one or two orders of magnitude larger than formaldehyde, toluene and acetaldehyde. The ratio ($D_{sf}K_{ma}/D_{mk}$) of hexanal is in the same order of magnitude, but not as large as that of benzaldehyde and butanol. It has a similarity coefficient of around 0.5 instead of a much lower value, which is possibly due to a significantly lower test concentration. It appears that similarity theory applies only to the cases where surface diffusion is not significant. It should be noted that the diffusion coefficient for surface diffusion of different VOCs is expected to vary; however, no relevant data have been found in the literature. Further study is needed to determine under what conditions the effect of surface diffusion becomes important.

3.4.4 Effect of the boundary layer mass transfer resistance

In order to verify the assumption of neglecting boundary layer resistance at the interface of chamber air and specimen, an order of magnitude analysis was conducted to compare the boundary layer mass transfer resistance and the mass diffusion resistance. At steady state, the total mass transfer resistance from chamber A to chamber B is the sum of the internal diffusion resistance plus the two boundary-layer mass transfer resistances:

$$\frac{1}{U} = \frac{1}{h_A} + \frac{L}{D_s} + \frac{1}{h_B} \tag{3.31}$$

where U is the overall mass transfer coefficient in m/s; h_A and h_B are the convective mass transfer coefficients in chambers A and B in m/s, respectively. L is the thickness of the material in m, and D_s is the diffusion coefficient of the material excluding boundary layer resistance in m^2/s.

Neglecting the mass transfer resistance would result in an overestimation of the internal diffusion resistance, and hence an underestimation of the diffusion coefficient. As established in (Haghighat et al. 2002), the error (e) due to neglecting the mass transfer resistance can be estimated by:

$$e = \frac{D_s - D_e}{D_s} \times 100\% \tag{3.32}$$

The air velocity over the test specimen surface was measured to be 1.64 m/s. Using the length of the specimen side as the length scale, the Reynolds number (Re) was calculated as 31874, which indicated that the flow was in a turbulent regime. The same convective mass transfer coefficient (h) was used in the boundary layers on two sides of the material, which means $h_A=h_B=h$. Assuming a fully developed turbulent flow over the specimen surface, Eq. (3.33) (Blondeau et al. 2008 and White 1991) was used to estimate the Sherwood number and then the convective mass transfer coefficient was obtained from Eq. (3.33) and (3.34):

$$Sh = 0.037 Sc^{\frac{1}{3}} \mathrm{Re}^{\frac{4}{5}} \tag{3.33}$$

$$Sh = \frac{hL}{D_{air}} \tag{3.34}$$

$$Sc = \frac{\nu}{D_{air}} \tag{3.35}$$

where Sh is the Sherwood number, Sc is the Schmidt number, h is the convective mass transfer coefficient in m/s, L is the characteristic length in m, D_{air} is diffusion coefficient of VOC in air in m^2/s, and ν is kinematic viscosity of air at 23°C, which equals $1.544x10^{-5}m^2/s$ (Cengel and Ghajar 2010). Using this estimated h value, the errors due to neglecting the mass transfer resistance were estimated by Eq. (3.32). As shown in Table 3.8, the resulting errors were within 6-8% except for benzaldehyde and butanol. These errors are similar to the uncertainty estimated for effective diffusion coefficient. Benzaldehyde and butanol had higher errors (18.3% and 11.9%, respectively). It should be noted that the above analysis should be considered as semi-quantitative because the air flow pattern inside the chamber due to the mixing fan were not characterized in detail, and the estimation of the mass transfer coefficient using Eq. (3.33) is a very rough approximation. Nevertheless, the analysis shows that the mass transfer resistance could possibly be important even under turbulent flow conditions for more accurate determination of the diffusion coefficients, especially when the diffusion coefficients are larger than 10^{-6} m^2/s. It was shown (Haghighat et al. 2002) that if laminar boundary layer flow was assumed, neglecting boundary layer mass transfer resistance could result in an underestimation error as high as 50% for typical indoor building materials and VOCs. Therefore, future measurements of the diffusion coefficient using the dual chamber approach should take into account the effects of mass transfer resistance for better accuracy.

Table 3.8 Effective diffusion coefficients using order of magnitude analysis for boundary layer resistance

No.	Compound	RH %	D_e (boundary layer resistance ignored) m^2/s	D (boundary layer resistance considered) m^2/s	Error(e) %
1	FOR	50	3.28×10^{-6}	3.60×10^{-6}	8.7
2	TOL	50	1.72×10^{-6}	1.84×10^{-6}	6.7
3	ACE	50	2.67×10^{-6}	2.92×10^{-6}	8.6
4	HEX	50	1.55×10^{-6}	1.67×10^{-6}	7.0
5	BZD	50	4.17×10^{-6}	5.10×10^{-6}	18.3
6	BUT	50	3.09×10^{-6}	3.50×10^{-6}	11.9
7	DEC	50	1.17×10^{-6}	1.25×10^{-6}	6.2
8	FOR^R	50	3.21×10^{-6}	3.51×10^{-6}	8.5
9	TOL^R	50	2.10×10^{-6}	2.29×10^{-6}	8.2
10	ACE^{R1}	50	2.61×10^{-6}	2.85×10^{-6}	8.4
11	ACE^{R2}	50	2.64×10^{-6}	2.89×10^{-6}	8.5

3.4.5 Comparison of the measured diffusivity of water vapor with results from the dry cup test

The Mew value of water vapor in the building material is usually quantified by the standard cup test, such as ASTM standard E96/E96M-05(ASTM 2005), which prescribes the procedure to measure water vapor transmission (i.e. mass transport rate per unit cup area per unit time) through materials. The dry cup test is the transport between environmental chamber air (maintained at 50%RH) and the dry cup condition created by desiccant. The relative humidity on each side of the specimen is recorded by the RH sensor placed adjacent to the surface. The weight gain/loss by diffusion in the specimen is measured continuously by electronic balance until an equilibrium state is reached. At the equilibrium state, the Mew value of water vapor can be acquired:

$$\mu = \frac{D_{air}}{R_v \cdot T \cdot \Delta x \cdot permeance} \tag{3.36}$$

where Δx = Thickness of the specimen (m)

D_{air} = 2.662×10^{-5} (m^2/s), Vapor diffusion resistance in free air

Rv = 462 (J/kg k) Gas constant for water vapor

T = 296.15 K (23ºC), Test temperature

Water vapour permeance is defined as (ASTM 2005):

$$Permeance = WVT / \Delta p = WVT / S(RH_1 - RH_2) \tag{3.37}$$

Δp = vapor pressure difference (Pa)

S = Saturation vapor pressure at the test temperature (Pa)

RH_1 =relative humidity at the vapor source expressed as a fraction

RH_2 =relative humidity at the vapor sink expressed as a fraction

WVT = rate of water vapor transmission ($g/s/m^2$)

The water vapor transmission rate is calculated from dry/wet cup test as:

$$WVT = \Delta m / (t \cdot A) \tag{3.38}$$

Δm = weight change (g)

t = time during which Δm occurred (s)

A = test area (cup mouth area, m^2)

The weight change is measurable by electronic scale at specified time intervals. In contrast, in a dual chamber test, the WVT calculation is based on the water vapor mass balance in chamber A (or chamber B), which is expressed by:

$$WVT = (\rho_{Ain} - \rho_{Aout}).Q_A / A \tag{3.39}$$

ϱ_{Aout} = density of water vapor in the outflow of chamber A (kg/m^3)

ϱ_{Ain} = density of water vapor in the inflow of chamber A (kg/m^3)

Table 3.9 shows the Mew values in different methods with the corresponding relative humidity for the test conditions. In the dual chamber, it was obtained from relative humidity in two chambers at steady state. For the cup test, it was obtained from the relative humidity in the cup and in the environmental chamber.

Table 3.9 Comparison of Mew value at equilibrium state by different methods

Dry cup		Dual chamber	Range 1	Range 2
Outside cup	50.0% RH	Chamber A	41.7% RH	70.0% RH
Inside cup	15.0% RH	Chamber B	35.5% RH	62.8% RH
Calculated μ_{vapor}	6.99	Calculated μ_{vapor}	8.75	8.71

The Mew values for the dual chamber test method were about the same for the two RH ranges tested. They were slightly larger than the dry cup test, but the difference was considered acceptable considering the different test procedure and a slight difference in moisture range. The dry cup test extended to a lower RH which might have opened up additional small pores in the material, resulting a slightly smaller resistance factor (Pazera 2007). Further confirmation of this hypothesis is needed. The effective diffusion coefficient (also called diffusivity in the field of

Building Physics) of water vapor in calcium silicate in a dual chamber is $3.04\times10^{-6}m^2/s$ since diffusivity is equal to water vapor diffusivity in free air divided by the Mew value.

3.4.6 Comparison of VOCs diffusion with mercury intrusion porosimetry

The diffusion coefficients of the VOCs were also calculated based on the pore volume distribution obtained via the mercury intrusion porosimetry (MIP) method (Blondeau et al. 2003). Table 3.10 compares the derived diffusion coefficients by MIP method and measured effective diffusion coefficients in a dual chamber test.

Table 3.10 Comparison of diffusion coefficient with MIP method (m^2/s)

Method	Formaldehyde	Toluene
MIP	1.07×10^{-6}	0.638×10^{-6}
Dual Chamber(50%RH)	3.29×10^{-6}	1.72×10^{-6}

The values obtained by the two methods are in the same order of magnitude, but the diffusion coefficient by dual chamber is larger than that in the MIP method. Possible reasons may include but are not limited to uncertainties in both the MIP and dual chamber measurements. Further investigation is needed.

3.4.7 Error analysis

Based on the error propagation theory (Taylor 1982 and Kline 1985), if the uncertainty of each parameter $\partial C_{Ass}, \partial C_{Bss}, \partial L, \partial A, \partial Q$ is independent and random, the overall uncertainty of the effective diffusion coefficient ∂D_e can be calculated by the following equations:

$$\delta D_e = \sqrt{(\frac{\partial D_e}{\partial C_{Ass}}\delta C_{Ass})^2 + (\frac{\partial D_e}{\partial C_{Bss}}\delta C_{Bss})^2 + (\frac{\partial D_e}{\partial L}\delta L)^2 + (\frac{\partial D_e}{\partial A}\delta A)^2 + (\frac{\partial D_e}{\partial Q}\delta Q)^2} \tag{3.40}$$

Refer to the Eq. (3.2), the partial derivatives of the D_e with respect to C_{Ass}(VOC concentration at steady state in chamber A), C_{Bss}(VOC concentration at steady state in chamber B), L, A and Q are:

$$\frac{\partial D_e}{\partial C_{Ass}} = -\frac{D_e}{(C_{Ass} - C_{Bss})} \tag{3.41a}$$

$$\frac{\partial D_e}{\partial C_{Bss}} = \frac{D_e C_{Ass}}{C_{Bss}(C_{Ass} - C_{Bss})} \tag{3.41b}$$

$$\frac{\partial D_e}{\partial A} = (\frac{C_{Bss}}{C_{Ass} - C_{Bss}} LQ)(-1)\frac{1}{A^2} = -\frac{D_e}{A} \tag{3.41c}$$

$$\frac{\partial D_e}{\partial L} = (\frac{C_{Bss}}{C_{Ass} - C_{Bss}} \frac{Q}{A}) = \frac{D_e}{L} \tag{3.41d}$$

$$\frac{\partial D_e}{\partial Q} = (\frac{C_{Bss}}{C_{Ass} - C_{Bss}} \frac{L}{A}) = \frac{D_e}{Q} \tag{3.41e}$$

Inserting Eqs. (3.41a) through (3.41e) in the Eq. (3.40), and the fractional uncertainty of the effective diffusion coefficient is derived as in Eq. (3.42):

$$\frac{\delta D_e}{D_e} = \sqrt{(-\frac{\delta C_{Ass}}{C_{Ass} - C_{Bss}})^2 + (\frac{C_{Ass}\delta C_{Bss}}{C_{Bss}(C_{Ass} - C_{Bss})})^2 + (\frac{\delta L}{L})^2 + (-\frac{\delta A}{A})^2 + (\frac{\delta Q}{Q})^2} \tag{3.42}$$

Take one test for example, which is the test for formaldehyde diffusion in calcium silicate under 25%RH, at equilibrium, C_{Ass}=230.9μg/m^3, and C_{Bss}=135.5μg/m^3. Considering the individual fractional uncertainty in Table 3.11 of the five parameters, the overall uncertainty via Eq. (3.42) of the effective diffusion coefficient is 6.96%.

Table 3.11 Uncertainty analysis for various factors in effective diffusion coefficient

Uncertainty	Variations	Estimate
VOC concentration in chamber A	PTRMS measurement	$\delta C_{Ass}=\pm 1.8\% C_{Ass}$ *
VOC concentration in chamber B	PTRMS measurement	$\delta C_{Bss}=\pm 1.8\% C_{Bss}$ *
Material thickness	Thickness measurements	$\delta L=\pm 0.1\% L$
Material area	Area measurements	$\delta A=\pm 0.66\% A$
Flow rate	Measurement of flow rate	$\delta Q=\pm 3.0\% Q$

* Only random error is considered here because D_e and K_{ma} are not affected by the absolute values of concentration per Eq. (3.2) and (3.24). The PTRMS was calibrated by the permeation tube with an estimated accuracy of ±10% of measured values.

For the uncertainty of partition coefficient, the same analysis method was applied. The overall uncertainty of the partition coefficient is more complicated than the effective diffusion coefficient because it involves the integration of the VOC concentration as in Eq. (3.24). To make the integration possible for the purpose of uncertainty estimation, we used the following

empirical equation for a curve fitting to approximate the formaldehyde concentrations in chambers: $C_A = C_{Ass} - 10^{(a-bt)}$, and $C_B = C_{Bss} - 10^{(c-dt)}$, where a, b, c and d are constants. The partial derivatives of K_{ma} with respect to C_{Ass}, C_{Bss}, L, A, Q and T are given in Eq. (3.45a) to (3.45f), to be consistent. Take formaldehyde under 25%RH test, for example: at equilibrium, it is known that a=2.32, b=0.021, c=2.19, d=0.019.

$$C_A = 230.9 - 10^{(2.32-0.021t)} \tag{3.43a}$$

$$C_B = 135.5 - 10^{(2.19-0.019t)} \tag{3.43b}$$

plug the above two equations in the Eq. (3.24), the partition coefficient is calculated as:

$$K_{ma} = \frac{2Q\left\{C_{Ain}T - \left[230.9T + \frac{10\text{^}(2.32-0.021T)}{0.049} - 4233\right] - \left[135.5T + \frac{10\text{^}(2.19-0.019T)}{0.044} - 3467\right]\right\}}{(C_{Aout} + C_{Bout})V_{mat}} \tag{3.44}$$

refer to Eq. (3.44), the partial derivatives of K_{ma} with respect to C_A, C_B, L, A and Q are calculated step by step in Eq. (3.45a) to (3.45e).

$$\frac{\partial K_{ma}}{\partial Q} = -\frac{K_{ma}}{Q} \tag{3.45a}$$

$$\frac{\partial K_{ma}}{\partial C_{Ass}} = -\frac{K_{ma}}{C_{Ass} + C_{Bss}} \tag{3.45b}$$

$$\frac{\partial K_{ma}}{\partial C_{Bss}} = -\frac{K_{ma}}{C_{Ass} + C_{Bss}} \tag{3.45c}$$

$$\frac{\partial K_{ma}}{\partial V_{mat}} = -\frac{K_{ma}}{V_{mat}} \tag{3.45d}$$

$$\frac{\partial K_{ma}}{\partial T} = \frac{2Q\left[10\text{^}(2.32-0.021T) + 10\text{^}(2.19-0.019T)\right]}{(C_{Aout} + C_{Bout})V_{mat}} \tag{3.45e}$$

The overall uncertainty of ∂K_{ma} can be calculated by the following equations:

$$\delta K_{ma} = \sqrt{(\frac{\partial K_{ma}}{\partial Q}\delta Q)^2 + (\frac{\partial K_{ma}}{\partial C_{Ass}}\delta C_{Ass})^2 + (\frac{\partial K_{ma}}{\partial C_{Bss}}\delta C_{Bss})^2 + (\frac{\partial K_{ma}}{\partial V_{mat}}\delta V_{mat})^2 + (\frac{\partial K_{ma}}{\partial T}\delta T)^2}$$

(3.46)

Plug the Eqs. from (3.45a) to (3.45e) into Eq. (3.46), and the fractional uncertainty of the partition coefficient is derived as in Eq. (3.47). Considering the individual fractional uncertainty in Table 3.12 of the six parameters, the overall uncertainty of partition coefficient is 3.35%.

$$\frac{\delta K_{ma}}{K_{ma}} = \sqrt{(\frac{\delta Q}{Q})^2 + (\frac{\delta C_{Aout}}{C_{Aout}+C_{Bout}})^2 + (\frac{\partial C_{Bout}}{C_{Aout}+C_{Bout}})^2 + (\frac{\delta V_{mat}}{V_{mat}})^2 + \{\frac{2Q[10\text{^}(2.32-0.021T)+10\text{^}(2.19-0.019T)]}{(C_A+C_B)V_{mat}K_{ma}}\delta T\}^2}$$

(3.47)

Table 3.12 Uncertainty analysis for various factors in partition coefficient

Uncertainty	Variations	Estimate
Material volume	Volume measurements	$\delta V_{mat}=\pm 0.67\% V_{mat}$
Flow rate	Measurement of flow rate	$\delta Q=\pm 3.0\% Q$
VOC concentration in chamber A	PTRMS measurement	$\delta C_{Aout}=\pm 1.8\% C_{Aout}$
VOC concentration in chamber B	PTRMS measurement	$\delta C_{Bout}=\pm 1.8\% C_{Bout}$
Time	Determination of test period	$\delta T=\pm 10\% T$

3.5 Verification of similarity theory by particleboard

The similarity coefficients calculated for formaldehyde, acetaldehyde, hexanal, toluene and decane were averaged to be 0.518 with a standard deviation of 0.039. Using the similarity theory, a simulation of the emission from particleboard in small chamber was conducted to compare with the emission profile under environmental conditions of 1 1/h in air change rate, 23 ºC and 50%RH. Two VOCs were selected from the emitted VOCs, which were acetaldehyde and hexanal. The initial VOC concentration and partition coefficient of VOCs in particleboard were directly measured by VOC extraction method under the temperature 23 ºC.

Table 3.13 summarizes the critical parameters in the simulation set up of emission test for particleboard. Figure 3.13 shows the comparison between simulated acetaldehyde and hexanal concentrations with measurements.

Table 3.13 Critical parameters in the simulation setup of emission test for particleboard

Compound	k_{voc}	K_{ma}	ACH (1/h)	C_0 (g/m^3)	Temperature (ºC)	Grid number
Acetaldehyde	0.518	4325	1	17.61	23	700
Hexanal	0.518	4419	1	40.18	23	700

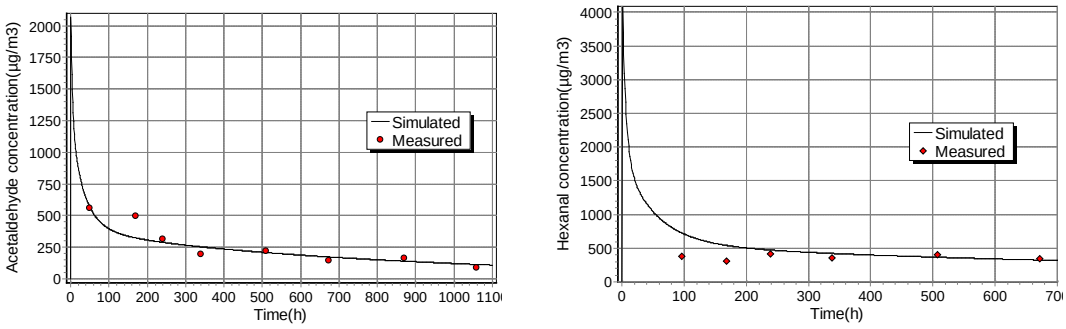

Figure 3.13 Comparison of simulated acetaldehyde and hexanal concentrations from particleboard with measurements

It is found that there is good agreement between predicted/simulated concentrations based on the pre-determined similarity coefficient and measured concentrations for acetaldehyde and hexanal, which supports the application of similarity theory in particleboard for the two compounds. It also indicates that similarity theory is not only valid for calcium silicate 0.3µm-0.8µm, but also for other porous material like particleboard, whose pore size covers a larger span of diameters 1.6µm-195µm as illustrated in Figure 3.14.

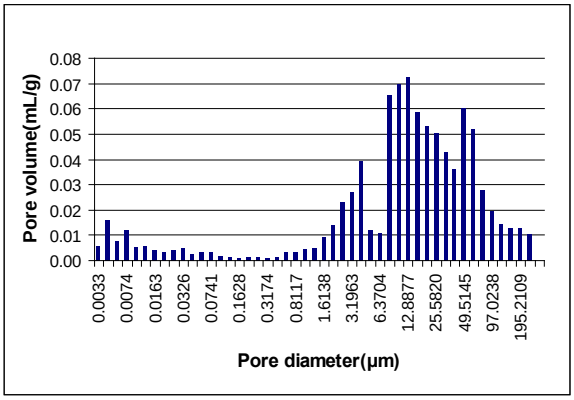

Figure 3.14 Pore volume distribution of particleboard

Besides acetaldehyde and hexanal, particleboard emitted more VOCs such as formaldehyde, α-pienene, pentanal, octanal and toluene. These compounds did not follow the decay trend, so

they were not selected for the comparison of CHAMPS-BES modeling. Their initial concentrations and partition coefficients are presented in Table 3.14.

Table 3.14 Initial concentrations and partition coefficients of unselected emitted compounds from particleboard

Compounds	$C_0(g/m^3)$	K_{ma}
Formaldehyde	61.06	28326
Alpha-pinene	27.25	2866
Toluene	1.86	
Pentanal	13.37	4413
Octanal	9.25	8207

3.6 Implementation of Similarity Theory in CHAMPS-BES

3.6.1 Governing equation

In the current CHAMPS-BES model, several assumptions are made regarding the VOC transport in storage in a porous medium:

1) Only one VOC component is present in the gas phase and in the adsorbed phase; no chemical reactions with other components are considered;

2) There is no VOC dissolution in the liquid water phase if capillary water condensation takes place; VOC adsorption and desorption is rather an interaction of the solid matrix with the gas phase;

3) Within an elemental representative volume, there is thermodynamic equilibrium between VOCs in the gas phase and the adsorbed phase; no differentiation between adsorbed surface layers and absorption in small pores;.

The total VOC flux consists of a convective and a diffusive part; the convective flux is caused by air convection only; all other VOC flux can be treated or approximated as a Fickian diffusion process, which includes diffusion in the gas phase, surface diffusion on the solid matrix and transport in micro pores.

With the assumptions above, the VOC mass balance can be written as

$$\frac{\partial}{\partial t}\rho_{REV}^{m_{voc},l+g} = -\frac{\partial}{\partial x}\left[j_{conv}^{m_{voc},g} + j_{diff}^{m_{voc},g} \right] + \sigma_{REV}^{m_{voc},l+g} \tag{3.48}$$

$\rho_{REV}^{m_{voc},l+g}$	VOC (liquid+vapor) density in reference volume	kg/m^3
$\sigma_{REV}^{m_{voc},l+g}$	VOC sources/sinks in reference volume	kg/m^{3}s

With known convective air flux, the calculation of the convective VOC flux in equation (3.48) is a straight forward procedure. The VOC mass concentration in the gas phase can be calculated by the total VOC density in the reference volume divided by a partition coefficient. The partition coefficient is a function of temperature. Using a reference partition coefficient and a VOC saturation density ratio as a temperature correction as shown below implies that partition coefficient is inversely proportional to the saturated vapor density of the VOC. The partition coefficient at reference temperature is experimentally determined for material-VOC combinations of interest. The dependence of the VOC saturation density is a thermodynamic property of the VOC.

$j_{conv}^{m_{voc},g} = c_g^{m_{voc}} j_{conv}^{m_a}$	Convective gas phase VOC flux	*k*g/m^{2}s
$c_g^{m_{voc}} = \frac{\rho_g^{m_{voc}}}{\rho_a}$	VOC mass concentration in the gas phase	*k*g/kg
$\rho_g^{m_{voc}} = \frac{\rho_{REV}^{m_{voc},l+g}}{K_{ma}(T)}$	Intrinsic VOC density in the gas phase	*k*g/m^3
$K_{ma}(T) = K_{ma,ref} \cdot \frac{\rho_{g,sat}^{m_{voc}}(20°C)}{\rho_{g,sat}^{m_{voc}}(T)}$	Partition coefficient	–
$K_{ma,ref}$	*R*eference *p*artition coefficient	–
$\rho_{g,sat}^{m_{voc}}(T)$	Saturation VOC density	*k*g/m^3

The diffusive VOC flux in equation (3.48) can be calculated using similarity theory. Similarly to the calculation method of the vapor diffusion flux in Building Physics, the VOC diffusion coefficient in free air can be related to a VOC diffusion resistance factor. In Building Physics, a water vapor diffusion resistance factor is attributed to the combined effect of both porosity and tortuosity. A resistance factor for VOC diffusion in a porous material can be introduced that

accounts for porosity and tortuosity effects as well as for surface diffusion on the solid matrix and transport in micro pores.

$j_{diff}^{m_{voc},g} = -\frac{M_{voc} D_{voc}^{air}}{\mu_{voc} RT} \frac{\theta_g}{\theta_{por}} \frac{\partial p_{voc}}{\partial x}$	Diffusive gas phase VOC flux	kg/m^{2}s
D_{voc}^{air}	VOC diffusivity in free air	m^2/s
μ_{voc}	VOC diffusion resistance factor	–
$\theta_g = \theta_{por} - \theta_l$	Volumetric fraction of gas phase	m^3/m^3
θ_l	Volumetric fraction of liquid phase	m^3/m^3
θ_{por}	Porosity	m^3/m^3
p_{voc}	VOC partial pressure in gas phase	Pa

The diffusion coefficient in free air is a known thermodynamic property of the VOC. The VOC-diffusion resistance factor depends on both the material and the VOC, and has to be determined experimentally, at least for groups of VOCs if not individually.

3.6.2 Model input

In order to perform simulations of VOCs emission from a porous material using CHAMPS-BES, the following input data are necessary: geometry and construction, materials and material properties, initial conditions, boundary conditions, outputs selections and formats, modeling options and solver settings.

3.6.2.1 Materials and Material Properties

Material properties include basic material properties such as density, specific heat, heat conductivity, porosity, effective porosity, torturosity and air permeability.

Material properties also include material functions such as water retention curve, reversed water retention curve, liquid water diffusivity and water vapor permeability.

3.6.2.2 VOC properties

VOC properties include VOC data and VOC/material data.

VOC data include the VOC name, alternative descriptive name(s), and/or CAS number, molecular formula, molar weight in kg/mol, and the liquid density of the VOC in [kg(VOC)/m^3(VOC)], $\rho_{g,sat}^{m_{voc}}(T)$ curve and $D_{air}(T)$ curve.

VOC-material data include the VOC name, material ID name, similarity coefficient (diffusion resistance correction factor), and partition coefficient as a function of temperature.

3.6.2.3 Created VOC database and material characterization for calcium silicate and particleboard

A VOC database in Textpad is created in appendix A. The VOC database includes VOC properties and VOC/material properties. Six VOCs are included: formaldehyde, acetaldehyde, benzaldehyde, hexanal, toluene and butanol. VOC/material properties include formaldehyde/calcium silicate, acetaldehyde/calcium silicate, benzaldehyde/calcium silicate, hexanal/calcium silicate, toluene/calcium silicate, butanol/calcium silicate, acetaldehyde/particleboard, and hexanal/particleboard.

The material characterization for calcium silicate and particleboard is implemented in the CHAMPS software.

The database can be used for simulation of these six VOCs from the materials which are available in the material characterization section.

3.7 Conclusion

1. A dynamic dual chamber method was developed to measure both water vapour and VOCs diffusion through porous building materials and furniture materials with good repeatability. The effective diffusion coefficient and partition coefficient were obtained independently, with an uncertainty of 6.96% and 3.35%, respectively. The water vapor diffusivity measured using the dual chamber method was in reasonable agreement with that measured by the conventional "dry cup method" for water vapor transmission tests for the

range of relative humidities tested. The VOC diffusivity measured by the dual chamber method was comparable to that measured by mercury intrusion porosimetry method.

2. The differences between three definitions of effective, apparent, and pore diffusion coefficients were elucidated. The relationships between these three diffusion coefficients were also established.

3. A similarity coefficient has been proposed to correlate the pore diffusion coefficient of VOCs with that of water vapor for hygroscopic moisture conditions in which open pore porosity does not change significantly. Values of the similarity coefficients were determined for formaldehyde, toluene, acetaldehyde, benzaldehyde, hexanal, butanol and decane for a reference material--the calcium silicate. The similarity coefficient can be used to estimate the VOC diffusion coefficient if the water vapor diffusivity is known for the same material based on the conventional "dry cup method". The application of similarity theory in particleboard was also validated by the comparison of measured acetaldehyde and hexanal with simulated concentrations.

4. VOCs database files containing VOC properties and VOC/material properties were established for two materials, and implemented as part of the input data file for modeling material emissions using the CHAMPS-BES software. The material characterizations for calcium silicate and particleboard were also implemented in CHAMPS.

Chapter 4 Effects of Relative Humidity on VOCs' Effective Diffusion Coefficient and Partition Coefficient in Porous Mediums

4.1 Introduction

The objectives of this study were: 1) to investigate the influence of relative humidity on the effective diffusion coefficient and partition coefficient of VOCs in a porous media. The purpose was to improve the understanding of the mechanism of VOC sorption and transport in a relatively simple material when subjected to moisture influence. Formaldehyde was chosen as a representative soluble compound and toluene as a non-soluble compound. 2) The relationship between effective diffusion and partition coefficients with VOCs' properties was explored. Besides formaldehyde and toluene, five more VOCs (acetaldehyde, hexanal, benzaldehyde, butanol, and decane) were measured at the same temperature 23ºC and humidity condition 50% RH for this investigation. 3) Finally, the competition between gas phase multi-VOCs was measured by testing a mixture of formaldehyde and toluene as well as individual compounds.

4.2 Experiment

4.2.1 Test setup and principle

The same dynamic dual chamber method (Xu et al. 2009) was still used. The schematic of the test system was provided in chapter 3. The effective diffusion coefficient obtained from dynamic dual chamber also included the effects of convective mass transfer resistance through the air film on either surfaces of the material, which are negligible as compared to in-material diffusion resistance except in very permeable materials. At steady state, mass balance for chamber B requires that $C_B Q_B = A D_e \frac{C_A - C_B}{L}$. Therefore, the effective diffusion coefficient of the VOC is calculated as:

$$D_e = \frac{C_B}{C_A - C_B} \frac{L}{A} Q_B \tag{4.1}$$

where D_e is effective diffusion coefficient in m^2/s. C_A and C_B are the VOC concentrations in the air phase of chamber A and B in kg/m^3, respectively (Note: $C_A=C_{Aout}$ and $C_B=C_{Bout}$ assuming perfect mixing in both chambers). C_A and C_B were averaged from the last three data points when the system reached steady state. L is the thickness of the material in m. A is the specimen material area exposed to the air in m^2. Q_B is the flowrate into chamber B in m^3/s. Partition coefficient K_{ma} (dimensionless) can be obtained as:

$$K_{ma} = \frac{2M / V_{mat}}{C_A + C_B} = \frac{2\int_0^T \left[Q_A(C_{Ain} - C_A) - Q_B C_B\right] dt}{(C_A + C_B)V_{mat}} \tag{4.2}$$

where V_{mat} is the volume of the test specimen in m^3. In Eq. (4.2), M is the total VOC mass in the material in kg, which can be obtained by the integration of the continuous concentration profile of C_A and C_B, while C_A and C_B were obtained as discrete data points. Q_A and Q_B are the flowrates into chamber A and B, respectively, in m^3/s. C_{Ain} is the inlet VOC concentration of chamber A in kg/m^3. The partition coefficient is a storage parameter and is the ratio of the VOCs' concentration in the material to its concentration in the air at equilibrium. In order to reproduce the continuous concentration file, a curve fitting process for C_A and C_B was needed based on the measured data points of C_A and C_B. The CHAMPS model (Grunewald et al. 2007, Li 2007 and Zhang 2005) that describes the diffusion and sorption process was used for obtaining the best-fit curve for numerical integration with a time interval of 1 minute. The calculation equation was:

$$M = \sum \left[Q_A(C_{Ain} - C_{Aout}) - Q_B C_{Bout}\right]\Delta t \tag{4.3}$$

4.2.2 Test specimens

Calcium silicate was still selected as a reference material in this study due to its well-characterized moisture diffusion properties and wide usage as a building insulation material. In addition, calcium silicate is a clean material, which means that it has no VOCs added in the fabrication. The specimen was cut into 30.5cm ×30.5cm ×1.0cm.

Conventional gypsum wallboard, "green" gypsum wallboard, and "green" carpet were shipped in the size of 30.5 cm ×30.5 cm ×1.27 cm, which was also the size of the test specimen. Upon receipt, all the materials were stored in a specimen storage room under 23 °C. Prior to the test, the four edge sides of the material were sealed with VOC-free tape to prevent formaldehyde diffusion through the edges. Pictures of the sealed test specimens (conventional wallboard, "green" wallboard, "green" carpet) are presented in Fig. 4.1. A picture of calcium silicate was already presented in Fig. 3.5.

The specimen was then placed in a specially prepared steel specimen holder between two chambers, and clamped tightly together.

(a) Front (b) Back

Conventional wallboard

(a) Front (b) Back

"Green" wallboard

(a) Front (b) Back

"Green" carpet

Figure 4.1 Pictures of conventional wallboard, "green" wallboard, and "green" carpet

4.2.3 Differences in the composition of two wallboards

The conventional wallboard and "green" wallboard were painted with the same paint and air dried for the same time period. The conventional wall board consisted primarily of gypsum, with a paper surfacing on the face, back and long edges. The "green" wallboard was paperless and featured fiberglass mats on both sides for superior moisture protection. Two kinds of wallboards were made by different companies.

4.2.4 Experimental Design

A total of 27 experiments were performed (Table 4.1) to achieve the research objectives.

4.2.4.1 Repeatability of test

As mentioned in chapter 3, in order to evaluate the accuracy and reliability of the dynamic dual chamber method for calcium silicate, repeat tests of formaldehyde, toluene, and acetaldehyde at 50%RH were conducted. Additionally, for conventional wallboard, one repeat test of formaldehyde at 50%RH was conducted.

4.2.4.2 Effect of relative humidity

For calcium silicate, water soluble formaldehyde and non-soluble toluene were tested for three relative humidity conditions: 25%, 50%, and 80% RH.

For conventional wallboard, "green" wallboard and "green" carpet, formaldehyde was tested for three levels of humidity conditions: 20%, 50%, and 70% RH.

4.2.4.3 Effect of mixture

In indoor air, there is not just one kind of VOC in the building; most of the time many kinds coexist. Gas phase VOCs can compete for the available adsorption site. Mixtures of formaldehyde and toluene were tested at 50%RH in calcium silicate to investigate if there was evidence of competition between the two compounds for adsorption.

4.2.4.4 Relationship between VOC properties and D_e&K_{ma}

In an effort to establish the relationship of diffusion/partition coefficients and VOCs' properties, besides formaldehyde and acetaldehyde, more VOCs in calcium silicate were tested. They were aldehyde, hexanal, benzaldehyde, butanol and decane, which are all common VOCs detected in material emissions. Physicochemical properties of the seven selected VOCs are listed in Table 4.2.

Table 4.1 Experimental design and the conditions

Calcium silicate					
No.	Compounds	RH	C_{Ain} ($\mu g/m^3$)	$Q_A=Q_B$ (m^3/h)	Test purpose
1	FOR	25	372	0.0658	Effect of relative humidity on effective diffusion coefficient and partition coefficient
2	FOR	50	372		
3	FOR	80	372		
4	TOL	25	383		
5	TOL	50	383		
6	TOL	80	383		
7	FOR^R	50	372	0.0658	Evaluate the accuracy and reliability of dynamic dual chamber method in measuring effective diffusion coefficient and partition coefficient
8	TOL^R		383		
9	ACE^{R1}		374		
10	ACE^{R2}		374		
11a	FOR^M	50	372	0.0658	Effect of VOC mixture
11b	TOL^M		383		
12a	$FOR^{M,R}$	50	372	0.0658	Repeat the mixture test
12b	$TOL^{M,R}$		383		
13	ACE	50	374	0.0658	Establish the relationship of diffusion/partition coefficient and VOC properties
14	HEX		128	0.0352	
15	BZD		401	0.0658	
16	BUT		383	0.0658	
17	DEC		372	0.0658	
Conventional wallboard					

18	FOR	20	4080	0.0307	Effect of relative humidity on effective
19	FOR	50	4080	0.0307	diffusion coefficient and partition coefficient
20	FOR^{R}	50	4080	0.0307	and evaluate the repeatability of the method
21	FOR	80	4080	0.0307	
			"Green" wallboard		
22	FOR	20	4080	0.0307	Effect of relative humidity on effective
23	FOR	50	4080	0.0307	diffusion coefficient and partition coefficient
24	FOR	80	4080	0.0307	
			"Green" carpet		
25	FOR	20	4080	0.0307	Effect of relative humidity on effective
26	FOR	50	4080	0.0307	diffusion coefficient and partition coefficient
27	FOR	80	4080	0.0307	

- In compound name, FOR represents formaldehyde; TOL represents toluene; ACE is acetaldehyde; HEX is hexanal; BZD is benzaldehyde; BUT is butanol; DEC is decane

- In superscript, R means repeat test; R1 means the first repeat test; R2 means the second repeat test; M means mixture test.

Table 4.2 Physicochemical properties of the selected VOCs

Compound	Chemical class	CAS #	Formula	MW (g/mol)	Density(23 °C,kg/m^3)	Vapor Pressure (23°C,mm Hg)	Polarity (debye)	Henry's law constant((mol/L^3)/atm),23°C
FOR	Aldehyde	50-00-0	CH_2O	30	1.09×10^{-3}	3643.8[a]	2.3[i]	2743[c]
ACE	Aldehyde	75-07-0	C_2H_4O	44	0.79×10^{-3}	837.5[h]	2.5[i]	12[c]
HEX	Aldehyde	66-25-1	$C_6H_{12}O$	100	0.83×10^{-3}	10.00[f]	na[d]	4.2[c]
BZD	Aldehyde	100-52-7	C_7H_6O	106	0.98×10^{-3}	1.06[g]	2.8[i]	35[c]
BUT	Alcohol	71-36-3	C_4H_9OH	74	0.81×10^{-3}	6.5[b]	1.8[i]	110[c]
TOL	Aromatic	108-88-3	C_7H_8	92	0.86×10^{-3}	25.8[b]	0.4[i]	0.14[c]
DEC	Alkane	124-18-5	$C_{10}H_{22}$	142	0.73×10^{-3}	1.18[b]	0.0[i]	$1.4\text{x}10^{-4}$ [e]

[a] Obtained from Lide, D.R. 2009, *CRC handbook of chemisty and physics*. 90th edition. CRC press

[b] Obtained from Vargaftik, N.B. 1975. *Tables on the thermophysical properties of liquids and gases*, John Wiley & Sons, Inc.

[c] Converted to 23°C from the value at 25°C obtained from [21] Sander R., 1999, Compilation of Henry's Law Constants for Inorganic and Organic Species of Potential Importance in Environmental Chemistry (Version 3), http://www.henrys-law.org

[d] Not available in the literature

[e] The value provided here is at 25°C. The conversion from 25°C to 23°C is not possible because of the lack of the necessary data

[f] Obtained from Bodalal, A., Zhang, J., Plett, E., Zhu, J., 2001. Correlations between the internal diffusion and equilibrium partition coefficients of volatile organic compounds (VOCs) in building materials and the VOC properties. *ASHRAE Transactions* 107(1), 789-800.

[g] Obtained from An, Y., Zhang, J., Shaw, C.Y., 1999. Measurements of VOC adsorption/desorption characteristics of typical interior building material surfaces. *International Journal of HVAC & R Research* 5(4), 297-316.

[h] Obtained from Boublik, T., Fried, V., and Hala, E. 1984, The vapour pressures of pure substances: selected values of the temperature dependence of the vapour pressures of some pure substances in the normal and low pressure region. Amsterdam: Elsevier

[i] Obtained from Korea thermophysical properties data bank. Korean national chemical engineering research information center. http://www.cheric.org/research/kdb/hcprop/showcoef.php?cmpid=1232&prop=PVP

4.2.5 Instrument conditions-calibration experiments

Two different VOC measurement instruments, HPLC and PTRMS, were adopted in the measurement of formaldehyde. They were calibrated against the certified permeation tube from VICI Corporation. The emission rates of the permeation tube for formaldehyde and toluene were 408ng/min and 420ng/min, respectively. PTRMS calibration was completed by adjusting the dilution flow from an isolated RH controlled system other than the dilution flow from the Dynacalibrator. The temperature was maintained at 23 ºC for all the calibrations. Figure 4.2 (a)-(f) displays the calibration results of both HPLC and PTRMS under different RHs. The linearity coefficient was around 0.99 for all the cases, which indicated a good linearity for both HPLC and PTRMS. Note that the HPLC response factor for formaldehyde was 0.91, and the PTRMS' response factor was around 0.40~0.50 for toluene. The PTRMS' response factor for formaldehyde was 0.91 at 25%RH, while it was 0.18 and 0.11 at 50%RH and 80%RH, respectively. The calibration results for the tests of conventional wallboard, "green" wallboard and "green" carpet are provided together with the test results in Appendix B.

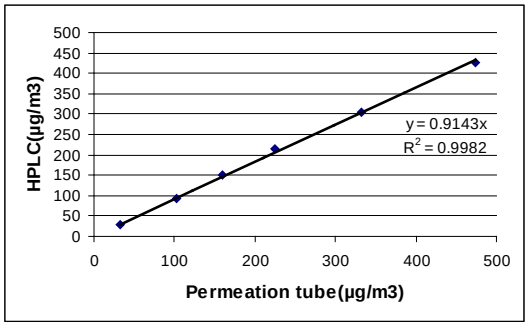

(a) Formaldehyde in 25%RH

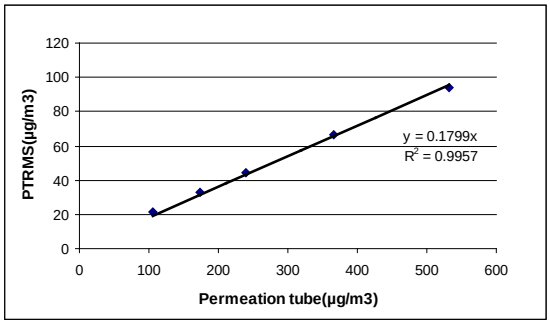

(b) Formaldehyde in 50%RH

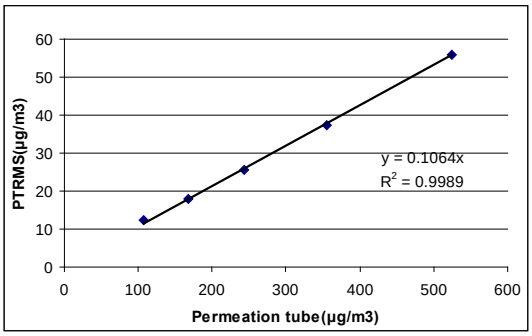

(c) Formaldehyde in 80%RH

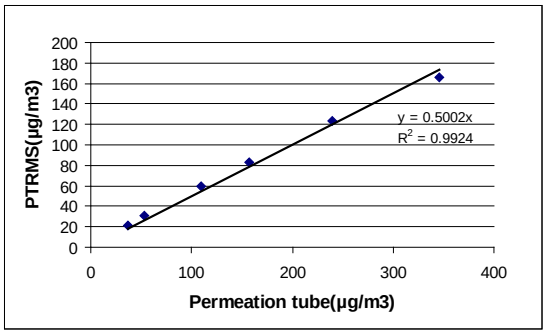

(d) Toluene in 25%RH

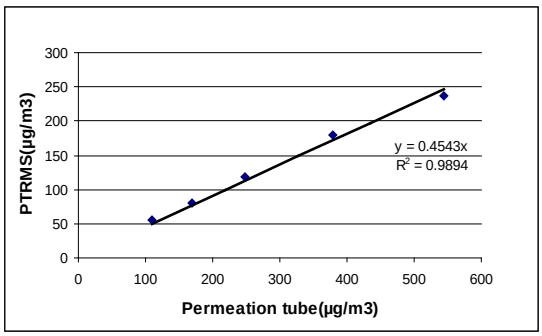

(e) Toluene in 50%RH

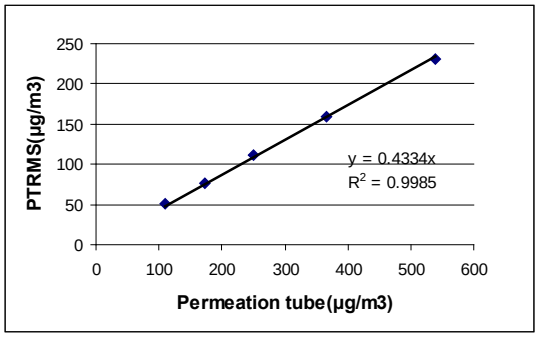

(f) Toluene in 80%RH

Figure 4.2 Calibration results for calcium silicate

4.3 Results and discussion

4.3.1 Calcium silicate

The test results of repeat tests of formaldehyde, toluene and acetaldehyde under 50%RH were already given in Fig. 3.12 (a, b and c). The repeated test of each VOC agreed well with the first test. The results presented in Table 4.3 include the relative humidity or VOCs concentration at equilibrium, the effective diffusion coefficients, the partition coefficient, μ_{voc} for VOCs (μ_{voc} is the diffusion resistance factor for VOC in the material, which is calculated as D_{air}/D_e), and the similarity coefficient k_{voc}. The similarity coefficient is the ratio of the diffusion resistance factor of VOC (μ_{voc}) to that of water vapor, which is calculated as μ_{voc}/μ_{vapor}. The diffusion coefficient in air is obtained from literature (Nelson 1992). μ_{voc} and k_{voc} in Table 4.3 are also needed as input parameters for the VOC database of CHAMPS-BES (Grunewald et al. 2007), a coupled heat, air, moisture and pollutant simulation program for porous media and building envelope systems.

Table 4.3 Results of 17 tests for calcium silicate

No.	Compound	RH %	C_{Ain} µg/m³	C_{Aout} µg/m³	C_{Bout} µg/m³	D_{air}(23°C) m²/s	D_e m²/s	K_{ma}	μ_{voc}
1	FOR	25	372.0	230.9	135.5	1.49×10^{-5}	3.08×10^{-6}	2574	4.83
2	FOR	50	366.4	226.1	136.1	1.49×10^{-5}	3.28×10^{-6}	2597	4.54
3	FOR	80	353.4	217.0	126.5	1.49×10^{-5}	3.03×10^{-6}	4057	4.91
4	TOL	25	354.7	238.1	105.8	8.40×10^{-6}	1.73×10^{-6}	288	4.84
5	TOL	50	372.7	267.4	118.2	8.40×10^{-6}	1.72×10^{-6}	133	4.89
6	TOL	80	363.4	266.5	114.3	8.40×10^{-6}	1.63×10^{-6}	76	5.15
7	FOR^R	50	385.6	231.4	138.1	1.49×10^{-5}	3.21×10^{-6}	2568	4.64
8	TOL^R	50	379.6	253.6	124.7	8.40×10^{-6}	2.10×10^{-6}	123	4.00

9	ACE^{R1}	50	359.2	222.2	121.3	1.12×10^{-5}	2.61×10^{-6}	232	4.29
10	ACE^{R2}	50	357.5	217.9	119.6	1.12×10^{-5}	2.64×10^{-6}	283	4.24
11a	FOR^{M}	50	370.8	248.2	147.2	1.49×10^{-5}	3.16×10^{-6}	3775	4.71
11b	TOL^{M}	50	433.7	320.8	147.8	8.40×10^{-6}	1.85×10^{-6}	134	4.53
12a	$FOR^{M,R}$	50	290.8	182.2	104.8	1.49×10^{-5}	2.94×10^{-6}	3656	5.07
12b	$TOL^{M,R}$	50	376.7	262.8	113.5	8.40×10^{-6}	1.65×10^{-6}	141	5.09
13	ACE	50	367.9	227.6	125.6	1.12×10^{-5}	2.67×10^{-6}	221	4.19
14	HEX*	50	128.1	60.8	34.8	6.71×10^{-6}	1.47×10^{-6}	7809	4.56
15	BZD	50	390.9	227.5	149.6	6.99×10^{-6}	4.17×10^{-6}	16111	1.68
16	BUT	50	370.5	218.7	128.4	8.52×10^{-6}	3.09×10^{-6}	18100	2.76
17	DEC	50	356.8	218.5	76.7	5.25×10^{-6}	1.17×10^{-6}	/	4.47

- The standard deviation of the mean for measured concentrations is +/- 1.8%
- The volume of the specimen $V_{mat}=8.53\times10^{-4}\ m^3$
- * means the flowrate for this test is different from other tests

4.3.1.1 Effect of relative humidity

Formaldehyde and toluene were tested under three different relative humidity conditions: 25%, 50% and 80% RH (see Fig. 4.3 and Fig. 4.4). Considering the uncertainty of the results, the influence of relative humidity on the effective diffusion coefficient of both formaldehyde and toluene is not significant. The partition coefficient of formaldehyde in calcium silicate did not change when the humidity changed from 25%RH to 50%RH, but it increased by 56% when the humidity further increased to 80%RH. The increase of the partition coefficient of formaldehyde was likely due to formaldehyde absorption into the liquid water under the higher humidity condition. The hygroscopic sorption isotherm of moisture in the material can be obtained using standard procedures (ASTM 2001). The partition coefficient of toluene decreased slightly with increasing humidity conditions from 25%RH to 80%RH. This finding agreed with those reported in (Huang et al. 2006), who presented that the partition coefficient of methanol decreased as relative humidity increased. It is likely that water vapor molecules competed with toluene molecule for available adsorption sites.

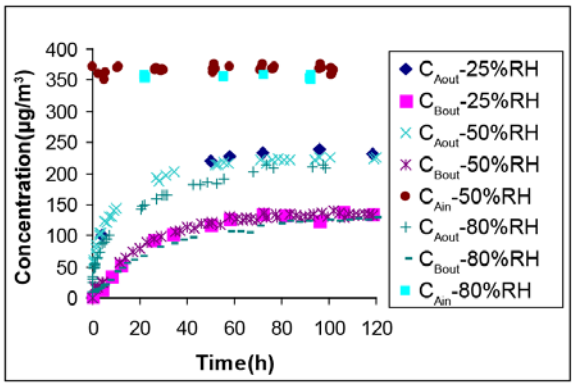

(a) Formaldehyde

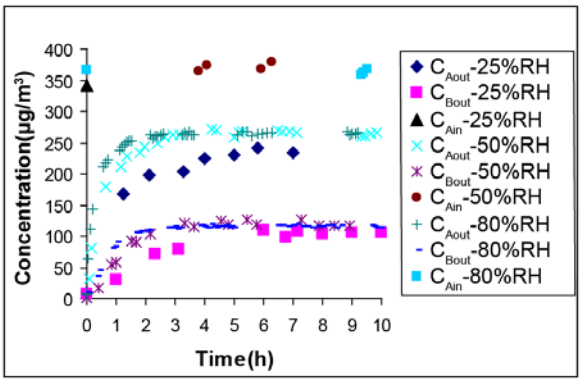

(b) Toluene

Figure 4.3 Test results under different relative humidity

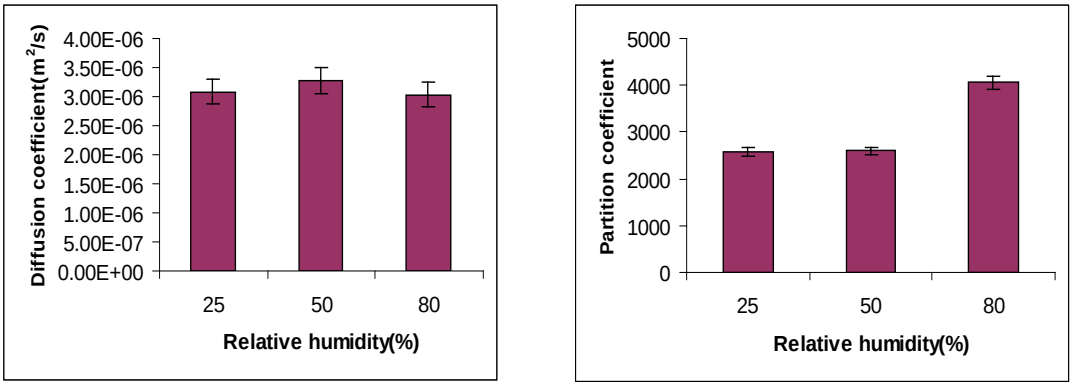

(a) Formaldehyde

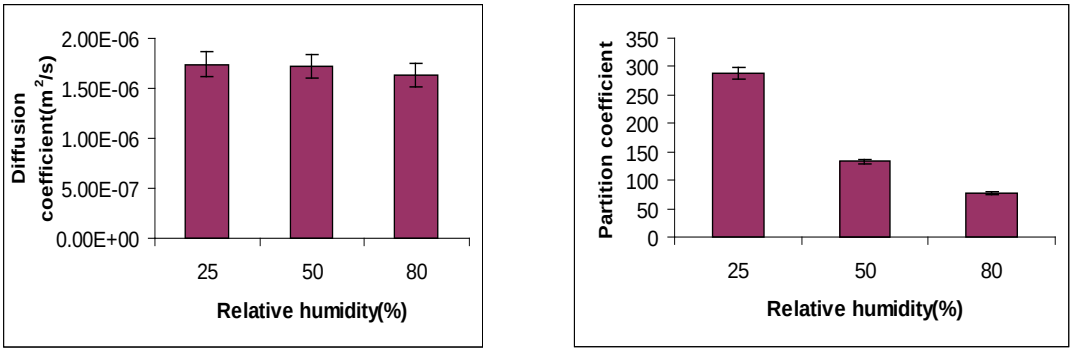

(b) Toluene

Figure 4.4 Effect of relative humidity on effective diffusion coefficients and partition coefficients

4.3.1.2 Effects of mixture

A mixture of formaldehyde and toluene was tested at 50%RH (see Fig.4.5). For toluene, there was also no obvious change compared to the single compound test of toluene. For formaldehyde,

the effective diffusion coefficient decreased in the mixture test. The partition coefficient of formaldehyde was also larger in the mixture test compared to formaldehyde alone test.

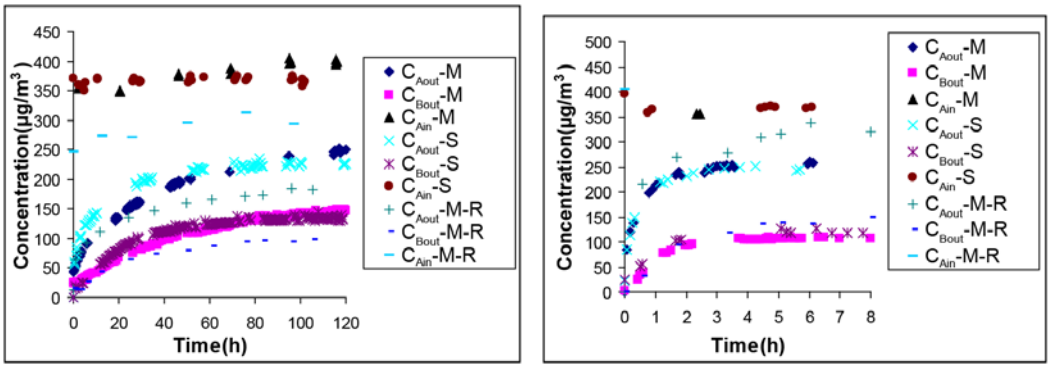

Figure 4.5 Comparison of results between mixture and single compounds

("M" represents "mixture test", " S" represents "single test", "R" means "repeat test")

To verify the phenomenon, another mixture test was performed. The test period was extended because the first test indicated that it took a longer time for formaldehyde to reach equilibrium in the mixture test. The results are shown in Fig. 4.5. The calculated diffusion and partition coefficients are consistent with the previous conclusion. It is not clear what could have caused such a phenomenon and further investigation is needed.

4.3.1.3 Relationship between K_{ma} & D_e and VOC properties

In addition to formaldehyde and toluene, butanol, benzaldehyde and hexanal were also tested at 50% (Fig. 3.13). For the VOCs in the same chemical class, the partition coefficients were inversely proportional to the vapor pressure of the compounds (Cox et al. 2001 and Bodalal et al. 2001). For the three aldehydes (benzaldehyde, hexanal and acetaldehyde), this relationship was further confirmed (Fig. 4.9). If the vapor pressure of formaldehyde was known as 3643.8 mmHg, based on the inversely relationship with the vapor pressure alone, the partition coefficient of formaldehyde predicted by the equation established from benzaldehyde, hexanal and acetaldehyde was 33.0. However, experimental data in Fig. 4.9 showed that the measured partition coefficient of formaldehyde, which was 2597, was obviously much higher than the

prediction. Compared to these three aldehydes, the Henry's law constant of formaldehyde was significantly larger than those of the other aldehydes. Therefore, the partition coefficient of VOCs was not simply inversely proportional to the vapor pressure of the compound, but also increased with the higher Henry's law constant. In other words, at relatively high relative humidity where moisture content is significant in the material, the partition coefficient of a water-soluble compound such as formaldehyde depends on the Henry's law constant as well as vapor pressure. Further study is needed to establish the relationship between them.

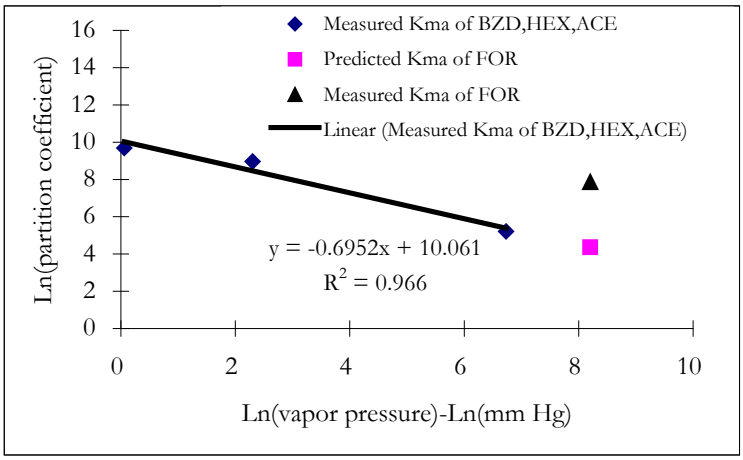

Figure 4.6 Comparison of predicted and measured partition coefficient of formaldehyde

4.3.2 Conventional and "Green" gypsum wallboard

Four tests of conventional wallboard and three tests of green wallboards were completed. During the test for carpet, the carpet was highly permeable, and hence significant effort was added to upgrade the system for controlling and measuring the pressure difference across the test specimen so that convective flux could be compensated for in the calculation of effective diffusion coefficient. The permeability of the carpet specimen has already been measured, which enabled the calculation of convective flux based on the online monitored minimal pressure difference across the test specimen (<2 Pa). The carpet test will be discussed separately in section 4.3.3.

The environmental conditions (temperature and relative humidity) were recorded continuously during all the tests. Table 4.4 shows the mean value and the standard deviation of actual measured values. RH_A and RH_B represent the relative humidity in chambers A and B, respectively. In the tests of green wallboard, the temperature was slightly lower than the designated temperature (23 °C), and also had a larger standard deviation than desired, but the temperature was consistent among the three green wallboard tests allowing direct comparison between these tests to identify the RH effect on the effective diffusion coefficient and partition coefficient for green wallboard. Relative humidity was controlled well within ±5% of the set points.

Table 4.4 Summary of recorded environmental conditions in wallboard tests

Specimen	Designated RH (%)	Measured Temperature(°C)	Measured RH_A (%)	Measured RH_B (%)
Conventional Wallboard	20	23.2±1.0	21.7±0.3	21.0±0.5
	50	23.7±0.7	51.2±0.3	49.3±0.5
	50 repeat	23.5±0.3	51.2±0.3	49.3±0.4
	70	23.7±1.1	70.4±0.9	68.2±1.2
Green wallboard	20	21.1±1.3	21.9±0.2	21.7±0.4
	50	21.6±1.9	51.7±0.5	50.7±0.6
	70	21.4±1.5	69.6±1.2	68.4±1.6

4.3.2.1 Repeatability between duplicate tests at the same humidity condition

In terms of the effective diffusion coefficient and partition coefficient, the repeatability for conventional wallboard at the same relative humidity was good. The relative difference between the two duplicate tests was 4.26% and 7.40% for the effective diffusion coefficient and the partition coefficient, respectively (Table 4.5).

Table 4.5 Repeatability of conventional wallboard at 50%RH

	50%RH	50%RH(repeat)	Difference	Average
$D_e(m^2/s)$	6.34×10^{-8}	6.61×10^{-8}	4.26%	6.48×10^{-8}
K_{ma}	446	479	7.40%	463

The detailed test results at different levels of relative humidity were presented in Appendix 4.1, which included the individual reports of ten tests (four conventional wallboards, three green

wallboards and three green carpets). The summarized results of two kinds of wallboards were listed in Table 4.6, which included five parameters: the supply formaldehyde concentrations into chamber A, the equilibrium concentrations at both chambers and the effective diffusion coefficients and partition coefficients at each test condition.

Table 4.6 Summary of test results of wallboard tests

No	Materials	RH condition (%)	C_{Ain} ($\mu g/m^3$)	C_{Aout} ($\mu g/m^3$)	C_{Bout} ($\mu g/m^3$)	D_e (m^2/s)	K_{ma}
18	Conventional	20	2662.8	2603.4	72.9	3.67×10^{-8}	304
19	wallboard	50	3106.0	2921.7	138.8	6.34×10^{-8}	446
20		50 (repeat)	2665.9	2500.8	124.1	6.61×10^{-8}	479
21		70	2443.2	2274.7	163.3	9.84×10^{-8}	404
22	"Green"	20	2649.5	2244.3	260.1	1.65×10^{-7}	1100
23	wallboard	50	2715.9	2178.8	330.2	2.24×10^{-7}	1205
24		70	1591.2	1007.6	275.7	4.73×10^{-7}	1325

4.3.2.2 Relative humidity effect

Figure 4.7 shows the derived effective diffusion coefficient and partition coefficient at three levels of relative humidity (20% RH, 50% RH, and 70% RH). A higher relative humidity led to a slightly larger effective diffusion coefficient for both conventional wallboard and green wallboard. The small increase is likely due to more frequent collisions between formaldehyde and water vapor molecules. At a higher relative humidity, the amount of adsorbed moisture in the material would also be higher. If the surface diffusion plays a role in the moisture transport, it is then plausible that the higher adsorbed moisture content at a higher RH value also contributed to the increase of the effective diffusion coefficient of formaldehyde due to its water solubility. These hypotheses need to be investigated further in future studies that also include detailed measurements of the moisture retention curve as well as the diffusion of a mixture of gases (formaldehyde and water vapor in this case). From 20% RH to 50% RH, the partition coefficient of formaldehyde in conventional wallboard became larger. From 50% RH to 70% RH, the partition coefficient of formaldehyde in conventional wallboard decreased slightly. Considering that the decrease was less than 3 times the level of experimental uncertainty, the relative humidity

effect from 50% RH to 70% RH on the partition coefficient in conventional wallboard may be considered insignificant. Again the higher adsorbed moisture content in the material at a higher RH value is likely to be responsible for the increase of the high partition coefficient due to the water-soluble nature of formaldehyde, but its impact is expected to be different from one RH range to another because of the non linear nature of the moisture retention curve. It is likely that from 20% RH to 50% RH, the increase of adsorbed moisture is higher than from 50% RH to 70% RH as most porous materials tend to have a relatively flat curve in the 30% to 70% RH range compared to the ranges of 0 to 30% RH and 70% to 100% RH.

The partition coefficient of formaldehyde in green wallboard increased slightly with the increase of relative humidity, probably due to the soluble nature of formaldehyde, which was absorbed more into the adsorbed moisture at a higher relative humidity.

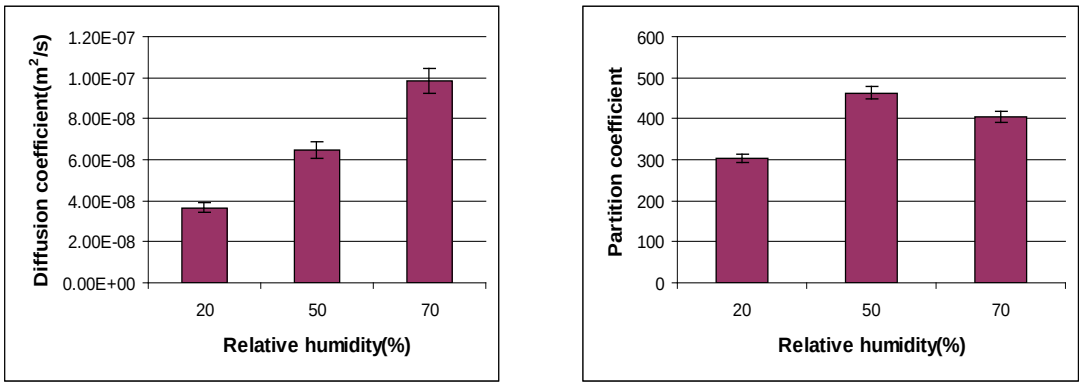

(a) Conventional wallboard

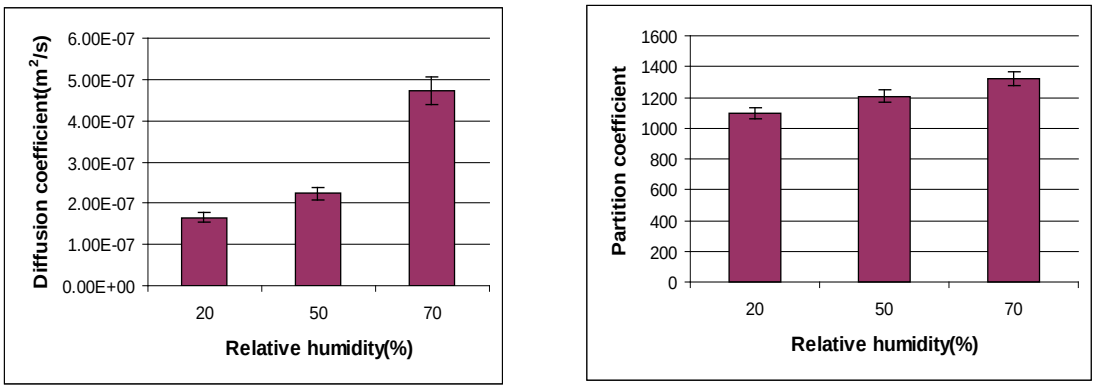

(b) Green wallboard

Figure 4.7 Comparison of effective and partition coefficients of wallboards at different RHs

4.3.2.3 Comparison of conventional and green wallboard

In Fig. 4.8, the results of conventional and green wallboard were plotted together. By comparison, the effective diffusion coefficient of green wallboard at each level of relative humidity was significantly larger than that of conventional wallboard. In other words, the diffusion resistance of green wallboard was smaller than the diffusion resistance of conventional wallboard. The partition coefficient of green wallboard at each level of relative humidity was also larger than conventional wallboard, indicating that the green wallboard had a larger storage capacity for formaldehyde. However, the lower test temperature in the "green" wall board test than in the conventional wall board test (21 vs. 23 ^{o}C) contributed, and may or may not account for all the increase in the partition coefficients. These parameters require further analysis to account for the temperature effect.

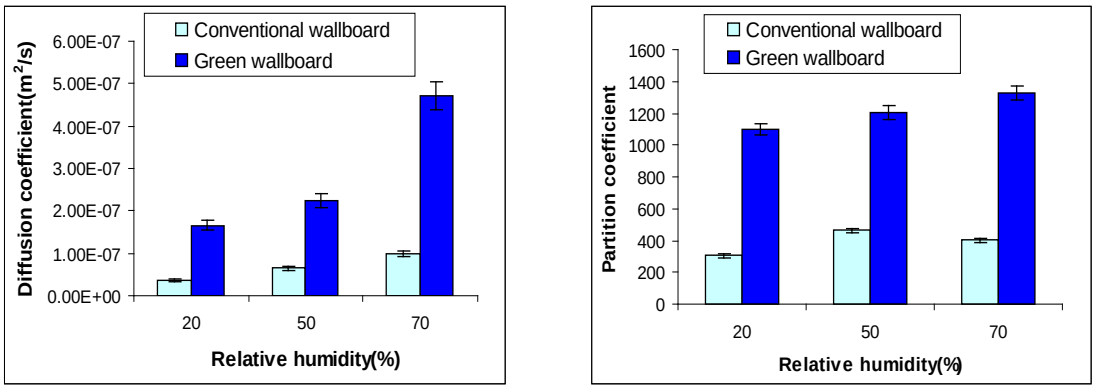

Figure 4.8 Comparison of conventional and "green" wallboard

Both the conventional and "green" wallboards had a water-based paint. As a result, the data represented above included the effects of RH on the formaldehyde transport and storage in the paint layer as well as the gypsum material. Separate tests would be needed to separate the effects on the two materials and determine the diffusion and partition coefficients for individual materials as well as the material systems (i.e., painted boards) in the current study.

4.3.3 "Green" carpet

4.3.3.1 Permeability test

The carpet was found to be very permeable. Even a small pressure difference across the test specimen (in the order of 0.2 Pa) can result in significant convection flux, which needs to be corrected in the calculation of the diffusion coefficient. In order to obtain the convection flux, a permeability test for the carpet was conducted.

In the permeability test, the outlet of chamber A and the inlet of chamber B were blocked. The fresh air Q_{Ain} was supplied into chamber A and the flow was out through the outflow of chamber B Q_{Bout} as shown in the Fig. 4.9 below:

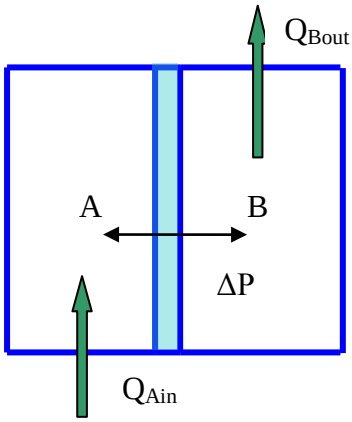

Figure 4.9 Principle of permeability test

During measurement, the flow of chamber A was adjusted from low to high to achieve different pressure drops (ΔP) between chamber A and chamber B. The pressure drop was measured by the differential pressure transmitter (Model DXLdp, ASHCROFT, Stratford, CT). The range of the pressure transmitter was -24.9Pa~24.9Pa and the accuracy was 0.25%. The volumetric flow rate Q_{Bout} was measured by a bubble flow meter (model 709, SKC UltraFlo, Orlando, FL). The range was 1~6000 cc/min and the accuracy was 0.5%. The permeability of the carpet was calculated by the following equation:

$$\delta \frac{\Delta P}{L} A = j \Rightarrow \delta = jL/(\Delta PA) \tag{4.4}$$

where

δ = air permeability (kg/m.Pa.s)

j = Air flow rate across an area A (kg/s)

L = Thickness of specimen (m)

A=Area of the specimen (m^2)

ΔP = Difference in air pressure across the specimen surfaces (Pa)

The thickness of the carpet was 1.27 cm and the exposed area of the installed specimen was measured as 0.085 m^2. Table 4.7 presents the measured Q_{Bout} and the corresponding pressure drops. The permeability of the carpet was also calculated under different flowrates. The average value of permeability is calculated in the last row of the table, at 1.05×10^{-5}.

Table 4.7 Results of permeability test

Q_{Bout}(cc/min)	496.7	1111	2181	3178	4052	5075
Q_{Bout} (m^3/s)	8.28×10^{-6}	1.85×10^{-5}	3.64×10^{-5}	5.30×10^{-5}	6.75×10^{-5}	8.46×10^{-5}
Air density ϱ at 23°C(kg/m^3)	1.192					
mass flux $j=\varrho Q_{Bout}$(kg/s)	9.87×10^{-6}	2.21×10^{-5}	4.33×10^{-5}	6.31×10^{-5}	8.05×10^{-5}	1.01×10^{-4}
Pressure drop under different flowrates ΔP(Pa)	0.12	0.34	0.61	0.91	1.18	1.51
Permeability (kg/mPas)	1.22×10^{-5}	9.81×10^{-6}	1.06×10^{-5}	1.03×10^{-5}	1.02×10^{-5}	9.94×10^{-6}
Average permeability (kg/mPas)	1.05×10^{-5}					

The relationship of pressure drop to mass flux is linear is illustrated in Fig. 4.10. The calculated permeabilities under six different flowrates are very close, except that the measured permeability under 496.7cc/min is slightly larger, which is mainly attributable to the relatively low pressure drop measured, since the accuracy of the pressure sensor was 0.06 Pa.

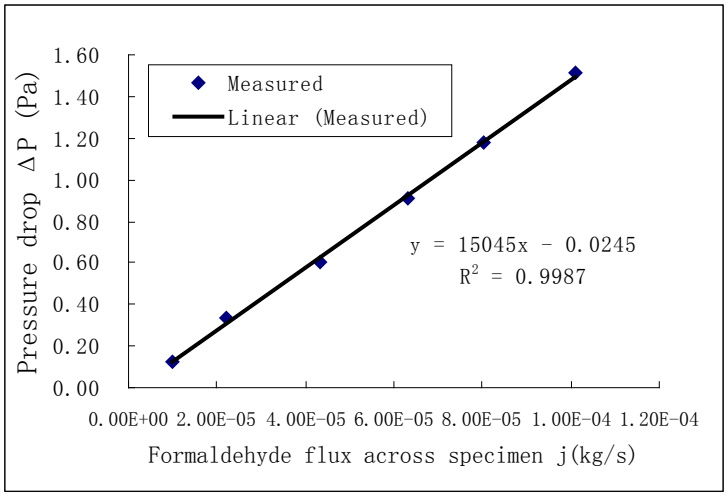

Figure 4.10 Measured air permeability of the carpet specimen

Compared to the permeability of OSB 9.6×10^{-10}, spruce 5.00×10^{-11} and gypsum board 4.16×10^{-9} kg/mPas, the permeability of the tested carpet was 1.05×10^{-5} kg/mPas, so carpet is 10937 times as permeable as OSB board and 2524 times as permeable as gypsum board.

4.3.3.2 Calculation procedure of effective diffusion coefficient of formaldehyde in carpet

Assuming a constant pressure difference at the steady state period, the air flux, associated convective formaldehyde flux, and total formaldehyde flux can be calculated as follows:

Convective formaldehyde flux:

$$j_{convection} = \frac{\delta.\Delta P.A}{L.\rho_{air}} C_{Bout} \tag{4.5}$$

where δ is the permeability of the carpet in kg/msPa; ΔP is the pressure drop between chamber A and chamber B in Pa; ϱ_{air} is the air density at the test temperature in kg/m^3, which is 1.192 kg/m^3 at 23 °C. L is the thickness of the material in m. A is the material area exposed to the air in m^2. C_{Bout} is the formaldehyde concentration in the outflow of chamber B in kg/m^3.$j_{convection}$ is the formaldehyde mass flux due to convection in kg/s.

Total formaldehyde flux from chamber A to chamber B:

$$j_{total} = C_{Bout} Q_B \tag{4.6}$$

where Q_B is the flow rate into chamber B in m^3/s.j_{total} is formaldehyde mass flux due to both convection and diffusion in kg/s.

Hence the flux due to diffusion can be calculated as:

$$j_{diffusion} = j_{total} - j_{convection} \quad (4.7)$$

where $j_{diffusion}$ is formaldehyde mass flux due to diffusion in kg/s. The above calculations provide an estimation of the effective diffusion coefficients based on the estimated pressure difference measured at the steady state period of the test. The partition coefficient can be calculated in the same way as for the other materials. In order to control and monitor the pressure difference across the test specimen for highly permeable materials such as the carpet, a more sensitive pressure sensor was purchased and installed together with an online monitoring data acquisition system.

4.3.3.3 Test results of carpet

Three tests were conducted for the carpet (20%, 50% and 70% RH). The test conditions and results are summarized in Table 4.7, 4.8 and 4.9. Figure 4.11 provides a comparison of effective diffusion coefficients and partition coefficients of carpet at different RHs. The measured pressure drop was corrected by subtracting the average of the noise signal (system error) from direct reading of the sensor in the test. The noise reading of the pressure sensor at 70%RH was relatively larger than the noises at 20%RH and 50%RH.

Table 4.8 Summary of recorded environmental conditions in carpet tests

Specimen	Designated RH (%)	Noise of pressure sensor before testing(Pa)	Direct reading of pressure sensor in the test(Pa)	Measured Pressure Drop(Pa)	Measured Temperature(°C)	Measured RH_A (%)	Measured RH_B (%)
"Green" carpet	20	-0.08	-0.27	-0.20±0.26	23.5±0.8	21.9±0.2	21.7±0.2
	50	-0.05	-0.27	-0.22±0.25	24.1±0.6	51.6±0.3	51.0±0.3
	70	0.22	-0.19	-0.41±0.24	23.9±0.3	70.0±1.0	68.9±1.1

Table 4.9 Summary of calculated mass fluxes in carpet tests

Specimen	Designated RH (%)	Total mass flux (μg/s)	Mass flux due to convection*(μg/s)	Mass flux due to diffusion(μg/s)
"Green" carpet	20	1.31×10^{-8}	-1.78×10^{-8}	3.09×10^{-8}
	50	1.25×10^{-8}	-1.85×10^{-8}	3.10×10^{-8}
	70	1.29×10^{-8}	-3.65×10^{-8}	4.94×10^{-8}

- Negative sign means that the flux is from chamber B to chamber A.

Table 4.10 Summary of test results of carpet tests

No	Materials	RH condition (%)	C_{Ain} (μg/m^3)	C_{Aout} (μg/m^3)	C_{Bout} (μg/m^3)	D_e (m^2/s)	K_{ma}
25	"Green" carpet	20	3346.71	1825.11	1530.71	1.56×10^{-5}	471
26		50	3294.84	1721.42	1451.83	1.71×10^{-5}	661
27		70	3388.96	1790.57	1491.51	2.46×10^{-5}	967

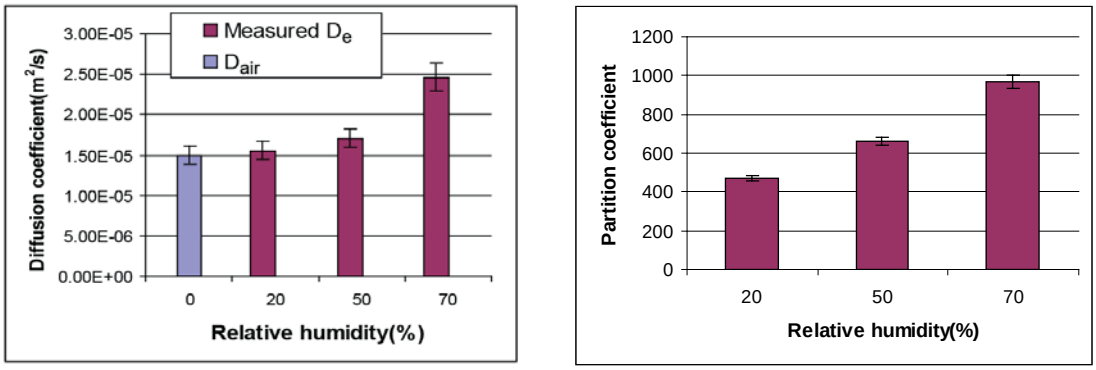

Figure 4.11 Comparison of effective diffusion and partition coefficient of carpet at different RHs

The calculated effective diffusion coefficients at different RHs were very close to the diffusion coefficient of formaldehyde in dry air (D_{air}) at 23 ºC(1.49×10^{-5}m^2/s), which indicates that the carpet had little resistance to formaldehyde diffusion. The diffusion coefficient of formaldehyde in dry air at a specific temperature and pressure was obtained by the Eq. (4.8):

$$D_{air} = \frac{0.0043\sqrt{T^3}\sqrt{\frac{1}{m_A}+\frac{1}{m_B}}}{(v_A^{1/3}+v_B^{1/3})^2 P} \tag{4.8}$$

where D_{air} was the diffusion coefficient of formaldehyde in m^2/s; m_A was the molecular weight of dry air in g/mol; m_B was the molecular weight of formaldehyde in g/mol; v_A was the molecular volume of dry air in mL/gmol; v_B was the molecular volume of formaldehyde in mL/gmol; T was the temperature in Kelvin; and P was the pressure in atm. A method to calculate the diffusion

coefficient of formaldehyde in humid air was not found in literature. If the diffusion coefficient was estimated by replacing the parameters of air in the equation by the parameters of the mixture of air and water vapor, in the presence of water vapor, the molecular weight of the mixture of air and water vapor was smaller than air since the molecular weight of water vapor (18.0 g/mol) was smaller than air (28.9 g/mol). The molecular volume of water vapor could be obtained by dividing the molecular weight by the density. The density of water vapor was slightly smaller than air at the same temperature. The molecular volume of water vapor was still smaller than air. As a result, the diffusion coefficient of formaldehyde predicted in humid air in this way was larger than the diffusion coefficient in air only, which agrees with the trend of the measured results despite the blockage of the carpet material matrix. More quantitative analysis will be needed in future studies.

Relative humidity in the range 20% RH ~70% RH led to a slightly larger effective diffusion coefficient of formaldehyde in the carpet. The partition coefficient of formaldehyde in carpet increased slightly with the increase of relative humidity, probably also due to the soluble nature of formaldehyde, which was absorbed more into the adsorbed moisture at a higher relative humidity.

4.4 Conclusion

A dynamic dual chamber system was used to investigate the repeatability of tests and effects of relative humidity, mixture, and physicochemical properties of VOCs on the effective diffusion coefficient and partition coefficient of VOCs in porous mediums (calcium silicate, conventional gypsum wallboard, "green" gypsum wallboard and "green" carpet). Tests at 25%, 50% and 80%RH were conducted for calcium silicate, while 20%, 50%, and 70%RH were conducted for the other three materials. The following conclusions can be made for calcium silicate:

1. The partition coefficient of formaldehyde (a water soluble compound) in calcium silicate did not change when humidity increased from 25%RH to 50%RH, but it increased by 56% when

humidity increased from 50%RH to 80%RH. The increase of the partition coefficient of formaldehyde was likely because the formaldehyde molecule is absorbed into the significantly more adsorbed water under the 80%RH condition. The partition coefficient of toluene (a water non-soluble compound) decreased slightly with increasing humidity conditions from 25%RH to 80%RH. This was possibly because of competition by water vapor molecules for available adsorption site with toluene molecules.

2. The humidity effect on the diffusion coefficient of formaldehyde and toluene in calcium silicate was not significant in the hygroscopic range from 25%RH to 80%RH, where blocking of diffusion paths due to capillary condensation is minimal.

3. In the test of a mixture of formaldehyde and toluene for calcium silicate, the effective diffusion coefficient of formaldehyde was smaller and the partition coefficient of formaldehyde was larger than in single compound tests. It is not clear what could have caused such a phenomenon and further investigation is needed. Both the effective diffusion and the partition coefficient of toluene did not differ significantly in a mixture test compared to the toluene only test.

4. Besides vapor pressure, the solubility of VOCs was also one factor that influenced the partition coefficient of the VOC. The partition coefficient of VOCs was not simply inversely proportional to the vapor pressure of the compound, but also increased with higher Henry's law constants. At a relatively high relative humidity where moisture content is significant in the material, the partition coefficient of a water-soluble compound such as formaldehyde depends on the Henry's law constant as well as vapor pressure. Further study is needed to establish the relationship between them.

The following conclusions can be made for conventional gypsum wallboard, "green" gypsum wallboard and "green" carpet:

5. The test method had good repeatability as verified by duplicate tests for conventional wallboard at 50% RH.

6. A higher relative humidity led to a larger effective diffusion coefficient for both conventional wallboard and green wallboard.

7. The partition coefficient of formaldehyde in conventional wallboard became larger from 20% RH to 50% RH, while the relative humidity effect was insignificant from 50% RH to 70% RH considering that the decrease was less than 3 times the experimental uncertainty.

8. The partition coefficient of formaldehyde in green wallboard and carpet increased slightly with the increase of relative humidity, probably due to the soluble nature of formaldehyde, which was absorbed more into the adsorbed moisture at a higher relative humidity.

9. The effective diffusion coefficient and partition coefficient of green wallboard at each level of relative humidity were significantly larger than those for conventional wallboard. The slightly lower temperature in the "green" wall board than in the conventional wall board tests (21 vs. 23 °C) contributed, but may or may not be responsible for all of the difference, which requires further investigation.

10. The carpet specimen was highly permeable and the measured diffusion coefficients at 20% RH, 50% RH and 70% RH were all at the similar level as the formaldehyde diffusion coefficient in dry air at 23 °C, and had insignificant difference among the different RH conditions. The partition coefficient, however, increased slightly with the increase of RH level.

Chapter 5 Modeling Emissions from a Multi-layer Furniture Material Assembly

5.1 Introduction

Many wood-based furniture is made of composite wood boards such as the work panel and table surface. VOCs are emitted from different layers of the multilayer assembly, not only from the top surface, but also from the core and bottom layer. It is important to understand the emission characteristics of common multilayer-structured materials in order to provide useful information for manufacturing process control and to finally reduce the VOCs released into the indoor air. This chapter discusses the method and application of modeling emissions from a multilayer furniture assembly with a specific focus on the emissions from wood-based office furniture.

5.2 Description of the Material Assembly

5.2.1 Composition and structure

The selected subject of interest in this dissertation is a wood assembly worksurface (Fig. 5.1(a), (b)) that consists of a painted veneer on the top, a particleboard core, and an unpainted veneer at the bottom. Particular paints or varnishes are applied to the top surface of the veneer (called painted veneer, Fig. 5.1(d)) to have more gloss and protect the worksurface from damage. Veneer layers (Fig. 5.1(e)) are very thin compared to particleboard layers, and they are usually glued and pressed onto core material. Particleboard (Fig. 5.1(c)) is a wood panel product made from wood particles, widely used in the manufacture of furniture, floor underlayment, shelving, cabinet, table tennis, kitchen worktops, and work surfaces in offices and domestic homes. The basic physical parameters are provided in Table 5.1.

a b c

d e

Figure 5.1 Photograph of (a) Worksurface top (b) Worksurface bottom (c) Particleboard core (d) Painted veneer (e) Veneer

Table 5.1 Basic physical parameters of each layer in the worksurface assembly studied

Material	Length (mm)	Width (mm)	Thickness (mm)	Density* (kg/m^3)	Location in assembly
Painted veneer	177.8	177.8	0.55	717.86	Top layer
Particleboard	177.8	177.8	28.62	749.86	Core layer
Veneer	177.8	177.8	0.55	643.65	Bottom layer

* The densities of the materials were calculated from the mass measured by a balance divided by specimen volume.

5.2.2 Manufacturing processes and emission characteristics of individual materials

Particleboard: The process of making particle board begins with wood. Most particle board manufacturers use waste wood products collected from commercial woodworking factories, although some virgin wood may be used as well. All of this recycled wood fiber and sawdust is stored in large containers before being processed into particle board.

The wood particles are usually dried, then sorted to eliminate overly large or small pieces. Once this mechanical sorting has been completed, the acceptable wood fibers are moved by conveyor belt to a blending hopper. Along the way, several overhead nozzles spray the wood fibers with a strong liquid resin or glue. Several different forms of formaldehyde-based resins may be used, depending on the specific quality of particle board desired. The resin or glue applied is the major VOCS source for particleboard. The distribution of theses VOCs are determined by the manufacturing process. Another VOC source is the VOC that originates from wood itself, so the distribution of these VOCs is more dependent on the species of the wood.

The resin-soaked wood particles are then blended to form a consistent paste. This combination is piped into a forming machine, which presses out a sheet of uncured particle board. The formed panels of particle board are then pressed down for easier transportation to the final curing ovens. Individual sheets of particle board are held under pressure as the air around them is superheated. This allows the resin to harden and form a very strong bond with the wood fibers.

Some forms of particle board are left in this rough state for use in flooring and other projects in which the panels will not be visible. In situations in which the appearance of the product is a concern, thin strips of wood, called veneers, are added to the surface of the particle board. Furniture manufacturers often use veneer-covered particle board as a cheaper alternative to natural hardwoods. Many assemble-it-yourself desks and other home furnishings may also be made from veneered particle board.

Wood veneer: Wood veneer is used to give furniture or other materials a fine wood grain appearance. Wood veneer comes in very thin sheets, less than 3 mm thick, and is made of various species of finished or unfinished wood.

Wood veneer can be made from the wood of various species of trees. It is often made from species such as cherry, oak, maple and birch, as well as rare and exotic species such as Brazilian rosewood and eucalyptus. There are hundreds of different types of wood veneer available. When

wood veneer is applied properly, it gives a piece the illusion that is made entirely from the same type of wood as the veneer.

Three typical procedures are needed to make wood veneer 1) Preparing: Logs must be prepared before they can be turned into wood veneer. After they are delivered, logs are washed and then run through a machine that removes the bark. After the bark has been removed, the log is sent through a machine that slices it in half lengthwise. 2) Slicing and drying: The cut log pieces are loaded into a saw that cuts them into very thin slices, sometimes as thin as 1/40th of an inch thick. The slices are then placed into a dryer, where all the moisture is removed from them. After the slices are dried, they are trimmed so that the edges are perfectly straight and will fit together smoothly. 3) Sheeting: After the slices are cut, workers sort and grade them. The small, graded slices are joined together to make larger sheets of various sizes depending upon their needs. The large sheets are then turned into either raw veneer or paper-backed veneer. To make raw veneer, the large sheets are simply sanded. To make paper-backed veneer, paper is applied to the back of the sheets. The sheets are then trimmed again to even out the paper backing and sanded to a smooth finish.

Wood veneer is applied with an adhesive such as carpenter's glue, using a specialized roller and clamps to hold the veneer in place while drying. The choice of adhesive should depend on the experience of the person applying the wood veneer, since some adhesives are so strong that they do not allow for any mistakes. Wood veneer should also be applied only to flat surfaces, because it doesn't adhere neatly to curves.

VOCs sources for veneer also depend on both the adhesives used and the species of wood used as the raw material.

Painted veneer: The procedures to paint the veneer are: 1) Fix any problems with the veneer - use wood glue to affix veneer back to the original surface. Unfortunately cracked or missing pieces of veneer cannot be fixed. You will need to remove the damaged piece and glue a new

piece in its place. 2) Clean the surface with hot water removing any grease or grime. A simple solution containing a few drops of dish soap should work, do not saturate the surface. Please note that if the veneer is cracked, peeling or missing you should hold off on cleaning and fix this problem first as veneer is usually covering particle board (MDF) which breaks down when wet. 3) After dry, lightly sand the veneer (do not sand through veneer) and use tack cloth to remove all of the dust created on the surface. You may also want to clean up any dust around the surface to be painted or you have the potential to have the dust blow into your fresh paint. 4) Apply primer - Kilz is great. - At least 2 coats. Allow to dry for 24 hours. - You may need to sand between coats of primer (depends on smoothness of surface desired) 5) Apply paint - 2 coats for light paint, generally more for darker colors. 6) Seal with 2-4 coats of varnish if the surface is going to be used as a work surface. The paint used in the manufacturing is a major VOC source, which mainly rests on the surface of the veneer, and some of the paint may diffuse into the inside of the veneer to some extent. It needs further research to quantify the depth that the paint can reach. Same as particleboard and veneer, wood itself is another VOCs source, and the VOCs due to wood distribute within all the wood material.

About the specific VOCs emitted from the three layered worksurface studies in this dissertation, small chamber tests were done for painted veneer, veneer and particleboard, respectively. The details related to these tests can be found in Appendix D.

5.2.3 Applications in office furniture

Veneering is widely used on fine furniture for decorative and architectural purposes; hence the multilayer layered panels make up the edges, partition, cabinet, drawer and so on in the office furniture. In a typical workstation system, some panel comprises the particleboard drawer sides that are wrapped with a vinyl material. The worksurface, the panels, the drawer fronts, and the internal supports for the file cabinets usually have a standard industrial particleboard core with urea-formaldehyde (UF) resin. The veneers are applied with UF adhesive. That is to say, most of

the components in the office furniture are multilayer structured instead of singe layered, although the thickness of the core and the exterior layer probably differ depending on the functions of the specific product.

VOCs emission is a long process, which may take years to completely deplete the VOCs from the multilayer assembly. Though testing gives specific VOCs emitted from the materials, however, it is not realistic to measure all the VOCs concentration level during its entire service life. Simulation models can be useful for predicting VOCs exposure quickly with much less expense and time, and the model can also easily answer the relevant questions like estimated VOCs exposure time, VOCs distribution after a certain amount of time. Based on these needs, model development for multilayer assembly becomes inevitable.

5.3 Multilayer model development

Consider a generic multilayer assembly inside a chamber as illustrated in Fig. 5.2. The chamber has a flow rate of Q_{in} at the inlet and Q_{out} at the outlet, and a fan is placed in the chamber to make sure the chamber air is well mixed. With zero leakage in chamber, we have $Q_{in}=Q_{out}$. The geometry is symmetrical in the x direction. The material width is 2w in the x direction. In y direction, the subject material is composed of n layers of different materials which are labeled 1, 2, …i-1, i, i+1, … n from bottom to top, and each material has a corresponding thickness of L_i. The side edges and bottom surface of the material specimen are completely sealed up by the tape in the VOCs emission tests. The purpose of the sealing is to prevent the VOCs leakage from the sides so that the transport only occurs in the y direction. Note that in a typical test, a small area right close to the border on the top surface is also sealed in both moisture and VOCs emission test in specimen treatment, but its effect on VOC transport is neglected due to its small area in comparison to the total exposed emission surface area.

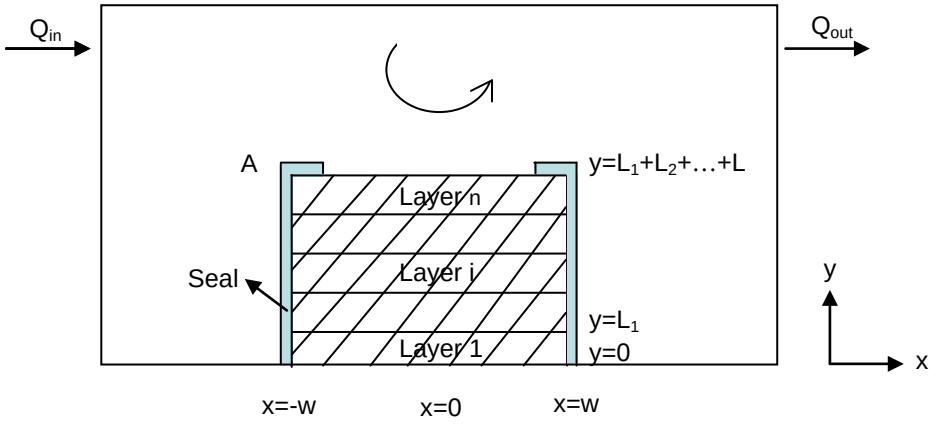

Figure 5.2 Schematic of 1D multilayer model

5.3.1 Physics and assumptions

In the manufacturing process of painted veneer, finish is applied to the surface of the veneer and later slowly diffuses into the inside of the veneer, which combines into the painted veneer. Although finish and veneer are made of different materials, in the modeling, they are treated together as a new material named painted veneer in the following part. Particleboard is also assumed to be homogeneous although density difference was observed due to the press in the manufacturing process (Zhao et al. 2009), which makes the density of exterior part slightly larger than the interior part. It is also assumed that there are perfect contact between painted veneer and particleboard, and between particleboard and veneer so that equilibrium condition exists at the interfaces governed by the partition law (Zhang et al. 1999).

5.3.2 Governing equations

In a numerical model approach, porous building materials that contain moisture and VOC(s) can be divided into a number of control volumes. Within a control volume (V_{REV}), the material consists of material matrix (adsorbent), macro and/or micro pores filled with gas phase mixture and/or liquid phase mixture. The gas phase consist of dry air, water vapor and/or gas phase VOC(s), while the liquid phase may consist of liquid water (including adsorbed phase water molecules), and/or adsorbed phase VOC(s). The equilibrium between liquid water and water vapor

can be described by sorption isotherm or moisture retention curve. The equilibrium between adsorbed phase VOC and the gas phase VOC can be described by VOC adsorption isotherm (e.g., a partition coefficient in its simplest form).

In the development of current multilayer model, several assumptions are adopted for the VOC mass balance:

- There are no interactions between different VOCs and hence each VOC component can be modeled independent of the others in the gas phase and in the adsorbed phase;
- No VOC dissolution in the water, if capillary water condensation takes place; VOC adsorption and release is rather an interaction between the adsorbed phase on solid matrix and the gas phase;
- Thermodynamic equilibrium (temperature, chemical potential) exists between VOC in the gas phase and the adsorbed phase;
- The total VOC flux consists of a convective and a diffusive part in general, but for the assembly system studied, the convection component can be neglected due to low air permeability of the materials; the diffusion part includes molecular diffusion and Knudsen diffusion through pore air.

With the assumptions above, the VOC mass balance can be written as

$$\frac{\partial}{\partial t}\rho_{REV}^{m_{vocc,l+g}} = -\frac{\partial}{\partial x}\left[j_{diff}^{m_{voc,g}}\right] + \sigma_{REV}^{m_{voc,l+g}} \tag{5.1}$$

where,

$\rho_{REV}^{m_{voc,l+g}}$	VOC (liquid+vapor) density in reference volume	kg/m^3
$\sigma_{REV}^{m_{voc,l+g}}$	VOC sources/sinks in reference volume	kg/m^{3}s

The diffusive VOC flux in equation (5.1) can be calculated as follows (in the same way as water vapor diffusion flux calculation in Building Physics:

$j_{diff}^{m_{voc},g} = -\frac{M_{voc} D_{voc}^{air}}{\mu_{voc} RT} \frac{\theta_g}{\theta_{por}} \frac{\partial p_{voc}}{\partial x}$	Diffusive gas phase VOC flux	kg/m^{2}s
D_{voc}^{air}	VOC diffusivity in free air	m^2/s
μ_{voc}	VOC diffusion resistance factor	–
$\theta_g = \theta_{por} - \theta_l$	Volume fraction of the gas phase	m^3 / m^3
θ_{por}	Porosity of material	m^3 / m^3
θ_l	Volume fraction of the liquid phase	m^3 / m^3
p_{voc}	Partial pressure of VOC in gas phase	Pa

The diffusion coefficient in free air is a known thermodynamic property of the VOC. The diffusion resistance factor is attributed to the combined effect of both porosity and tortuosity. The VOC-diffusion resistance factor depends on both the material and the VOC, and has to be determined experimentally. Using the analogy between VOC and water vapor diffusion in porous media, the resistance factor for VOC can be determined as the product of a similarity coefficient, k_{voc} and the resistance factor for water vapor.

5.3.3 Boundary conditions

5.3.3.1 Boundary conditions between interior material layers (from layer 2 to layer n-1)

It is known that for each VOC-material combinations, there is a partition coefficient. Similarly, for each material-material combination, the VOC density in each material will be obtained by another partition coefficient between each layer $K_{mm}^{i-1,i}$. $K_{mm}^{i-1,i}$ is the ratio of K_{ma} in VOC-material to another VOC-material.

$$K_{mm}^{i-1,i} = \frac{K_{ma}^{i-1}}{K_{ma}^{i}} \tag{5.2}$$

VOCs diffusion in porous media includes molecular diffusion and Knudsen diffusion. Within the material, partition coefficient $K_{ma}^{i-1,i}$ correlates the VOCs concentration between the material i-1 and i. The governing equations for VOCs in any layer i read:

$$\rho_g^{i-1,m_{voc}} = \frac{\rho_g^{i,m_{voc}}}{K_{mm}^{i-1,i}} \tag{5.3}$$

5.3.3.2 Boundary conditions for layer 1 and n

For layer 1, there is no mass flux of VOCs through the wall of the chamber if the bottom of the material is sealed against the chamber wall:

$$\frac{\partial \rho_g^{1,m_{voc}}}{\partial x} = 0 \tag{5.4}$$

However, if the bottom surface is also exposed to the chamber air, the boundary condition will be the same as layer n.

For layer n, the VOCs concentration in layer n is governed by linear Langmuir isotherm:

$$\rho_g^{n,m_{voc}} = K_{ma}^{n} C \tag{5.5}$$

Where, C is the VOCs concentration in the chamber air in kg/m^3. This assumes that the mass transfer resistance over the material surface is negligible and the equilibrium is reached instantaneously.

5.3.4 VOC mass balance in the chamber

As illustrated in Fig. 5.2, for the VOCs concentration in the chamber, it complies with the following mass balance equations:

$$\frac{\partial C}{\partial t} V = Q_{in} C_{in} - Q_{out} C_{out} + D_{m,1} \frac{\partial C_{m,1}}{\partial y}\bigg|_{y=L_1+L_2+\ldots+L_n} \tag{5.6}$$

Where, C is the VOCs concentration in the chamber air in kg/m^3; V is the chamber volume in m^3; Q_{in} and Q_{out} are the flow rates into and out of the chamber in m^3/s; C_{in} is the VOCs concentration in the inlet in kg/m^3, which is zero in this paper; C_{out} is the VOCs concentration in the outlet in kg/m^3; $D_{m,1}$ is the diffusion coefficient of VOC in the layer 1 in m^2/s.

It is assumed that the boundary layer is negligible in the painted veneer and chamber air, which indicates that the convective mass transfer resistance in the boundary layer is insignificant compared to diffusion resistance inside the multilayer material.

5.3.5 Initial conditions

Initial conditions:

$$\rho_g^{i,m_{voc}} = F_i^0 \tag{5.7}$$

Where, $\rho_g^{i,m_{voc}}$ is the initial VOCs concentration in layer i in kg/m^3; F_i^0 is the function of VOCs concentration distribution in layer i.

5.3.6 Model implementation

The above model has been implemented in the CHAMPS-BES software (Grunewald et al. 2007). More details can be found in the CHAMPS-BES help file.

5.4 Parametric analysis for k_{voc}, K_{ma} and C_0 of each layer

The objectives of parametric analysis were to 1) study the influence of each parameter (k_{voc}, C_0, K_{ma}) of VOC in the studied layer on the entire emission rate of VOC from the whole worksurface 2) determine the most important input parameters needed for the multilayer model for the assembly case under study.

Fig. 5.3 is a schematic of a typical multilayered worksurface which is composed of painted veneer (including a thin finish layer and veneer), particleboard and veneer sequentially from top to bottom.

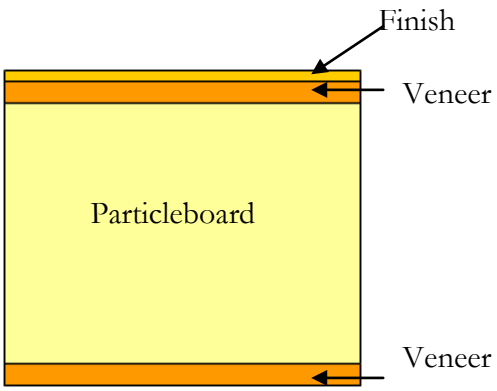

Figure 5.3 Schematic of multilayered typical worksurface

To study the influence of three parameters (similarity coefficient k_{voc}, partition coefficient K_{ma} and initial concentration C_0) on the emission rate of the entire worksurface, changes of only one studied parameter were made while the other two parameters were kept unchanged. Acetaldehyde was chosen in all the parametric studies because it is a major emitted VOC from all three layers.

5.4.1 Parametric study for painted veneer

Table 5.2 summarizes all the values for three sets of parametric studies. Fig. 5.4 presents the parametric results for painted veneer, while the reference values are used for particleboard and the unpainted veneer as given in Table 5.4. The reference values were chosen based on previous experience and experimental results on similarity coefficient, emission test results on initial concentration, diffusion and partition coefficients measurements ((Xu et al. 2009, Smith et al. 2009, Bodalal et al. 2000, An et al. 1999). These reference values are somewhat arbitrary, but are considered to be adequate for parametric analysis.

Table 5.2 Input parameters for three layers in parametric study for painted veneer

Material	Parameters studied	Initial concentration C_0 (g/m^3)	Similarity coefficient k_{voc}	Partition coefficient K_{ma}
Painted Veneer	k_{voc}	0*	0.10,0.26, 0.52,1.00	1000*
	K_{ma}	0*	0.518*	100,1000,5000,10000
	C_0	0,10,25,50	0.518*	1000*
Particleboard		17.61*	0.518*	4325*
Veneer		0*	0.518*	1000*

* used as reference value when other parameters are varied.

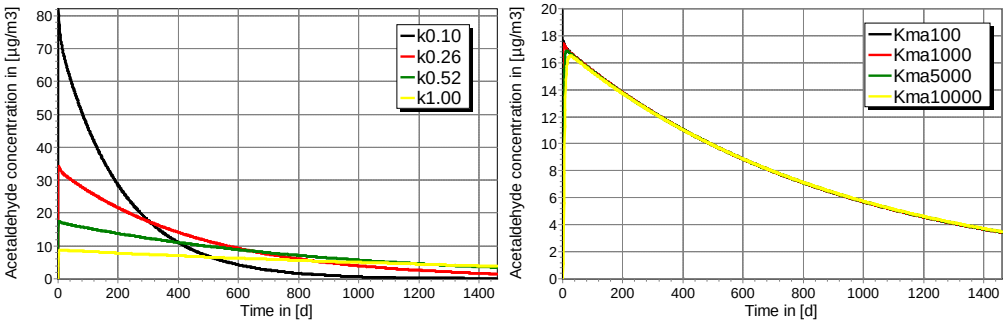

(a) Similarity coefficient (b) Partition coefficient

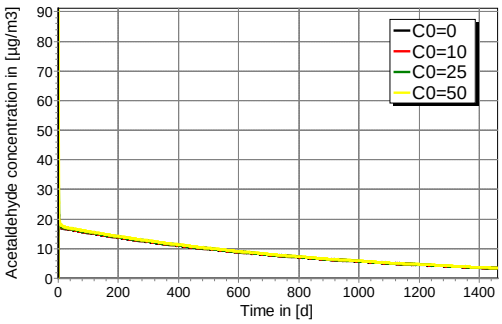

(c) Initial concentration

Figure 5.4 Parametric study of three critical parameters of painted veneer on the emission rate of the multilayered worksurface

For similarity coefficient, four values of each parameter were studied: 0.10, 0.26, 0.52, 1.00. The selection of the similarity coefficient was based on the findings of previous study in Chapter 3. The possible values for similarity coefficient by the experiment data were in the range of 0.1-

0.6. The extreme case of 1.0 was also studied when the diffusion resistances for VOC and water vapor were equal. As discussed in Chapter 3, the relationship between apparent diffusion coefficient and similarity coefficient is:

$$D = \frac{D_e}{K_{ma}} = \frac{D^{air}}{k_{voc}\mu_{vapor}K_{ma}} \tag{5.8}$$

That is, the apparent diffusion coefficient is inversely proportional to the similarity coefficient. Figure 5.7a shows that the similarity coefficient is the most important parameter of painted veneer in determining the emission rate of acetaldehyde from worksurface assembly. Considering the relationship of similarity coefficient and diffusion coefficient, we can conclude that the emission rate of acetaldehyde increases significantly with respect to the increase of diffusion coefficient. So, the change of the diffusion coefficient of the top painted veneer can control the emission rate from the whole worksurface. The top material with smaller diffusion coefficient can prevent VOCs emission from the material below it.

For partition coefficients, the five values in the parametric study were: 100, 1000, 5000, and 10000. The selection of the range of partition coefficient was based on the published literature by other researchers (Bodalal et al. 2000, Cox et al. 2001) and measured values in chapter 3 and 4. Fig. 5.4b shows that: 1) There is no observable change of acetaldehyde concentration in the chamber when the partition coefficient of acetaldehyde ranges from 10 to 5000; 2) The peak concentration slightly decreases at the first 2 to 3 days when the partition coefficient increases from 5000 to 10000; 3) There is no observable change of long-term chamber concentration when the partition coefficient of acetaldehyde changes in the studied range; 4) Partition coefficient of acetaldehyde in painted veneer has very small effect on the whole emission rate of acetaldehyde from the worksurface.

The main reason of this phenomenon is the small thickness of painted veneer relative to that of the core particleboard. The thickness of the painted veneer is only 0.55 mm, and

correspondingly the volume of the painted veneer and veneer are only 1.92% of the volume of particleboard. The storage for VOCs in small volume of the painted veneer (and veneer, see the parametric study for veneer in the later section) is negligible compared to the large storage capacity of particleboard. So, the value of partition coefficients in painted veneer (and veneer) is not the dominant factor that determines the emission rate of the VOCs from the three layered assembly.

For initial concentrations, the studied values were: 0, 10, 25 and 50, respectively. The range of the initial concentration was determined within the same order of magnitude including the extreme case when there was zero VOC content in the material. The simulation result shows that: the peak concentration for each case increased with the initial concentration in the material; after 2 days, there was no significant change for the acetaldehyde concentration in the chamber with respect to the increase of initial concentration in the painted veneer in the first 300 days.

By the comparison of the three parametric studies, we can see that the similarity coefficient is the most important parameter for painted veneer in simulating the concentration of the worksurface assembly in the chamber. For partition coefficient and initial concentration, their effects are minor. Therefore, in order to obtain accurate simulation results for the assembly, is it important to obtain accurate estimation of the similarity coefficient, while the values for the partition coefficient and initial concentration can be set somewhat loosely---e.g., using the estimated reference values would be adequate.

5.4.2 Parametric study for particleboard

Table 5.3 summarizes all the values for three sets of parametric studies. Fig. 5.5 presents the parametric results for particleboard.

Table 5.3 Input parameters for three layers in parametric study for particleboard

Material	Parameters studied	Initial concentration (g/m^3) C_0	Similarity coefficient k_{voc}	Partition coefficient K_{ma}
PB	k_{voc}	17.61*	0.10,0.26, 0.52,1.00	4325*
	K_{ma}	17.61*	0.518*	100,1000,5000,10000
	C_0	10,25,50	0.518*	4325*
PV		0*	0.518*	1000*
Veneer		0*	0.518*	1000*

* used as reference value when other parameters are varied.

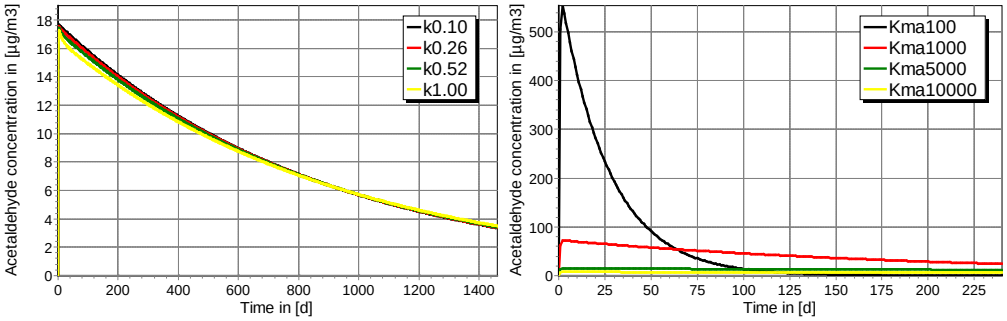

(a) Similarity coefficient (b) Partition coefficient

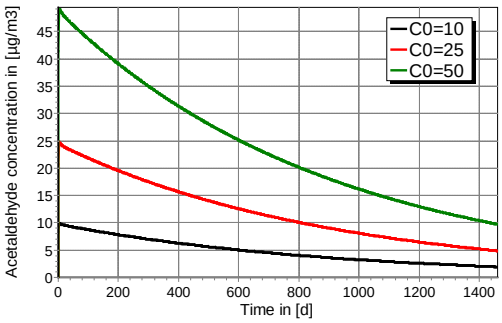

(c) Initial concentration

Figure 5.5 Parametric study of three critical parameters of particleboard on the emission rate of the multilayered worksurface

Same procedures of parametric studies were conducted for particleboard. Based on the simulation results of parametric study of similarity coefficient, the following findings are drawn: 1) higher diffusion coefficient leads to higher acetaldehyde concentration in the chamber in the first 280 days, but the trend reverses after 280 days. 2) Higher diffusion coefficient also depletes the

acetaldehyde mass in the material faster than the smaller diffusion coefficient does. Therefore, the effect of diffusion coefficient on the acetaldehyde concentration is different in the entire emission period of the worksurface.

Based on the parametric study for the partition coefficient, it is seen that 1) Smaller partition coefficient of acetaldehyde in particleboard leads to a relatively large peak acetaldehyde concentration. 2) Smaller partition coefficient also depletes the acetaldehyde mass in the material faster than big partition coefficient.

For the parametric study of initial concentration, it is seen very clearly that the initial concentration plays a big role in determining the acetaldehyde concentration from the worksurface.

In summary, we can see that all three parameters of particleboard are very important in determining the acetaldehyde concentration in the chamber for the worksurface assembly. It can be concluded that for the core layer of the multilayer materials, all three input parameters are very important when using this developed multilayered model.

5.4.3 Parametric study for veneer

Table 5.4 summarizes all the values for three sets of parametric studies. Fig. 5.6 presents the parametric results for particleboard.

Table 5.4 Input parameters for three layers in parametric study for veneer

Material	Parameters studied	Initial concentration (g/m^3)	Similarity coefficient	Partition coefficient
Veneer	k_{voc}	0*	0.10,0.26, 0.52,1.00	1000*
	K_{ma}	0*	0.518*	100,1000,5000,10000
	C_0	0,10,25,50	0.518*	1000*
PB		17.61*	0.518*	4325*
PV		0*	0.518*	1000*

* used as reference value when other parameters are varied.

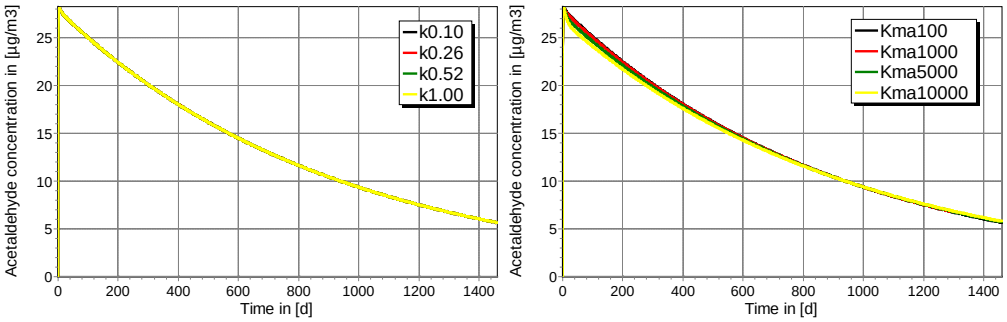

(a) Similarity coefficient (b) Partition coefficient

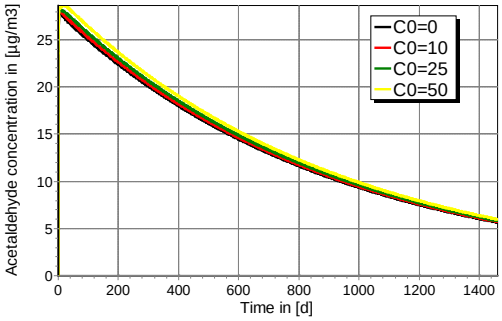

(c) Initial concentration

Figure 5.6 Parametric study of three critical parameters of veneer on the emission rate of the multilayered worksurface

Same parametric studies were also conducted for veneer. It can be seen from the simulation results that 1) No obvious concentration change has been observed for the diffusion coefficient and partition coefficient in the studied ranges. 2) There is no pronounced increase of acetaldehyde concentration in the chamber with the increase of initial concentration.

5.5 Determination of model parameters

Obviously, in order to make a successful simulation using the multilayered model developed, three critical parameters need to be input: similarity coefficient, partition coefficient and initial VOC concentration. Two important VOCs are selected in the following studies including sections of model verification and model application: acetaldehyde and hexanal. The diffusion coefficients of the VOCs are from the similarity coefficients obtained. The partition coefficients and initial emittable VOCs concentrations of acetaldehyde and hexanal in particleboard are

determined experimentally by VOC extraction method (referred to chapter 3). Based on the findings of parametric study, the partition coefficients of VOCs in painted veneer and veneer are negligible, so one general value 1000 is adopted as the input for the multilayer model. There is no acetaldehyde in painted veneer and veneer, so the initial acetaldehyde concentration is zero. Hexanal concentrations in painted veneer and veneer are very minor, so the initial concentration can also be treated as zero. Table 5.5 lists all the final values for each parameter in every layer used in the model.

Table 5.5 Critical coefficients used in modeling for worksurface

Material	Compound	Initial concentration (g/m^3)	Similarity coefficient	Partition coefficient
Painted veneer	Acetaldehyde	0	0.518	1000[a]
	Hexanal	0	0.518	1000[a]
Particleboard	Acetaldehyde	17.61	0.518	4325
	Hexanal	40.18	0.518	4419
Unfinished Veneer	Acetaldehyde	0	0.518	1000[a]
	Hexanal	0	0.518	1000[a]

Note a: the value is assumed based on the parametric study

5.6 Model verification

For a three-layer work surface assembly, limited data were collected. A standard emission test was performed for work surface panel consisting of painted veneer, particleboard and veneer using a 50 L chamber ventilated at 1 ACH. The specimen has a dimension of 7.5"x7.5" and thickness of 30 mm. Experiment details are presented in appendix D. The tests were conducted at constant temperature 23°C and 50%RH. The ventilation rates were 1 ACH. Acetaldehyde and hexanal were chosen in the comparison with the simulation results because they were important compounds emitted from the worksurface.

Simulations for the same tested scenarios were conducted. The simulated material is three layered worksurface, with the same exposed area as in the tests. The selected VOCs are still acetaldehyde and hexanal, which are two major emitted VOCs from the worksurface.

Table 5.6 Parameters of acetaldehyde in worksurface before considering redistribution effect

Material	Initial concentration (g/m^3)	Similarity coefficient	Partition coefficient
PV	0	0.518	1000[a]
PB	17.61	0.518	4325
Veneer	0	0.518	1000[a]

Table 5.7 Parameters of hexanal in worksurface before considering redistribution effect

Material	Initial concentration (g/m^3)	Similarity coefficient	Partition coefficient
PV	0[a]	0.518	1000[a]
PB	40.18	0.518	4419
Veneer	0[a]	0.518	1000[a]

[a] means that the value is assumed.

For the tested materials, before testing, the materials were stored in the storage room under 23°C constant temperature. The stored materials were subject to redistribution effect (Hui et al. 2007), and the VOCs concentrations in each layer reached an equilibrium between each other. The final concentrations in each layer and input parameters in CHAMPS are presented in the following tables:

Table 5.8 Input parameters for the simulation of acetaldehyde in worksurface after considering redistribution effect

Material	Initial concentration (g/m^3)	Similarity coefficient	Partition coefficient
PV	4.05	0.518	1000[a]
PB	17.5	0.518	4325
Veneer	4.05	0.518	1000[a]

Table 5.9 Input parameters for simulation of hexanal in worksurface after considering redistribution effect

Material	Initial concentration (g/m^3)	Similarity coefficient	Partition coefficient
PV	7.3	0.518	1000[a]
PB	39.8	0.518	4419
Veneer	9.0	0.518	1000[a]

[a] means that the value is assumed.

Below is the comparison of simulation considering the redistribution effect (Hui et al. 2007) with the measured multilayer emission data of acetaldehyde and hexanal from three layered worksurface.

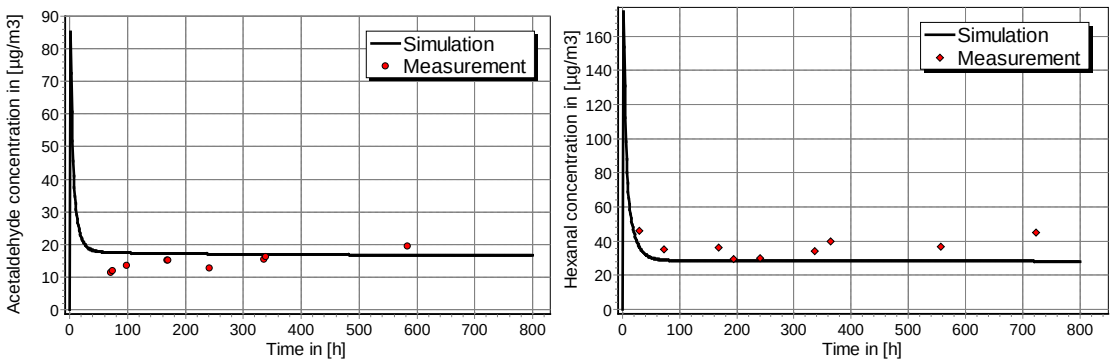

Figure 5.7 Comparison of simulation results with the experiment results

It can be seen that the simulation results match the measured data points well, which proved that the multilayer model developed was able to simulate the emission from multilayered furniture or building materials in accuracy. However, the comparison also showed that the no sufficient data that covered the transient status for the VOCs concentrations were presented in the comparison with simulated results. Therefore, the measurement data for acetaldehyde in the first 2 days and for hexanal in the first day in the small chamber emission tests are needed in the future study.

5.7 Application of the multilayer model

The developed multilayer model can be used to many real scenarios. The model can be used to study the emission characteristics of VOCs from any layer or all layers of the material, and it can also be used to study the effect of the top (or outer) layer in preventing the emission from the lower (or inner) layers. Several application cases are discussed in the following sections.

5.7.1 The emission characteristics of acetaldehyde from three layers

Acetaldehyde is chosen because it exists only in the particleboard, but it doesn't exist in the veneer and painted veneer. This simulation studies the emission characteristics of acetaldehyde from the entire worksurface. It also studies how the acetaldehyde from particleboard diffuses in the three layers. The input parameters for the model are provided in Table 5.10. The simulation results are shown in Fig. 5.8.

Table 5.10 Input parameters for the simulation of acetaldehyde in worksurface

Material	Initial concentration (g/m^3)	Similarity coefficient	Partition coefficient
PV	0	0.518	1000
PB	17.61	0.518	4325
Veneer	0	0.518	1000

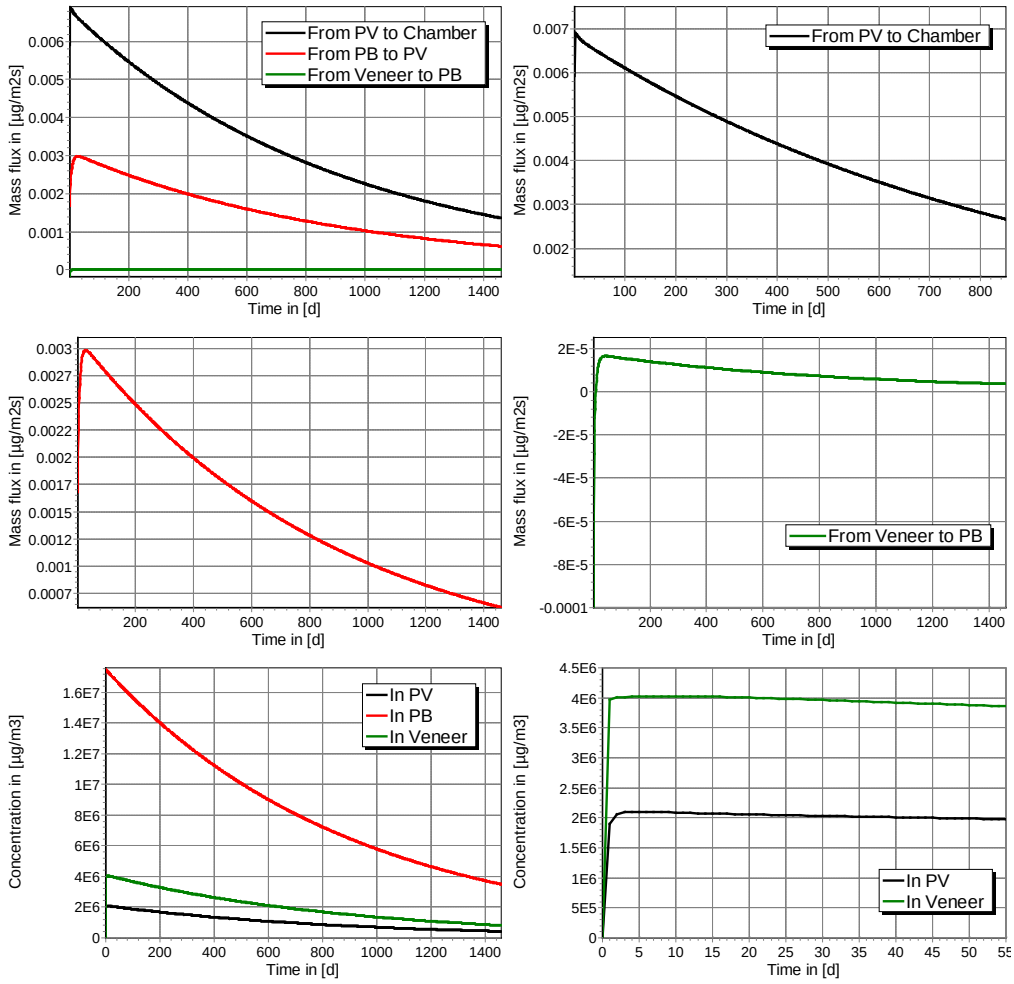

Figure 5.8 Simulation of acetaldehyde from worksurface: a,b,c,d for mass fluxes, and e, f for average concentration in the materials.

The acetaldehyde mass fluxes from veneer to particleboard, from particleboard to painted veneer and from painted veneer to chamber are plotted in the first graph of Fig. 5.10. We can see that the mass flux from painted veneer to chamber decreases with elapsed time in the entire emission period. The mass flux from particleboard to painted veneer increases with elapsed time in the first 20 days, and then decreased with elapsed time in the latter period. From fourth graph, we can see that the mass first diffuses from the particleboard to veneer, and then changes the direction in about 25 days. The reason is that: in the first 25 days, the acetaldehyde concentration in particleboard reached equilibrium with the acetaldehyde concentration in the veneer because of

zero initial concentration in the veneer, and then acetaldehyde in the veneer diffuses from veneer to particleboard.

The fifth and sixth graph showed that the concentration in painted veneer and veneer increased from zero to peak value in about 1 day, and then decreased with elapsed time.

5.7.2 Comaprison between multi-layer co-presence and single layer presence for hexanal

In some cases, one VOC exists either in one layer, as discussed in section 5.8.1. For some VOC, it may also exist simultaneously in three layers. These two cases are also studied together in this part. In case one, hexanal only exists in the particleboard, and in case two, hexanal exists in all three layers. The input parameters for these two scenarios are provided in Table 5.11 and 5.12. The simulation results are shown in Fig. 5.9.

Table 5.11 Simulation of hexanal in three layers- only particleboard has hexanal

Material	Initial concentration (g/m^3)	Similarity coefficient	Partition coefficient
PV	0[a]	0.518	1000[a]
PB	40.18	0.518	4419
Veneer	0[a]	0.518	1000[a]

Table 5.12 Simulation of hexanal in three layers: all layers have hexanal

Material	Initial concentration (g/m^3)	Similarity coefficient	Partition coefficient
PV	40.18[a]	0.518	1000[a]
PB	40.18	0.518	4419
Veneer	40.18[a]	0.518	1000[a]

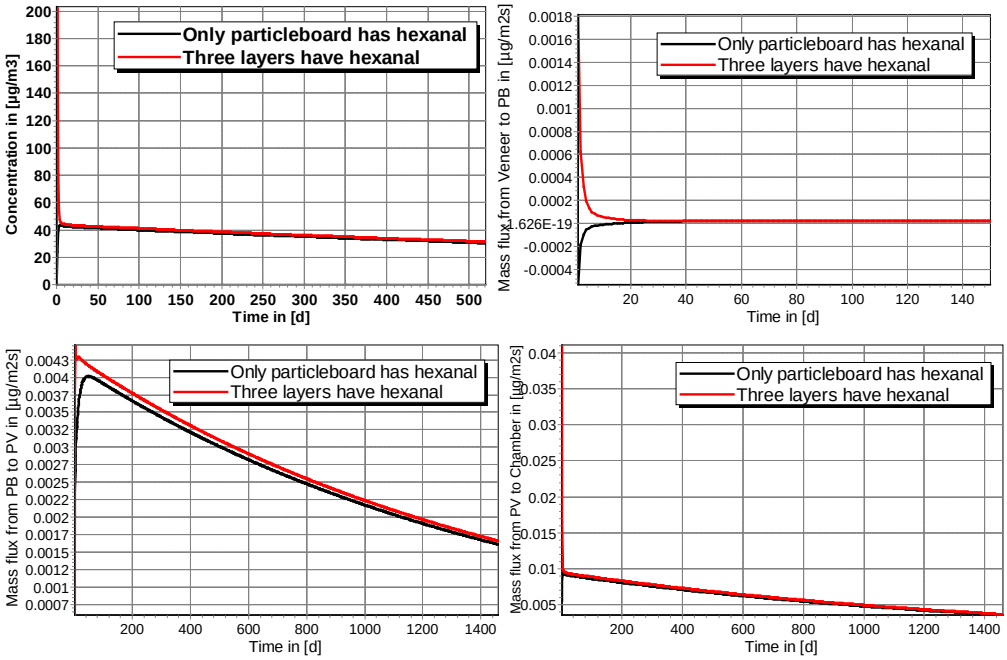

Figure 5.9 Simulation of hexanal in three layers and one layer

The first and fourth graphs of Fig. 5.9 show that there is not too much difference for the chamber concentration or mass flux of hexanal in two cases, which is consistent with the findings of previous parametric study. The second graph of Fig. 5.9 shows that the mass flux of hexanal from veneer to particleboard decreases with elapsed time when hexanal exists in three layers, which is different from the case when hexanal only exists in particleboard. The third graph of Fig. 5.9 shows that the mass flux from particleboard to painted veneer when hexanal exists in three layers (case 2) is higher than that when hexanal exists in only particleboard (case 1) during the first 20 days. It is because there is more hexanal in veneer and particleboard in case 2 than that in case 1.

5.7.3 Effect of painted veneer in reducing the emission rate from the worksurface

To study of the effect of painted veneer, two simulations were run. The first one is the emission test of acetaldehyde only in the particleboard. The second case is the emission of acetaldehyde from the whole worksurface. The input parameters are summarized in Table 5.13. The simulation results are presented in Fig. 5.10.

Table 5.13 Input parameters in the models to study the effect of painted veneer

Pure particleboard			
Material	Initial concentration (g/m^3)	Similarity coefficient	Partition coefficient
PB	40.18	0.518	4419
Three layered worksurface			
Material	Initial concentration (g/m^3)	Similarity coefficient	Partition coefficient
PV	0	0.518	1000[a]
PB	40.18	0.518	4419
Veneer	0	0.518	1000[a]

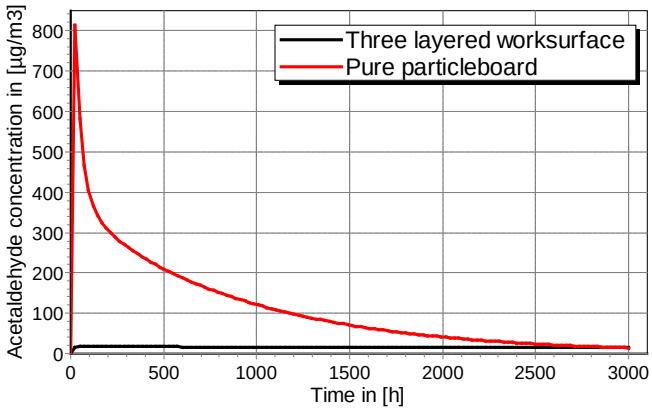

Figure 5.10 Comparison of chamber concentrations between pure particleboard and three layered worksurface

From the comparison of Fig. 5.10, we can see that the chamber concentration in the three layered worksurface is lower than that of the pure particleboard in the first 1600hours (67 days), but it is higher than that of the pure particleboard after 1600 hours. The existence of painted veneer prevents acetaldehyde emission from the particleboard in the first two months, but in the long term, it takes longer time to completely deplete the acetaldehyde from the worksurface than pure particleboard. If the purpose of adding additional layer on the top of a particleboard is to keep VOC emission below the target VOC concentration, then careful attention must be paid to select this additional layer with a very small diffusion coefficient, otherwise, though it will lower VOC concentration in the first two months, it lengthens the exposure time that residents are subject to.

5.7.4 Effect of source location on emission characteristics

The location of VOCs sources may affect the emission characteristics for the multilayer materials. In order to study the influence of source location on emission characteristics, three simulation cases were conducted. To eliminate the influences of material thickness and material type, in the simulation, one uniform material particleboard was assumed, and it was assumed that the particleboard was divided into three layers with the same thickness. It was assumed that the hexanal emitted from the top layer, middle layer and bottom layer, respectively. The area of the material was still in the dimension of 7.5" x7.5" and the total thickness was 30 mm (each layer was 10 mm). Four edges and bottom were sealed by the VOC-free tape, so no VOCs could diffuse through the tape. The amount of hexanal was the same in each case, and the only difference was the source location in the material. More detailed information was provided in Table 5.14.

Table 5.14 Simulation of effect of source location of hexanal on emission characteristics

Source location is top veneer			
Layer name	Initial concentration (g/m^3)	Similarity coefficient	Partition coefficient
Top layer	40.18	0.518	4419
Middle layer	0	0.518	4419
Bottom layer	0	0.518	4419
Source location is middle layer			
Layer name	Initial concentration (g/m^3)	Similarity coefficient	Partition coefficient
Top layer	0	0.518	4419
Middle layer	40.18	0.518	4419
Bottom layer	0	0.518	4419
Source location is bottom layer			
Layer name	Initial concentration (g/m^3)	Similarity coefficient	Partition coefficient
Top layer	0	0.518	4419
Middle layer	0	0.518	4419
Bottom layer	40.18	0.518	4419

Simulation results are given in Fig. 5.10. We can see that if the source location is in the bottom layer, then the peak concentration can be lowered greatly compared to that of the top layer. After 30 days elapsed time, VOC concentration for the source in the bottom layer case is lower than that either in the top layer or middle layer. In conclusion, though the VOC amount in the material is the same for all three cases, the source location does influence the VOC emission characteristics.

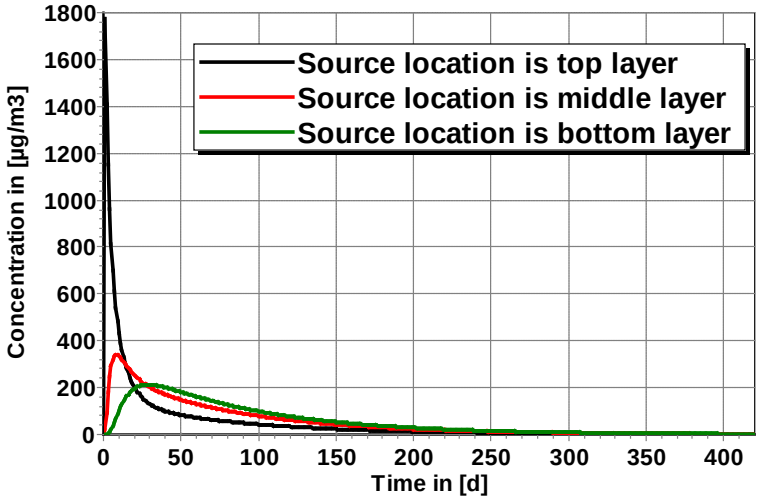

Figure 5.11 Effect of source location on emission characteristics

5.8 Conclusions

1. A numerical 1D multilayer model that can simulate VOCs emissions from porous media was developed. The model can be used to simulate the VOCs emission from one layered or multilayered building/furniture materials.

2. The one layer case of the model was verified by one layer analytical solution, and it showed good agreement between the developed model and the one layer analytical solution. The multilayered case was validated by the experimental emission test of the worksurface.

3. Parametric studies of the influence of similarity coefficient, partition coefficient and initial concentration of VOC on the emission rate of worksurface has been conducted. The

studies showed that the initial concentration and partition coefficient of VOC in painted veneer were not the dominant factor in determining the emission rate of VOC from the entire worksurface. All three parameters of VOC in veneer had also very minor effect on the total emission rate. The main reason was that the thickness and volume of painted veneer and veneer was too small compared to core particleboard. However, the diffusion coefficient of VOC in painted veneer played a big role in determining the entire emission rate.

4. The model can be applied to many real scenarios, and can be potentially used to solve the relevant problems encountered in the manufacturing, e.g., what outer layers may be necessary to limit the emissions from the particle core of the assembly; the VOCs emission characteristics of the multilayer wood assembly; the VOCs distribution with elapsed time in each layer of the assembly.

Chapter 6 Conclusions and Recommendations

6.1 Summary and conclusions

The first part of this research investigated the similarity between water vapor and VOC transport, and the ultimate goal was to build a database of mechanistic emission model parameters for the simulation of VOC emission from different materials in both the short term and the long term. The following major conclusions can be drawn from this part of the study:

1) The dynamic dual chamber method developed to measure both water vapour and VOCs diffusion through porous building materials and furniture materials had good repeatability. Effective diffusion coefficients and partition coefficients were obtained independently, with uncertainties of 6.96% and 3.35%, respectively.

2) The water vapor diffusivity measured using the dual chamber method were in reasonable agreement with that measured by the conventional "dry cup method" for water vapor transmission tests for the range of relative humidity 25%~80% RH. The VOC diffusivity measured by the dual chamber method was comparable to that measured by the mercury intrusion porosimetry method.

3) The differences between three definitions of effective, apparent, and pore diffusion coefficients were elucidated. The relationships between these three diffusion coefficients were also established.

4) A similarity coefficient was proposed to correlate the pore diffusion coefficient of VOCs with that of water vapor for hygroscopic moisture conditions in which open pore porosity did not change significantly. Values of the similarity coefficients were determined for formaldehyde, toluene, acetaldehyde, benzaldehyde, hexanal, butanol and decane for a reference material-- calcium silicate. The similarity coefficient could be used to estimate the VOC diffusion coefficient if the water vapor diffusivity was known for the same

material based on the conventional "dry cup method". The application of similarity theory in particleboard was also validated by the comparison of measured acetaldehyde and hexanal emission in a small chamber with a simulated concentrations.

5) An approach for establishing the database of model parameters by using the similarity theory and properties of VOCs and materials was established.

6) The material characterizations for calcium silicate and particleboard were also obtained in the material characterization of CHAMPS-BES. The materials can be used for simulations of VOCs emission in the future.

The second part of this research investigated the effects of relative humidity on the effective diffusion coefficient and partition coefficient of VOCs in porous media. The same dynamic dual chamber system was used. Additional experiments were also conducted to investigate the repeatability of tests, mixture effects, and the relationship between physicochemical properties of VOCs and the effective diffusion coefficient/partition coefficient of VOCs in porous media. Tests at 25%, 50% and 80%RH were conducted for calcium silicate, while tests at 20%, 50%, and 70%RH were conducted for conventional gypsum wallboard, "green" gypsum wallboard and "green" carpet. Major conclusions are described below.

For calcium silicate:

1. The test method showed good repeatability for the measurement of diffusion coefficients and partition coefficients of formaldehyde, acetaldehyde and toluene in calcium silicate at 50%RH.

2. Humidity's effect on the diffusion coefficient of formaldehyde and toluene in calcium silicate was not significant in the hygroscopic range from 25%RH to 80%RH, where blocking of diffusion paths due to capillary condensation was minimal.

3. The partition coefficient of formaldehyde (a water soluble compound) in calcium silicate did not change when humidity increased from 25%RH to 50%RH, but it increased by 56% when humidity increased from 50%RH to 80%RH. The increase of the partition coefficient of formaldehyde was likely because formaldehyde molecule was absorbed into the significantly more adsorbed water under the 80%RH condition. The partition coefficient of toluene (a water non-soluble compound) decreased slightly with increasing humidity conditions from 25%RH to 80%RH. This was possibly because of the competition of water vapor molecules for available adsorption sites with toluene molecules.

4. In the test of a mixture of formaldehyde and toluene, the effective diffusion coefficient of formaldehyde was smaller and the partition coefficient of formaldehyde was larger than in single compound tests. It was not clear what could have caused such a phenomenon and further investigation was needed. Both the effective diffusion and partition coefficients of toluene did not differ significantly in the mixture test compared to the toluene only test.

5. Besides vapor pressure, the solubility of VOC was also one factor that influenced the partition coefficient of VOC. The partition coefficient of VOCs was not simply inversely proportional to the vapor pressure of the compound, but also increased with a higher Henry's law constant. At a relatively high relative humidity where moisture content is significant in the material, the partition coefficient of a water-soluble compound such as formaldehyde was found to depend on the Henry's law constant as well as vapor pressure. Further study is needed to establish the relationship between them.

For conventional gypsum wallboard, "green" gypsum wallboard and "green" carpet:

1) The test method had good repeatability as verified by the duplicate tests for conventional wallboard at 50% RH.

2) A higher relative humidity led to a larger effective diffusion coefficient for both conventional wallboard and green wallboard.

3) The partition coefficient of formaldehyde in conventional wallboard became larger from 20% RH to 50% RH, while the relative humidity effect was insignificant from 50% RH to 70% RH, considering that the decrease was less than 3 times the experimental uncertainty.

4) The partition coefficient of formaldehyde in "green" wallboard and carpet increased slightly with the increase of relative humidity, probably due to the soluble nature of formaldehyde, which was absorbed more into the adsorbed moisture at a higher relative humidity.

5) The effective diffusion coefficient and partition coefficient of green wallboard at each level of relative humidity were significantly larger than the ones of conventional wallboard. The slightly lower temperature in the "green" wall board than in the conventional wall board tests (21 vs. 23 °C) contributed, but may or may not be responsible for all of the difference, which requires further investigation.

6) The carpet specimen was highly permeable and the measured diffusion coefficients at 20% RH, 50% RH and 70% RH were all at a similar level compared to the formaldehyde diffusion coefficient in dry air at 23 ^{o}C, and had insignificant differences among the different RH conditions. The partition coefficient, however, increased slightly with an increase in the RH level.

The third part of this study focused on the numerical multilayer model development. Parametric studies were used to help determine the diffusion coefficient, partition coefficient and initial VOC concentration. The model was verified by experiment data from both individual layer tests and multilayer tests. Major conclusions are summarized below.

1) The numerical model can be used to simulate the VOCs emission from single-layered and multilayered building/furniture materials.

2) The single layer simulation result from the numerical model was verified by an analytical solution with good agreement between the two solutions. The multilayered case was also validated by an experimental emission test of a work surface assembly.

3) Parametric studies of the influences of the similarity coefficient, partition coefficient and initial concentration of VOC on the emission rate of worksurface were conducted. The studies showed that the initial concentration and partition coefficient of VOC in painted and unpainted veneer were not the dominant factors in determining the emission rate of a VOC from the entire worksurface. The main reason was that the thickness and volume of painted veneer and veneer was 2 orders of magnitude smaller than the core material (particleboard). However, the diffusion coefficient of a VOC in painted veneer played a big role in determining the entire emission rate. All three parameters of VOCs in the unpainted veneer had a very minor effect on the total emission rate when a non-permeable boundary condition was applied on the veneer surface. Three critical parameters, Co, D and K of each layer were determined based on the experimental data and the findings of parametric studies.

4) The multilayer model was applied to several realistic scenarios, and the simulation of acetaldehyde from the worksurface showed that the mass flux from painted veneer to the chamber decreased with elapsed time over the entire emission period. The mass flux from particleboard to painted veneer increased with elapsed time during the first 20 days, and then decreased with elapsed time in the later period. The acetaldehyde mass first diffused from the particleboard to the veneer, and then changed the flux direction in about 25 days. The reason was that in the first 25 days, acetaldehyde from the particleboard first

saturated the veneer, and then acetaldehyde in the veneer diffused out of its material into the particleboard.

5) The simulation of hexanal in a particleboard only case and in three layers of worksurface showed that (1) there was not too much difference for the chamber concentration or mass flux of hexanal in the two cases. (2) The mass flux of hexanal from veneer to particleboard decreased with elapsed time when hexanal existed in three layers, which was different from the case when hexanal only existed in particleboard. (3) The mass flux from particleboard to painted veneer when hexanal existed in three layers was higher than that when hexanal existed in only particleboard during the first 20 days. It was because there was more hexanal in the veneer and particleboard in three layers than that in only a particleboard layer.

6) The simulation also showed the possibility of reducing the VOCs concentration by adding an additional layer on the top of VOCs source layer. However, careful attention should be paid to select an additional layer with a proper diffusion coefficient. Otherwise, the extended emission time caused by adding additional layers may affect the health of residents in the room.

7) The location of VOC source influences the emission characteristics greatly, so it is useful to determine the best position for the VOC source based on the analysis of this multilayer modelling.

6.2 Recommendations for future research

The following subjects are recommended for future research on characterizing and predicting VOC emissions from building materials and furnishings:

1. To generalize the similarity theory, it would be helpful to conduct further experiments for more kinds of VOCs in several more porous materials. In addition, the water vapor transport in such porous materials should be further compared with VOC transport.

2. It would be interesting to further study when the surface diffusion would be significant in indoor air conditions. It would also be valuable if the diffusion coefficient of surface diffusion for the important VOCs in porous media could be quantified exactly. Those values would provide more accurate information than estimated values in interpreting the experimental results.

3. A relative shorter experimental method for the determination of diffusion and partition coefficient is needed in the future. Using the current dynamic dual chamber method, for acetaldehyde and toluene in calcium silicate, the tests can be finished in one day. However, for butanol and benzaldehyde in calcium silicate, it takes about 2 weeks to complete the measurement. It is also expected that the test will take much longer for materials with larger diffusion resistance such as particleboard, plywood or Oriented Strand Board (OSB). It would be worthwhile to reduce the test period in the future both to save time and to reduce cost.

4. A possible efficient way to measure partition coefficients is to use either static(Smith et al. 2008) or dynamic small chamber tests (Zhang et al. 2002), and then obtain the VOC concentrations in both the gas phase and the material phase. The partition coefficient can be calculated by those two concentrations. The size of the material should be small enough so that a relative shorter time is needed to reach steady sate.

5. Only random error was considered for the measurement of VOC concentrations since the effective diffusion coefficient and partition coefficient were not affected by the absolute value of the VOC concentrations. However, it would be more convincing that

an approach needs to be developed in the future to give a more complete account of all the uncertainty factors involved in such experiments.

6. For the effect of relative humidity on the diffusion and partition coefficients, it would be very worthwhile to develop a mathematical model to calculate the effect of humidity on those parameters. Further study on the underlying mechanisms of the humidity effect is also needed.

7. To further study the competition between VOCs molecular and water vapor molecule, it is suggested that more tests about transport and storage for mixtures in porous media be done.

8. More study is needed to quantify the exact relationship of the partition coefficients of VOCs with their corresponding Henry's law constants.

9. The incorporation of a relative humidity effect is recommended for the source code of CHAMPS-BES; if added, it can be used to cover the humidity effect in the simulation.

10. The developed multilayered model can be used for other common multilayered structures such as walls, floors, and cabinets, and it can also be used to analyze the emission characteristics for more complicated cases like having both top and bottom layers exposed to air.

11. The simulation of the VOC emissions from complicated workstation systems is also suggested in the future, which will reduce or replace full scale chamber tests for the workstation system.

Appendices

Appendix A VOC database

```
# VOC Database File
#
#
# Note: Lines beginning with a hash character '#' are comments and ignored
#
# The first table contains the VOC data with the following format:
#
# ENTITY <string: VOC name>
#       <string: alternative descriptive name(s)>
#       <string: molecular formula>
#       <double: molar weight in kg/mol>
#       <double: liquid density of the VOC in [kg(VOC)/m3(VOC)]>
#       <double vec: temperatures for saturation densities in K>
#       <           saturation densities in kg/m3(gas)>
#       <double vec: temperatures for diffusion coefficients in K>
#       <           diffusion coefficients in air in m2/s>
#
# Use the keyword 'undefined' for all _string_ entries to indicate missing information
#
# For constant "linear splines" simply store one x and one y value.


TABLE: VOC_DATA

ENTITY Formaldehyde
        50-00-0
        CH2O
        3.00E-02
        1083
        253.15  258.15  263.15  268.15  273.15  278.15  283.15  288.15  293.15  296.15  298.15
        303.15  308.15  313.15  318.15  323.15  328.15  333.15
        1.393E+00     1.698E+00     2.052E+00     2.458E+00     2.922E+00     3.449E+00
        4.042E+00     4.707E+00     5.447E+00     5.930E+00     6.268E+00     7.173E+00
        8.166E+00     9.252E+00     1.043E+01     1.171E+01     1.310E+01     1.459E+01

        296.15  306.15 316.15
        1.455E-05   1.6E-05   1.8E-05

ENTITY Toluene
        108-88-3, methylbenzene, phenylmethane, toluol
        C7H8
        9.21E-02
        865
        253.15  258.15  263.15  268.15  273.15  278.15  283.15  288.15  293.15  296.15  298.15
        303.15  308.15  313.15  318.15  323.15  328.15  333.15
```

9.532E-03 1.366E-02 1.924E-02 2.665E-02 3.635E-02 4.888E-02
6.485E-02 8.497E-02 1.100E-01 1.278E-01 1.409E-01 1.787E-01
2.243E-01 2.791E-01 3.442E-01 4.211E-01 5.112E-01 6.161E-01

296.15
7.280E-06

ENTITY n-Butanol
71-36-3
C4H10O
7.41E-02
810
253.15 258.15 263.15 268.15 273.15 278.15 283.15 288.15 293.15 296.15 298.15
303.15 308.15 313.15 318.15 323.15 328.15 333.15
3.694E-04 6.622E-04 1.146E-03 1.919E-03 3.122E-03 4.942E-03
7.630E-03 1.151E-02 1.700E-02 2.128E-02 2.463E-02 3.502E-02
4.896E-02 6.738E-02 9.136E-02 1.222E-01 1.614E-01 2.105E-01

296.15
7.838E-06

ENTITY Hexanal
66-25-1
C6H12O
1.00E-01
818
253.15 258.15 263.15 268.15 273.15 278.15 283.15 288.15 293.15 296.15 298.15
303.15 308.15 313.15 318.15 323.15 328.15 333.15
2.604E-03 3.878E-03 5.669E-03 8.146E-03 1.152E-02 1.604E-02
2.201E-02 2.981E-02 3.985E-02 4.716E-02 5.264E-02 6.874E-02
8.882E-02 1.136E-01 1.439E-01 1.806E-01 2.247E-01 2.774E-01

296.15
6.672E-06

ENTITY Acetaldehyde
75-07-0
C2H4O
4.41E-02
780
253.15 258.15 263.15 268.15 273.15 278.15 283.15 288.15 293.15 296.15 298.15
303.15 308.15 313.15 318.15 323.15 328.15 333.15
3.669E-01 4.596E-01 5.710E-01 7.038E-01 8.610E-01 1.046E+00
1.262E+00 1.513E+00 1.803E+00 1.997E+00 2.136E+00 2.517E+00
2.950E+00 3.441E+00 3.993E+00 4.614E+00 5.307E+00 6.080E+00

296.15
1.109E-05

The next table contains properties for a combination of materials and VOCs
with the following format:
#
ENTITY
<VOC name>
<Material ID name>
<double: diffusion resistance correction factor(similarity coefficient)>
<double: partition coefficient>

TABLE: VOC_MATERIAL_DATA

ENTITY
Formaldehyde
Calcium silicate
0.52
2597

ENTITY
Toluene
Calcium silicate
0.56
133

ENTITY
n-Butanol
Calcium silicate
0.32
18100

ENTITY
Hexanal
Calcium silicate
0.49
7809

ENTITY
Hexanal
Particleboard
0.518
4419

ENTITY
Acetaldehyde
Calcium silicate
0.48
221

ENTITY
Acetaldehyde
Particleboard

0.518
4325

ENTITY
Benzaldehyde
Calcium silicate
0.19
16111

Appendix B Individual Test Results for conventional gypsum board, "Green" gypsum wallboard and "Green" carpet

Material: Conventional wallboard

Relative humidity: 20%RH

Chamber Operating Conditions

Temperature:	73.4 °F (23 °C)
Relative humidity (%):	20% RH
Air mixing:	~100%
Air leakage calculation:	difference between outflow and inflow of each chamber

- CALIBRATIONS:

Calibration curve of PTRMS against HPLC:

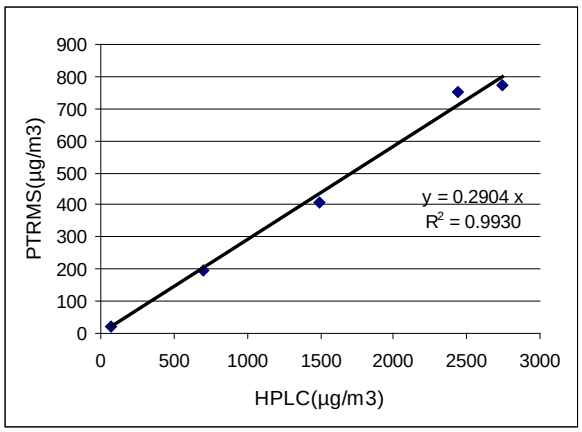

- TEST RESULTS

1) Concentrations for C_{Ain}, C_{Aout} and C_{Bout} during the test:

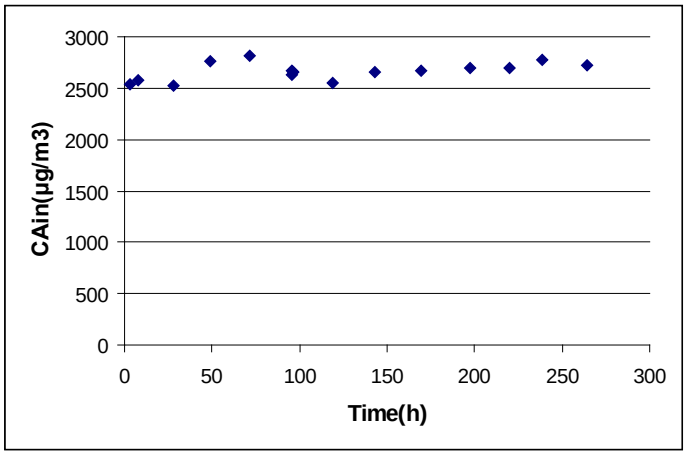

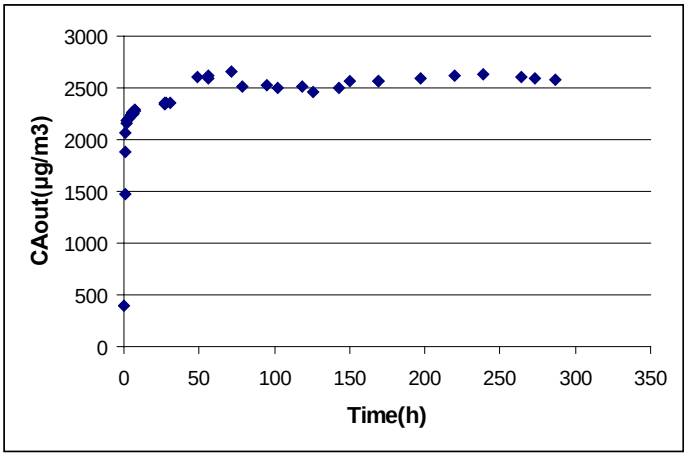

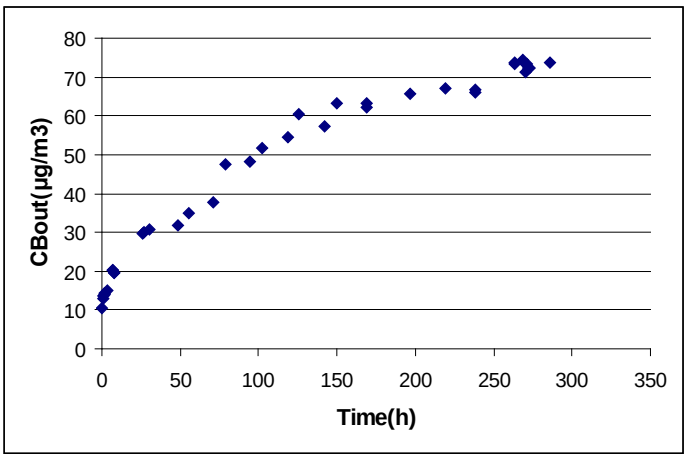

2) The calculated effective diffusion coefficient and partition coefficient are:

Effective diffusion coefficient $D_e(m^2/s)$	$3.67x10^{-8}$
Partition coefficient K_{ma}	304

Material: Conventional wallboard

Relative humidity: 50%RH

Chamber Operating Conditions –

Temperature:	73.4 ºF (23 ºC)
Relative humidity (%):	50% RH
Air mixing:	~100%
Air leakage calculation:	difference between outflow and inflow of each chamber

- CALIBRATIONS:

Calibration curve of PTRMS against HPLC:

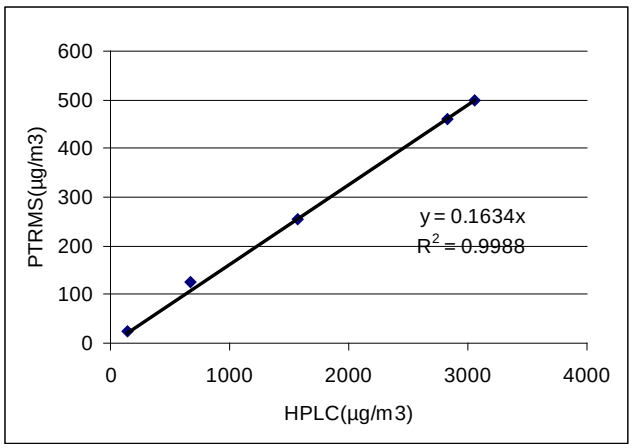

- TEST RESULTS:

1) Concentrations for C_{Ain}, C_{Aout} and C_{Bout} during the test:

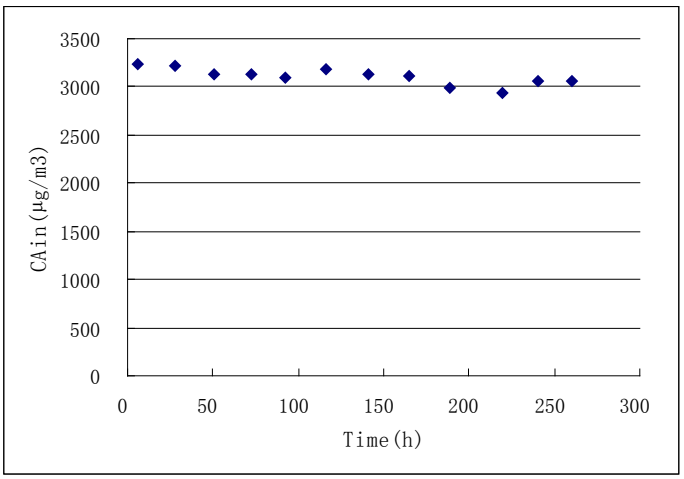

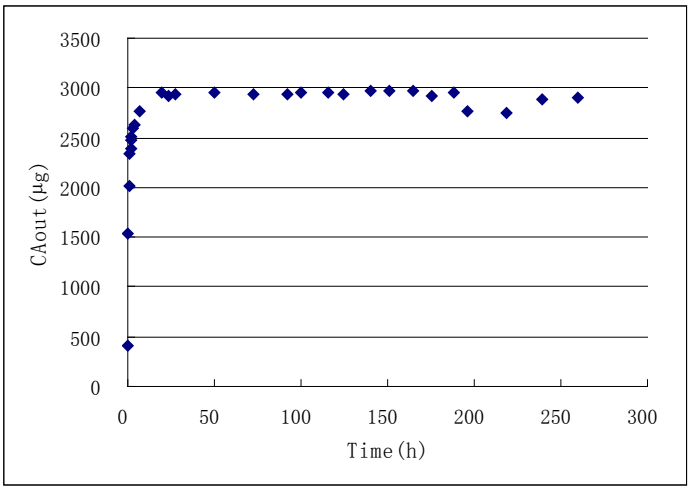

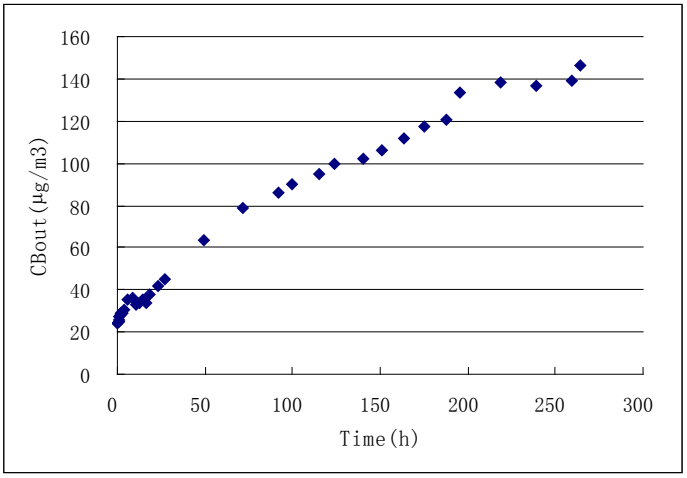

2) The calculated effective diffusion coefficient and partition coefficient are:

Effective diffusion coefficient $D_e(m^2/s)$	6.34×10^{-8}
Partition coefficient K_{ma}	446

Material: Conventional wallboard

Relative humidity: 50%RH (repeat)

Chamber Operating Conditions –

Temperature:	73.4 ºF (23 ºC)
Relative humidity (%):	50% RH
Air mixing:	~100%
Air leakage calculation:	difference between outflow and inflow of each chamber

- CALIBRATIONS:

Calibration curve of PTRMS against HPLC:

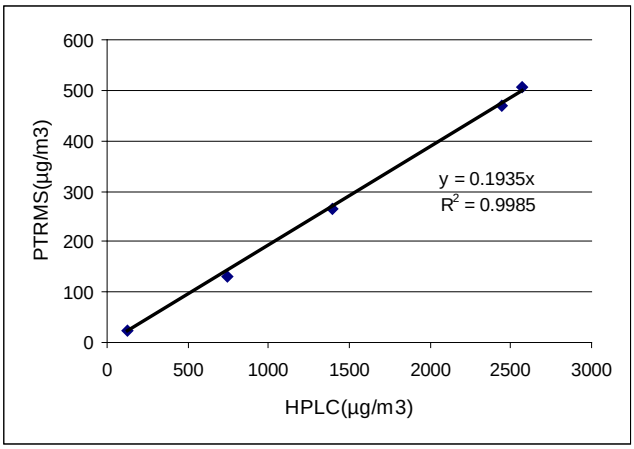

- TEST RESULTS:

1) Concentrations for C_{Ain}, C_{Aout} and C_{Bout} during the test:

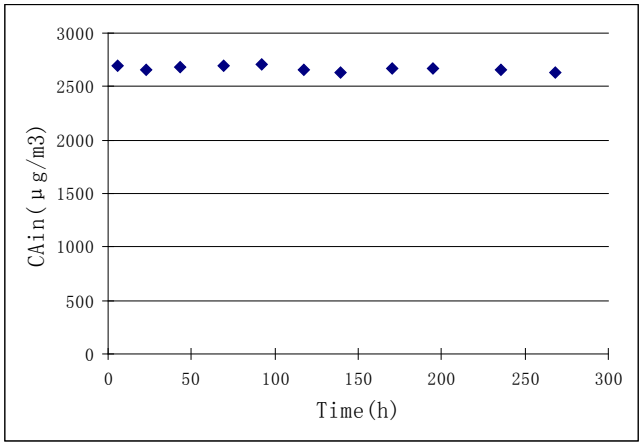

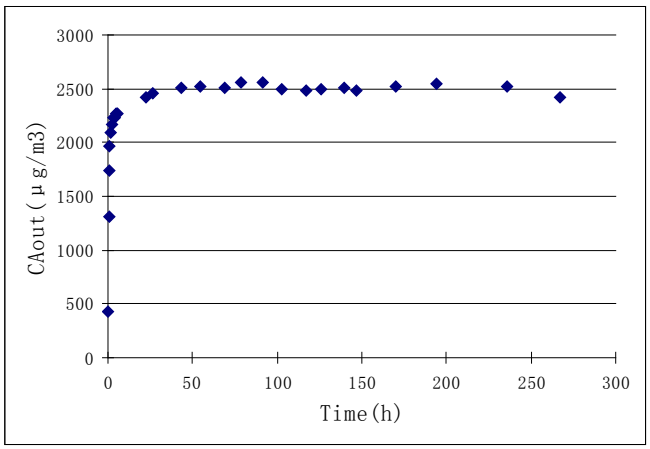

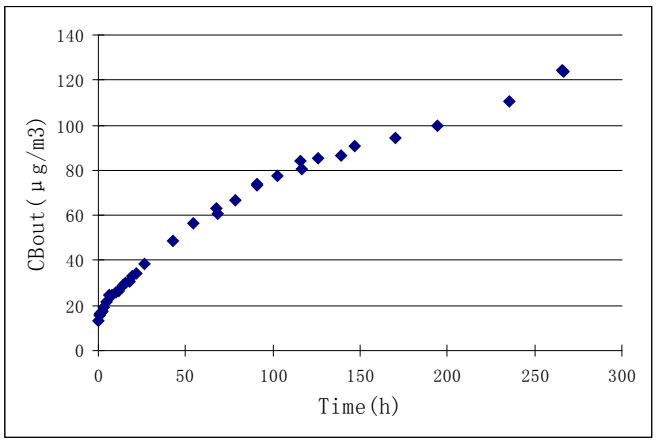

2) The calculated effective diffusion coefficient and partition coefficient are:

Effective diffusion coefficient $D_e(m^2/s)$	$6.61x10^{-8}$
Partition coefficient K_{ma}	479

Material: Conventional wallboard

Relative humidity: 70%RH

Chamber Operating Conditions –

Temperature:	73.4 ºF (23 ºC)
Relative humidity (%):	70% RH
Air mixing:	~100%
Air leakage calculation:	difference between outflow and inflow of each chamber

- CALIBRATIONS:

Calibration curve of PTRMS against HPLC:

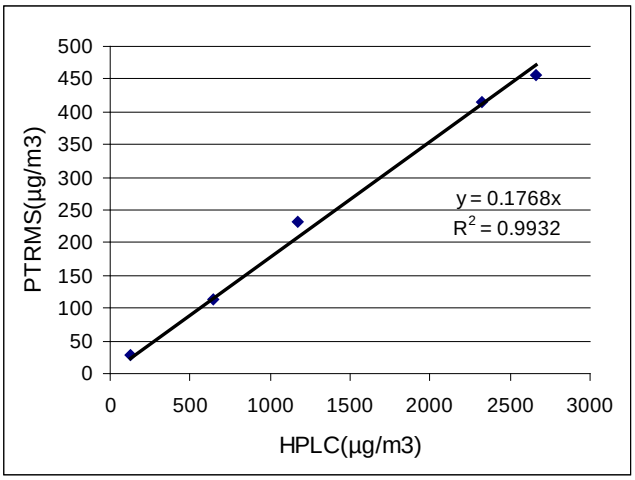

- TEST RESULTS:

1) Concentrations for C_{Ain}, C_{Aout} and C_{Bout} during the test:

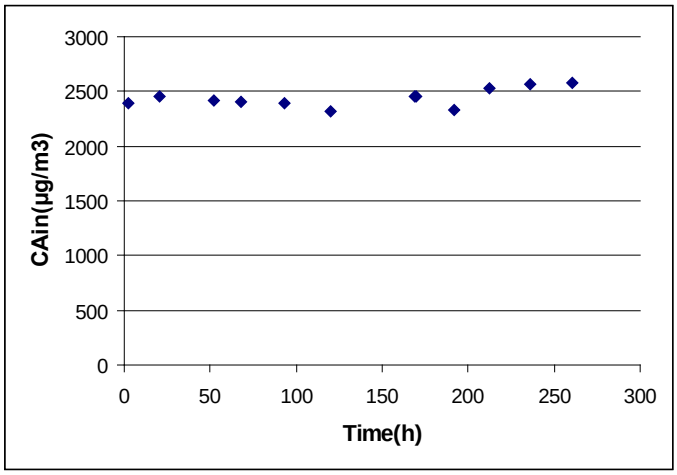

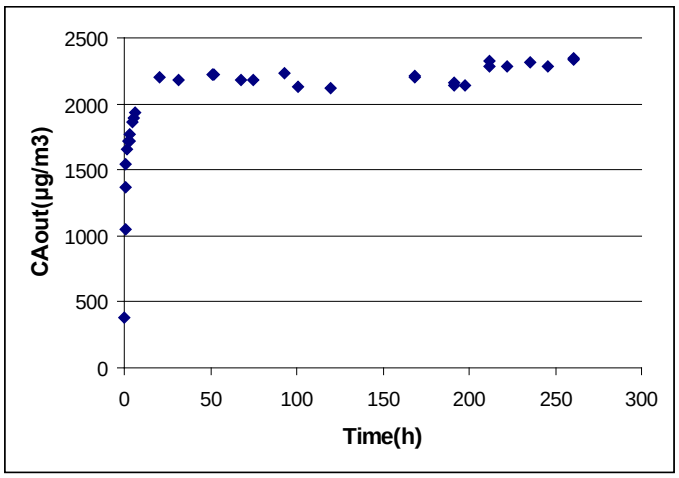

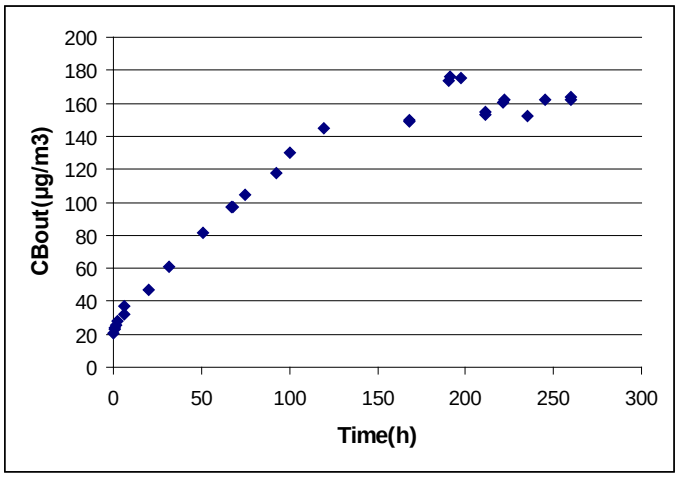

2) The calculated effective diffusion coefficient and partition coefficient are:

Effective diffusion coefficient $D_e(m^2/s)$	$9.84x10^{-8}$
Partition coefficient K_{ma}	404

Material: Green wallboard

Relative humidity: 20%RH

Chamber Operating Conditions –

Temperature:	73.4 ºF (23 ºC)
Relative humidity (%):	20% RH
Air mixing:	~100%
Air leakage calculation:	difference between outflow and inflow of each chamber

- CALIBRATIONS:

Calibration curve of PTRMS against HPLC:

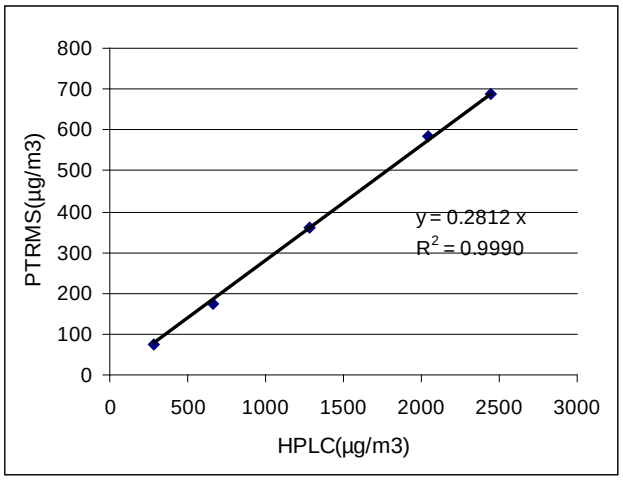

- TEST RESULTS:

1) Concentrations for C_{Ain}, C_{Aout} and C_{Bout} during the test:

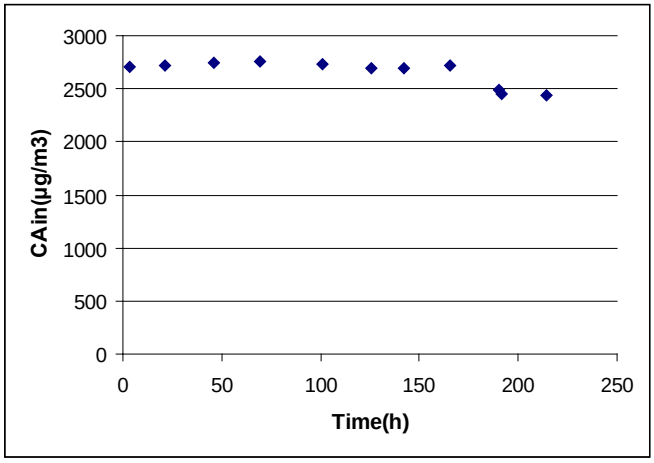

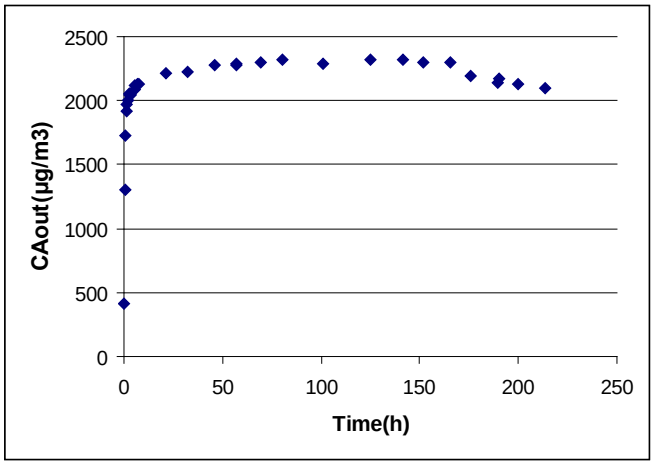

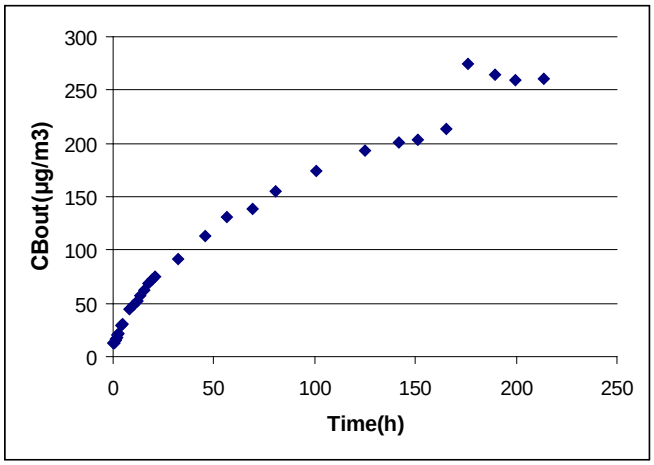

2) The calculated effective diffusion coefficient and partition coefficient are:

Effective diffusion coefficient $D_e(m^2/s)$	$1.65x10^{-7}$
Partition coefficient K_{ma}	1100

Material: Green wallboard

Relative humidity: 50%RH

Chamber Operating Conditions –

Temperature: 73.4 ºF (23 ºC)

Relative humidity (%): 50% RH

Air mixing: ~100%

Air leakage calculation: difference between outflow and inflow of each chamber

- CALIBRATIONS:

Calibration curve of PTRMS against HPLC:

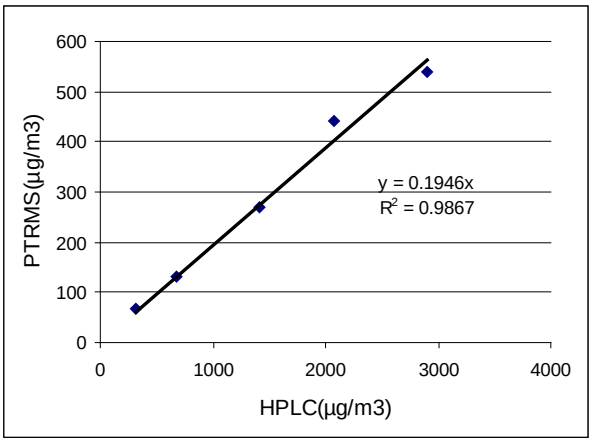

- TEST RESULTS:

1) Concentrations for C_{Ain}, C_{Aout} and C_{Bout} during the test:

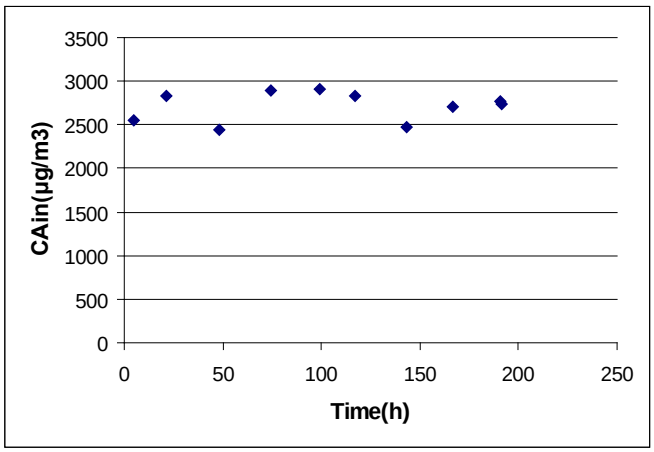

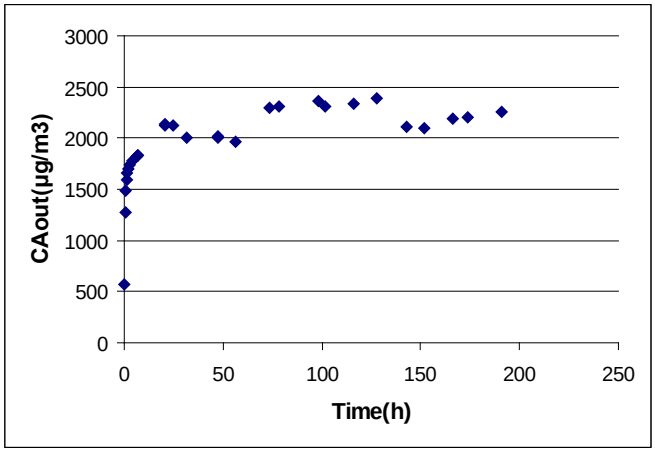

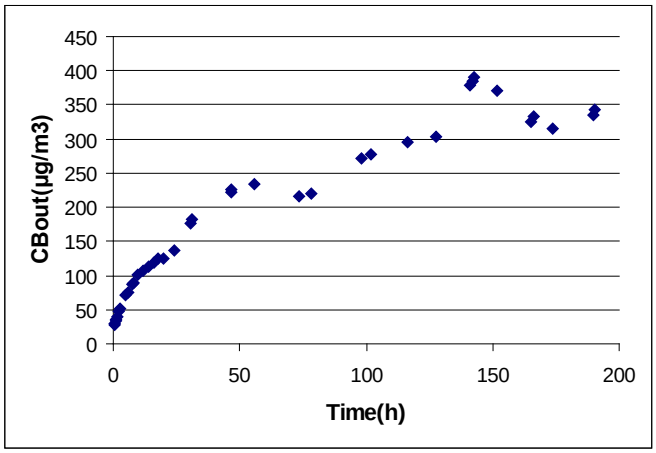

2) The calculated effective diffusion coefficient and partition coefficient are:

Effective diffusion coefficient $D_e(m^2/s)$	$2.24x10^{-7}$
Partition coefficient K_{ma}	1205

Material: Green wallboard

Relative humidity: 70%RH

Chamber Operating Conditions –

Temperature:	73.4 ºF (23 ºC)
Relative humidity (%):	70% RH
Air mixing:	~100%
Air leakage calculation:	difference between outflow and inflow of each chamber

- CALIBRATIONS:

Calibration curve of PTRMS against HPLC:

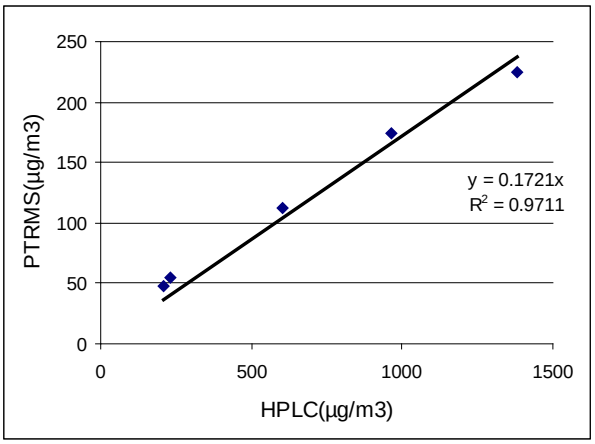

- TEST RESULTS:

1) Concentrations for C_{Ain}, C_{Aout} and C_{Bout} during the test:

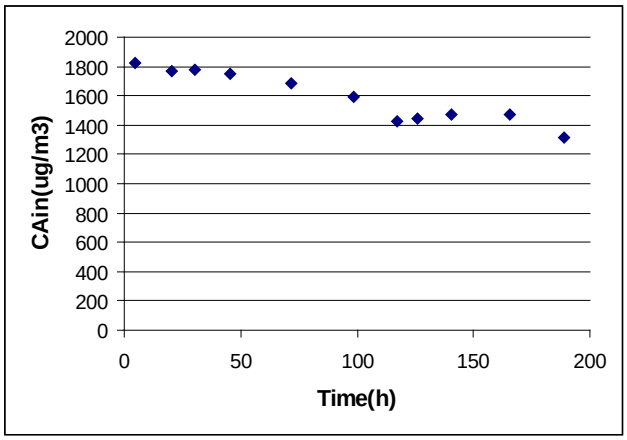

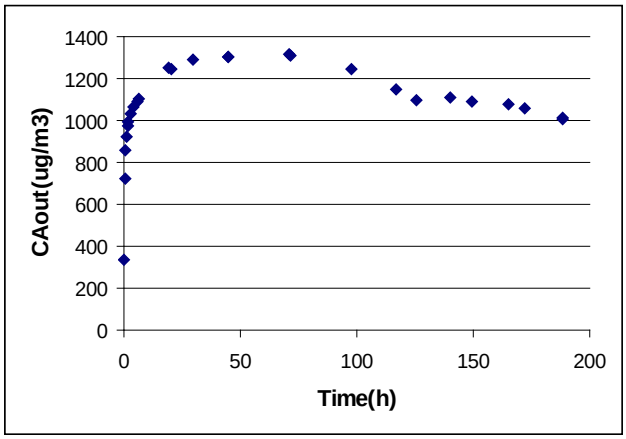

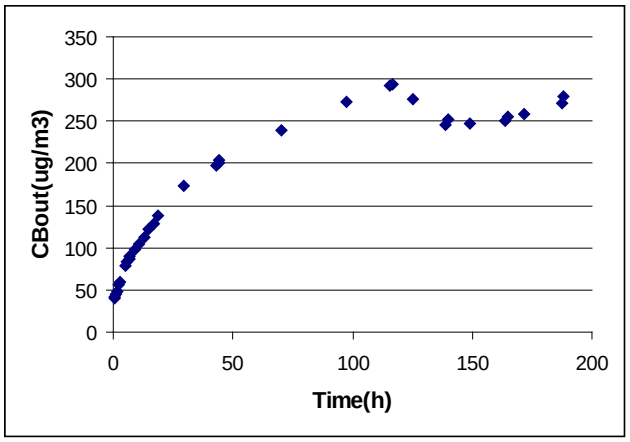

2) The calculated effective diffusion coefficient and partition coefficient are:

Effective diffusion coefficient $D_e(m^2/s)$	$4.73x10^{-7}$
Partition coefficient K_{ma}	1325

Material: Green carpet

Relative humidity: 20%RH

Chamber Operating Conditions –

Temperature: 73.4 ºF (23 ºC)

Relative humidity (%): 20% RH

Air mixing: ~100%

Air leakage calculation: difference between outflow and inflow of chamber A while the inflow and outflow of chamber B were blocked

- CALIBRATIONS:

Calibration curve of PTRMS against HPLC:

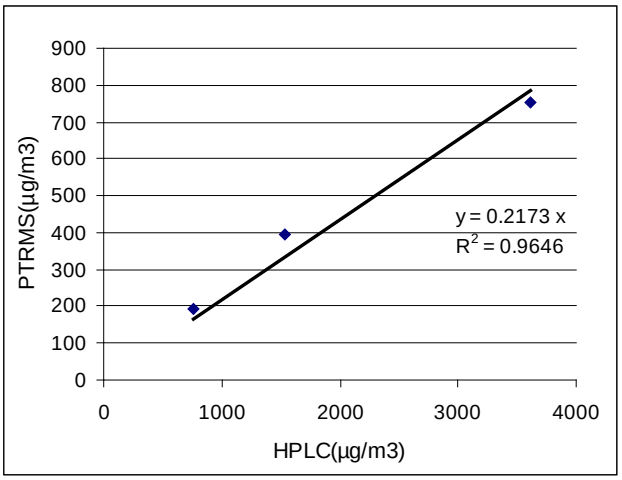

- TEST RESULTS:

1) Continuous pressure drop monitoring in the test:

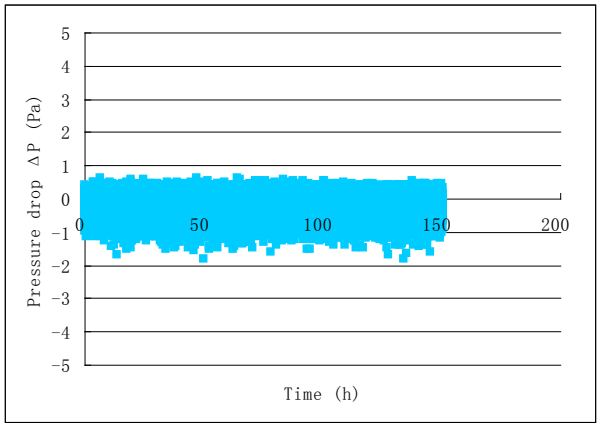

2) Concentrations for C_{Ain}, C_{Aout} and C_{Bout} during the test:

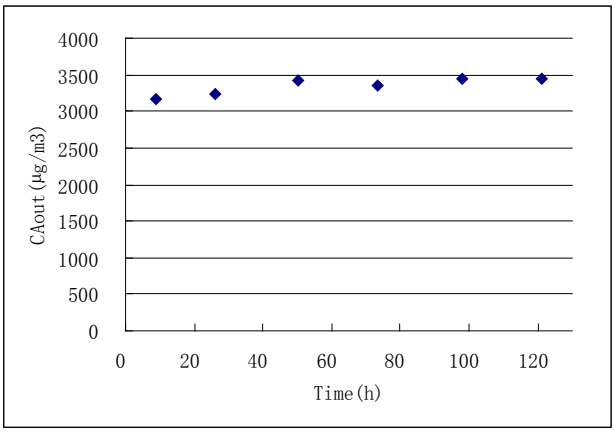

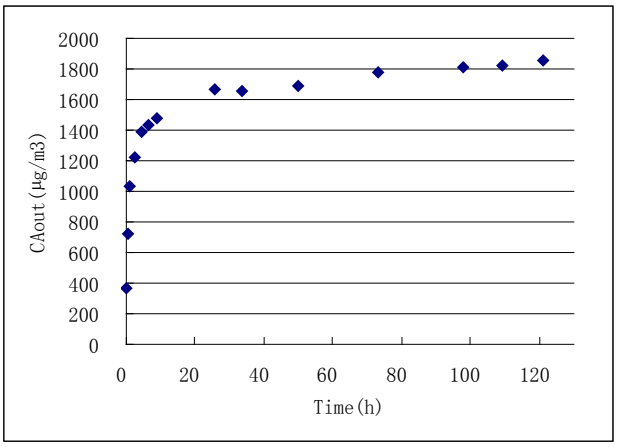

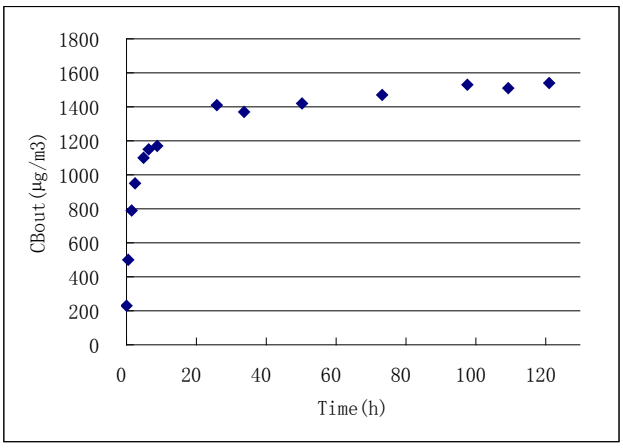

3) The calculated effective diffusion coefficient and partition coefficient are:

Effective diffusion coefficient $D_e(m^2/s)$	$1.56x10^{-5}$
Partition coefficient K_{ma}	471

Material: Green carpet

Relative humidity: 50%RH

Chamber Operating Conditions –

Temperature: 73.4 ºF (23 ºC)

Relative humidity (%): 50% RH

Air mixing: ~100%

Air leakage calculation: difference between outflow and inflow of chamber A while the inflow and outflow of chamber B were blocked

- CALIBRATIONS:

Calibration curve of PTRMS against HPLC:

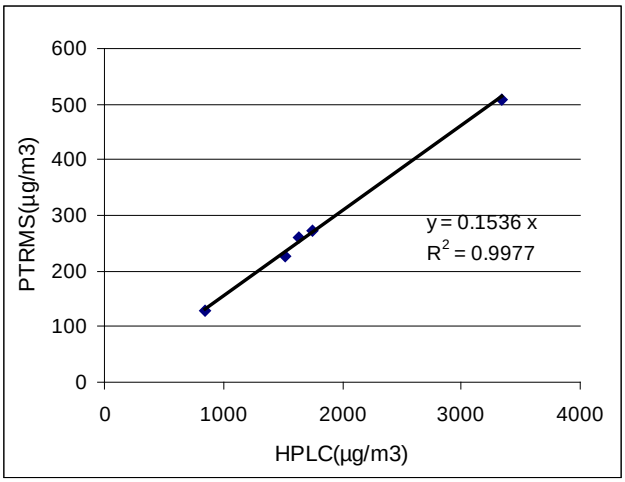

- TEST RESULTS:

1) Continuous pressure drop monitoring in the test:

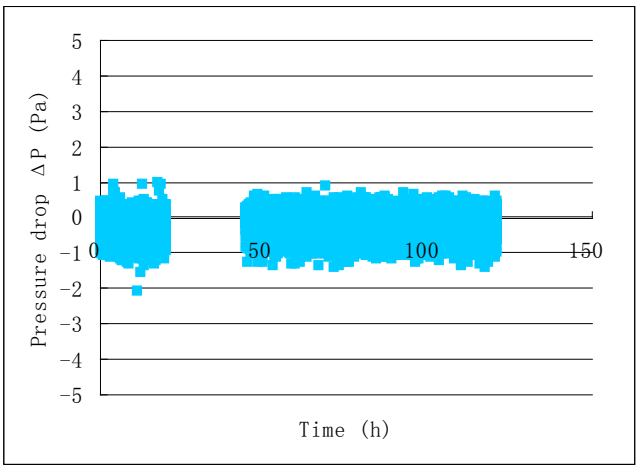

2) Concentrations for C_{Ain}, C_{Aout} and C_{Bout} during the test:

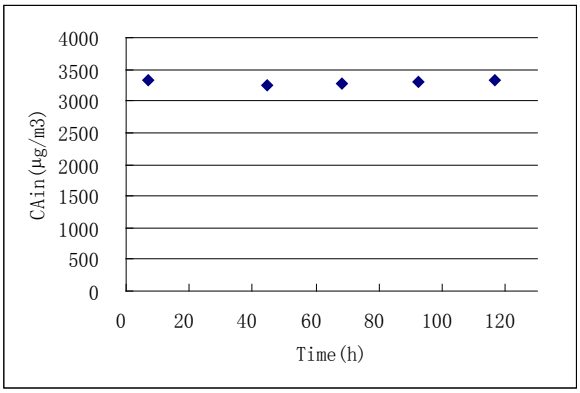

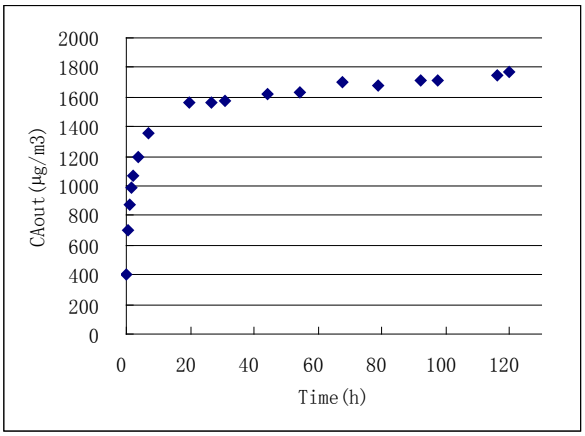

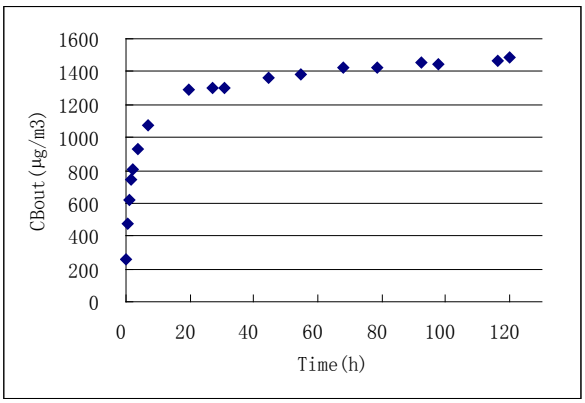

3) The calculated effective diffusion coefficient and partition coefficient are:

Effective diffusion coefficient $D_e(m^2/s)$	$1.71x10^{-5}$
Partition coefficient K_{ma}	661

Material: Green carpet

Relative humidity: 70%RH

Chamber Operating Conditions –

Temperature:	73.4 ºF (23 ºC)
Relative humidity (%):	70% RH
Air mixing:	~100%
Air leakage calculation:	difference between outflow and inflow of chamber A while the inflow and outflow of chamber B were blocked

- CALIBRATIONS:

Calibration curve of PTRMS against HPLC:

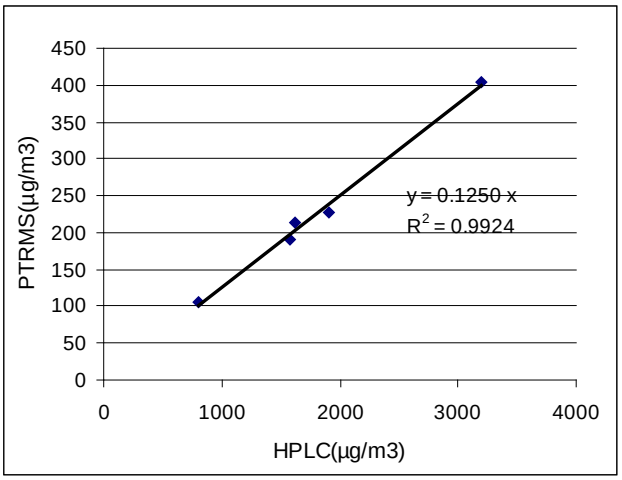

- TEST RESULTS:

1) Continuous pressure drop monitoring in the test:

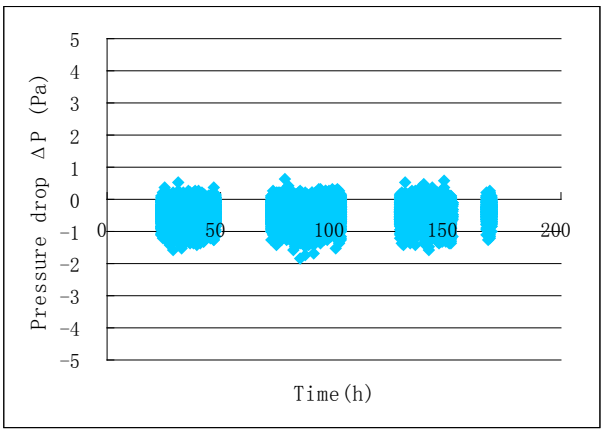

2) Concentrations for C_{Ain}, C_{Aout} and C_{Bout} during the test:

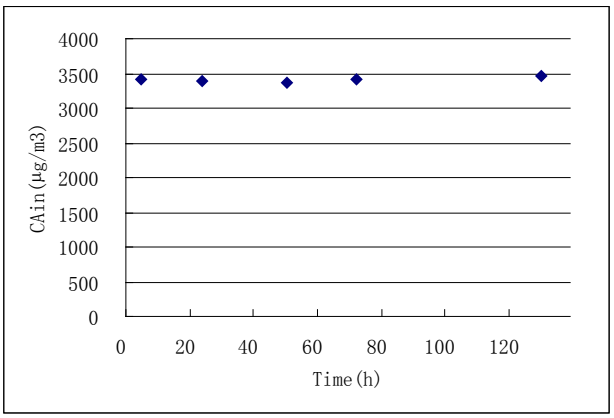

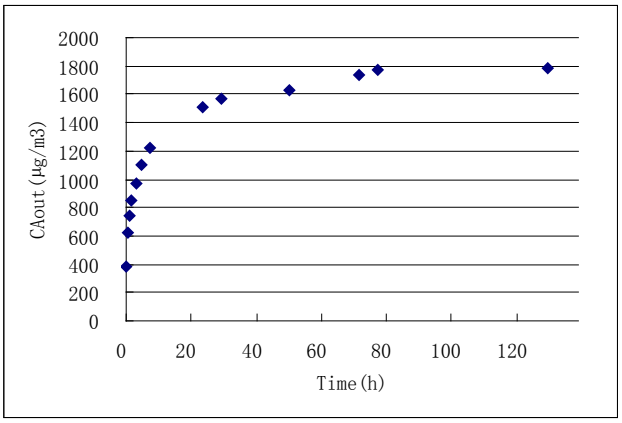

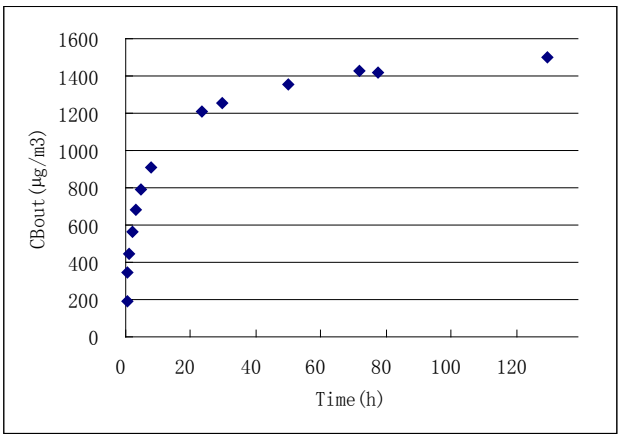

3) The calculated effective diffusion coefficient and partition coefficient are:

Effective diffusion coefficient $D_e(m^2/s)$	$2.46x10^{-5}$
Partition coefficient K_{ma}	967

Appendix C Summary of Standard Operating Procedures (SOPs) cited in the dissertation

Title: BEESL SOP 2002-HIGH PRESSURE LIQUID CHROMATOGRAPHY (HPLC) STANDARD PREPARATION PROCEDURE

Scope: Procedures for HPLC standard preparation

Purpose: To have a written and repeatable procedure for preparing HPLC standards in the Lab444.

Training: Chemical safety class is required; 8 hours for being able to operate; Significant more time for being experienced personnel.

Procedure:

This procedure is written with the assumption that the concentration of each analyte in the purchased standard is 100µg/ml. The solution comes with the certificate form issued by Supelco, which is NIST traceable. However, a purchased standard with different concentrations can be used. In that case, the dilution calculation should be adjusted in order to achieve appropriate amount for column injection.

1. Purchase appropriate standard, which contains the target compounds for a specific analysis.
2. Draw 500µl of the purchased standard. Dilute it with acetronitrile into a 5ml volumetric flask. Mixed well and store in clean bottle with Telfon lined cap. Use this standard solution as standard #1. Concentration of each analyte in this solution is 10µg/ml.
3. Draw 250µl of the purchased standard. Dilute it with acetronitrile into a 5ml volumetric flask. Mixed well and store in clean bottle with Telfon lined cap. Use this standard solution as standard #2. Concentration of each analyte in this solution is 5µg/ml.

4. Draw 100µl of the purchased standard. Dilute it with acetronitrile into a 5ml volumetric flask. Mixed well and store in clean bottle with Telfon lined cap. Use this standard solution as standard #3. Concentration of each analyte in this solution is 2µg/ml.
5. Draw 50µl of the purchased standard. Dilute it with acetronitrile into a 5ml volumetric flask. Mixed well and store in clean bottle with Telfon lined cap. Use this standard solution as standard #4. Concentration of each analyte in this solution is 1µg/ml.
6. Draw 25µl of the purchased standard. Dilute it with acetronitrile into a 5ml volumetric flask. Mixed well and store in clean bottle with Telfon lined cap. Use this standard solution as standard #5. Concentration of each analyte in this solution is 0.5µg/ml.
7. Draw 1ml of the solution #5. Dilute it with acetronitrile into a 5ml volumetric flask. Mixed well and store in clean bottle with Telfon lined cap. Use this standard solution as standard #6. Concentration of each analyte in this solution is 0.1µg/ml.

All standard solutions should be stored in refrigerator room and new standards should be made at a minimum of every 6 months.

Reference Documents:

IAQ MOP No.840, High performance liquid chromatography (HPLC) standard preparation procedure, EPA IAQ Source Characterization Laboratory.

Title: BEESL SOP 2009-HIGH PRESSURE LIQUID CHROMATOGRAPHY (HPLC) ANALYTICAL PROCEDURES

Scope: Analytic procedures for cartridge samples analyzed by HPLC.

Purpose: To have a written and repeatable procedure for HPLC analysis to quantify aldehydes and ketones in the Lab444.

Training: Chemical safety class is required; 2 days for general operation training.

General: For more specific and detailed information relating to the operation of this instrument, refer to the operation manuals of ProStar 220/230/240 Solvent Delivery Module and ProStar 310 UV/Vis Detector and the software instruction manual Galaxie Software. These manuals are stored with the instrument.

Procedures:

Part 1 Setting Up:

1. Fill the solvents in the reservoirs and empty the waste bottle (the method using Water 60%, ACN 30%, THF 10%, total running time for 7 minutes per sample);
2. Turn on the power of Solvent Delivery Module and UV Detector;
3. Empty the waste bottle;
4. Open Galaxie Software on desktop by using default user name and ignoring the password;
5. Click System in the bottom bar, select "check mark" on HPLC;
6. At Overview, first click on/off button to turn on pump first, then click D2 Lamp to turn on the sensor. Ignore VIS lamp; Usually need to pump 15-20 minutes to get a stable ready to measure system;

7. If bubbles in the line are observed while pumping, open the Prime Valve on Solvent Delivery Module by turning it counterclockwise about one turn; Prime using solvent A until the liquid flow from detector discharge line is regular and free of bubbles, then repeat with solvent B & C respectively; Purge using solvents with selected composition; Close the Prime Valve and pump the selected solvent composition through the entire system for 10-15 minutes;
8. Now the system is ready for sample analysis, pressure reading should be stable.

Part 2 Diluting/Extraction Samples:

1. Open the cartridge package and remove both ends of the cartridge;
2. Place the wider bottom of the cartridge on top of the mini-volumetric flask (5ml);
3. Use blunt syringe to load and inject 3ml of pure ACN into the cartridge. Make sure the syringe is joined snugly to the top opening of the cartridge. Remember this rinse should be done very slowly and steadily, drop by drop taking about 80 seconds;
4. Add additional ACN to fill the flask to the line etched into the glass (5ml);
5. Cap flask with stopper and shake well;
6. Place aside and ready to use.

Part 3 Making Injections:

1. Rinse the 25-uL flat-needle syringe 3 times using ACN ;
2. Rinse the syringe 3 times in the sample solution to be injected;
3. Verify that the computer's status is Waiting, and the knob is in the Load position;
4. Inject the 20 uL of solution by syringe to the injection port;
5. Turn knob from Load to Inject position, the computer status will change from Waiting to Running;
6. Wait for at least 30 seconds, then pull the syringe out and switch the injector back to Load status;

7. Wait for the equipment to finish one analysis;
8. Wait the status from Running to Waiting status;
9. Repeat as necessary.

Part 4 Recording Data:

1. Create Sequence: File→New sequence→ System name: hplc → Next → Then fill necessary columns, Table below is given as an example:

Run name	Run ID	Description	# of injection
Bev-ACT-0122-09-std	1	0.1ug/ml Formaldehyde	1
Bev-ACT-0122-09-std	2	0.5ug/ml Formaldehyde	1
Bev-ACT-0122-09-S	1	S1 sample, 60L, 500ml/min	2
Bev-ACT-0122-09-S	2	S2 sample, 60L, 500ml/min	2
Bev-ACT-0122-09-S	3	S3 sample, 60L, 500ml/min	2

2. To begin the sequence run, click the green arrow at the top of the sequence to start the run; to stop the sequence, click red stop;
3. Make sample injection;
4. Wait for the equipment to finish one analysis;
5. Repeat injection for other analysis.
6. Click System button to view the running status, to view the Real Time Plot: Response Amu vs. Time (minutes);
7. Click Data button, at File→ open "Chromatogram"→ to view the data file, click Results to get value of "RT and response Area" ;
8. After finished all analyses, turn off the Pump and Lamp and uncheck HPLC before closing the Galaxie software;
9. If the equipment is used daily, the power is not necessary to be turned off. Otherwise, turn off the power and cap well the injection port.

(Note: By clicking "Syringe picture" → quick start→select method→ data file name, one will also be able to run sample one by one.)

For each group of test, one should run 5 point standard calibration at the beginning of the sequential analysis. Each sample can be injected twice and the average result of the two injections can be taken to minimize errors caused by syringe injection. To be acceptable, the two injections from the same sample should be within ± 15% of the average. In addition, one blank cartridge should be analyzed for each production lot. Ensure that the blank values are in the normal range.

Reference Documents:

1. Operation Manual: ProStar 220/230/240 Solvent Delivery Module
2. Operation Manual: ProStar 310 UV/Vis Detector
3. Software Instruction Manual: Galaxie Software
4. LAB444 MOP HPLC1, High Performance Liquid Chromatography (HPLC) Standard Preparation Procedure
5. LAB444 MOP HPLC2, Procedure for collection of air samples on DNPH-Silica cartridges and preparation for analysis
6. IAQ MOP No.842, High Pressure Liquid Chromatography (HPLC) Analytical Procedures, EPA IAQ Source Characterization Laboratory.
7. SOP2002, BEESL
8. SOP 2003, BEESL

Title: BEESL SOP 2010-DUAL CHAMBER OPERATING PROCEDURES

Scope: The SOP covers specimen preparation, installation, precondition, test condition verification, sampling and analysis

Purpose: Ensure reliable and repeatable test results in experiments using the Dual Chamber system

Training: One day for general operation, some knowledge about fundamental principle of dual chamber system

General: The inlet concentration is dependent on the generation of the dynacalibrator, which is not within the scope of this SOP. The sampling of the concentration is taken by PTRMS (refer to SOP 2012 PTRMS).

Procedures:

Part one: material preparation and installation

1. Examine the edge sealing and integrity of the test specimen. The size of the sample shall have the dimensions of 12 inch x12 inch. The thickness shall be no more than half inch. The cut edges are sealed with non-VOC aluminum tape. The tape covers the four cut side edges with ¼ inch overlay on both faces. This is necessary to achieve a satisfactory seal as the tape does not completely stick to bare composite wood edges. Thus, the nominal emitting surfaces are typically 11.5 inch by 11.5 inch.
2. Install the specimen in the specimen holder and assemble it air-tight with the dual chambers by six clamps. Adjust the inflows of both chambers to the desired flow rates. Measure the

inflows Q_{in} (cc/min) and outflows Q_{out} (cc/min) of both chambers. The leakage rate of the two chambers should be less than 3% of the total supply air flow rate as determined by the difference between the inlet and outlet flow rates of the two chambers. i.e.,

$$Leakage = \frac{Q_{in} - Q_{out}}{Q_{in}} \times 100\% \leq 3\%$$

3. Measure the absolute pressure of chamber A and chamber B, and make sure they are positive pressures compared to the ambient. This prevents the contamination from ambient air.
4. Measure the pressure drop between two chambers and verify that it is negligible (less than 4 Pa).
5. Document the measured values in the above procedures (2, 3, and 4) in the logbook as future reference in the data analysis period.

Part two: precondition of the material under the desired environmental condition

1. Adjust the RH value in the RH control panel.
2. Precondition the dual chamber facility by supplying the desired flow rates under the specified RH into both chambers.
3. Record the RH condition in the preconditioning period, download it from the computer. Analyze the RH data for two chambers until the RH in the outflows of the chamber A and B reach stable. The time needed for precondition varies for different specimens.

Part three: testing

1. When the airflow rate, temperature and relative humidity are stable, take formalehyde background sample for chamber A and B, respectively.
2. Start the test by injecting constant formaldehyde concentration into chamber A. In the meantime, record the formaldehyde concentration change continuously. As the dotted line indicates in Fig. (1), only one PTRMS is employed in the test, so PTRMS switches among the

lines of C_{Aout}, C_{Bout} and C_{Ain} in the test period. For each of these data points, the PTRMS will be used to take an air sample every 10 seconds for 5 minutes, and the average value will be used to determine the concentration. The test measured concentrations are considered to reach steady state when the moving average of C_{Aout} and C_{Bout} do not change more than 1% between two adjacent data points.

3. Record the temperature, airflow rate and relative humidity for the inflow and outflow of the chambers simultaneously when the test begins.
4. Stop the test once the formaldehyde concentrations in two chambers reach steady state---i.e., the difference between two adjacent sampling time points is less than 1%.
5. Verify the test conditions and download all recorded data including PTRMS and environmental conditions.

Part four: after test finishes

1. Stop the inflows of the chamber A and B.
2. Put the relative humidity control into "off" status in the control panel.
3. Remove all the clamps around the chambers.
4. Take the specimen holder out of the chambers.
5. Remove the specimen from the specimen holder and put in the storage or dispose it.

Reference Documents:

1. SOP 2011 Dynacalibrator
2. SOP 2012 PTR-MS

Title: BEESL SOP 2011-VICI Model 500 DYNACALIBRATOR OPERATING PROCEDURES

Scope: Operating procedures for Dynacalibrator (VICI product, Serial#M-2028)

Purpose: Ensure consistent operation of the device and achieve reliable and repeatable air supply with known stable concentration.

Training: Two hours for general operation, require some knowledge about permeation tube

General: For more specific and detailed information relating to the operation of this instrument, refer to the operation manuals of the Dynacalibrator. These manuals are stored with the instrument.

Procedures:

Power on the instrument

1. To ensure high quality, flush it by setting the empty chamber to 100ºC and set flow rate at highest mark, press Vent run for 1 hour, press Span 1/2 hour, then turn off heater and flow.
2. For a specific VOC generation task, determining its required temperature, flow rate, and type of permeation tube by doing homework first. Refer or better remember some basic information from Manual: expanded temperature unit: 2ºC above 110ºC, standard unit: 50º C; output pressure: 0-5 psi, 50 psi optional (option H); Maximum permeation device length: 23.5 cm and max. diameter:1.6 cm; Tube connection:1/4"tubing; No internal pump; Precision rotameter dilution flow has 150mm graduated scale furnished with 15 individual calibration setting, exact flow value for each setting need to check "Dynacalibrator Flowmeter Calibration Data Table" in the manual (two small balls: top float, bottom float).

3. Open the chamber door, carefully using special tong to insert the permeation tube to the glass chamber, then close the chamber door; Wear gloves for best safety when touching permeation tube.
4. Set the temperature and flow rate as pre-determined for current task, refer to the manuals for understanding the flowmeter reading mark on the front of the instrument
5. Remember press Vent which leads to waste line, a default safe position
6. Usually need to run 4-12 hours to get a stable voc generation depending on type of VOCs
7. Press Span to do injection whenever necessary
8. After test is done, reduce Temperature to 23ºC, keep flow Vent, continue run for a few hours, till to room temperature
9. At room temperature, open chamber door, take permeation tube out and restore it to its original container; Wear gloves for safety.
10. Power off the instrument

Reference Documents:

1. Manual of Dynacalibrator Model 500 from VICI
2. Permeation tube product description

Title: BEESL SOP 2012-HIGH SENTIVITIVITY PROTON TRANSFER REACTION MASS SPECTRA (PTR-MS) OPERATING PROCEDURES

Scope: Operating procedures for high sensitivity PTR-MS

Purpose: To ensure consistent operation of PTR-MS for achieving reliable and repeatable measurements

Training: One day for general operation, some knowledge about Proton Transfer Reaction

General: For more specific and detailed information relating to the operation of this instrument, refer to the operation manuals of PTRMS Viewer 2_5 manual and PTRMS Control 2_5 software manual. These manuals are stored on BEESL server (T:\software\PTR-MS)

Procedures:

Part 1 Cold Start (System Power is off)

1. Take PTR-MS log book and read through the most recent record of previous status;
2. Turn on the power of the PTR-MS; Wait 5-10 minutes till all the front panel light indicates are Green;
3. Turn on the Laptop (no password required), make sure the cable connection is tight well;
4. Open the software by clicking PTR-MS Control icon on the desktop;
5. Click PCU -> load PCU set -> Select the most recent one, for example: Dec0109.pvs; (Sometimes, if the actual reading not matching the setting values, may click the box of set value, change it to 0, then change back)

6. Click Tools -> Enable Export Control if visually see the "U draft[v], U QL[v], U NC[v] reading is not active;
7. Make sure system values are fine refer to the record of the log book, for example:

   Detector voltage: 3010 [v], Pressure REA [mbar]: 2.21, PC [mbar]: 355,

   FC [sccm]:7.5; USO [v]:70, US [v]:110, U drift [v]: 600, UQL [v]:50, UNC [v]:6.0, and Source [mA]: 6.0.
8. From cold start to get stable accurate measurement, may need to wait above 5 hours;
9. Select MID mode, keep the reserved 6 channels (channel 0 to channel 5) unchanged, that are set to measure p-mass of 18, 21, 25, 30, 32, 37 to provide system measurement information in case water reservoir problem happen; Remember p-mass at 25 is a fake one. Its actual function is controlling the sampling time intervals.
10. To measure a specific target compound, one should manually select a channel, fill the values for "mass, dwell time, K value, multiplier", the rest can be default values. Refer to the Manuals of PTR-MS for questions.
11. One may click cps (counts per minute) or ppb as concentration unit view in plot window
12. One may click Quick for a quick measure. The data file is only temporally stored and will be automatically replaced by next Quick measure.
13. Click Record to start the measurement, make sure to create and save the Data File Name; remember the data will be automatically stored at "Desktop / My Document / Shared Documents / Lab view data / PTR data"
14. After the measurement, Click Stop to stop the measurement
15. Simply close the software as "Standby mode" if one will measure within three days. This will protect SEM detector, while all flows will stay same.

Part 2 Standby Mode (while the all the power and flow are on)

1. Simply start the software, all settings should be as before

2. System should be ready to do measurement after 3-5 minutes

Part 3 Scan Mode

1. Click Scan to perform scan, click Stop to stop;
2. The scan mode setting reference are: Detector: IonCount, Mode: Bargraph, Dwell/mass: 10ms (range 0.5ms to 60s), Start mass:21, End mass: 60, (mass range can up to 512), K-rate:2, Resoluition:25, Pause cal: 0.10

Part 4 How to Turn off

1. Click PCU -> Load PCU sets ->select Set all zeros.pvs
2. Make sure all PCU settings changed to 0, then close software
3. Wait all pump noise diminish, takes about 10 minutes, then turn off power of PTRMS

Part 5 Data Processing

1. There are two data files for each measurement, *.tdm and *.tdx, both should store under "Desktop / My Document / Shared Documents / Labview data / PTR data";
2. Copy both files to your computer, import to Excel to do analyze;
3. Remember your computer must install a drive software first, which is "NI TDMS Excel Importer" located at SU:\T\software\PTR-MS"

Reference Documents:

1. Iconic Analytic PTRMS Manual- hard copy binder
2. PTRMS Control 2_5 software manual-hard copy binder
3. On BEESL server (T drive) updated pdf files: PTRMS Viewer 2_5 manual and PTRMS Control 2_5 software manual
4. Log book for PTR-MS stayed with the PTR_MS which had all the using record for the instrument

Appendix D Small chamber tests for three individual layers and worksurface

Worksurface is composed of three layers: painted veneer, particleboard and veneer from top to bottom. In the experiment, total four materials have been tested: painted veneer, particleboard, veneer and worksurface. For each individual material, a small chamber test was conducted, in which the material was placed in a dynamic chamber and two duplicate samples were taken at the equilibrium status. The purpose of the small chamber tests for the three individual materials was to identify each significant VOC in every single layer and the concentration level of each emitted VOC. The purpose of conducting emission test for worksurface was to verify the multilayer model by the measured emission data. In order to better quantify the VOCs, the 14 most popular and clearly identified VOCs by a GC/MS and HPLC were selected as the target VOCs listed in Table D.1.

Table D. 1 Target compounds in emission tests

Target compounds	CAS #	Retention time(min)
2-Methyl-1-propanol	78-83-1	4.78
n-Butanol	71-36-3	5.68
Toluene	108-88-3	7.7
Isobutyl acetate	110-19-0	8.01
Hexanal	66-25-1	9.3
m/p-Xylene	108-38-3/106-42-3	11.12
o-Xylene	95-47-6	12.06
3-Ethyltoluene	620-14-4	14.34
1,3,5-Trimethylbenzene	108-67-8	14.58
1,2,4-Trimethylbenzene	95-63-6	15.58
1,2,3-Trimethylbenzene	526-73-8	16.66
Phenol	108-95-2	18.12
Formaldehyde	50-00-0	3.09
Acetaldehyde	75-07-0	4.54

Note: Formaldehyde and acetaldehyde were analyzed by HPLC, while the other VOCs were measured by GCMS.

D. 1 Test conditions

Four tests were conducted in small stainless steel chamber with standard 50 L volume (0.5 by 0.4 by 0.25 m) inside a temperature controlled enclosure to maintain the chamber test conditions

to be at 23±1°C, 50±5% RH, with air change rate equal to 1(refer to Fig. D.2). Duplicate samples were taken by two precision gas flow controller (Model MC-5SLPM-D, Alicat Scientific, refer to Fig. D.1 (c)) to make sure the quality of the samples. Sulfur Hexafluoride was injected occasionally into the chamber to confirm the air change rate using photoacoustic field gas monitor (1412, Innova, AirTech Instruments). The exhaust air of the chamber was drawn through the cartridges (Waters Sep-pak DNPH-silica cartridge, Waters) where aldehydes was trapped by 2, 4-Dinitrophenylhydrazine (DNPH) into a DNPH derivative. Water Sep-Pak Plus cartridges were constructed of high-purity polyethylene components with triaxially - compressed packed beds and Luer fittings. Finally, all the cartridges were analyzed by high performance liquid chromatography (Model 310, Varian Prostar UV Detector and Model 230, Varian Prostar Solvent Delivery Module, refer to Fig. E.1 (b)) together. Other VOCs were collected by stainless tubes containing Tenax-TA sorbent (refer to Fig. E.1(d). The VOCs collected on the tube are then thermally desorbed to a GC/MS (Fig. E.1 (a)) system for identification and quantification.

(a)

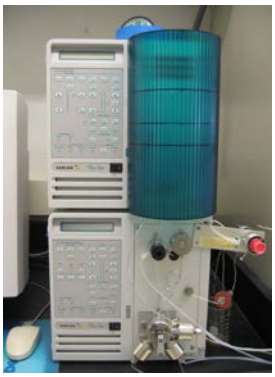

(b)

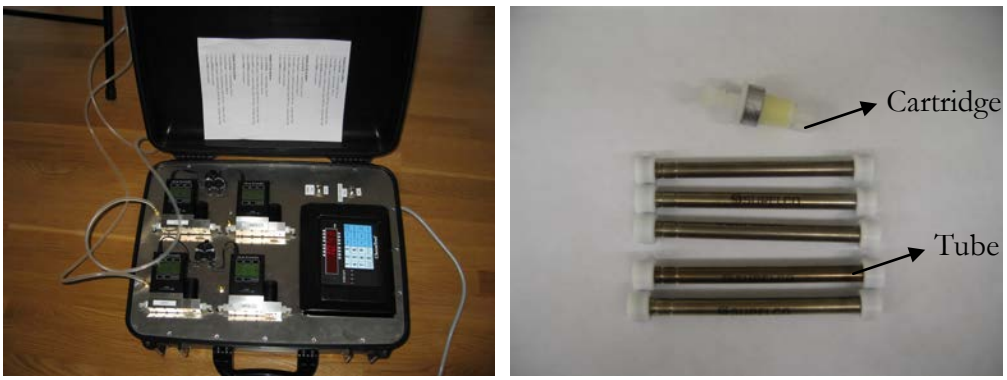

(c) (d)

Figure D 1 (a) GC/MS (b) HPLC (c) Mass flow controller (d) Cartridge and Tenax-TA tube

Figure D 2 Small-scale environmental chamber test system

D.2 Treatment of the specimens

Test specimens were collected from the same batch of production and separately wrapped using Tedlar bags and stored in a storage room (23±1°C and 50%±5% RH). Before testing in the small chamber, test specimen was then unwrapped and cut in the dimension of 7.5"×7.5" (19.05cm×19.05cm), with sealed edges and bottom.

An often used approach to specimen preparation and the first one considered in this study is to treat each material face as a separate emitting surface and to attempt to isolate this face by sealing the other face with a metal plate. The cut edges were sealed with non-VOC aluminum tape. The tape covered the cut edges and was folded over both faces covering a border 0.64-cm wide (refer to Fig. D.3). This was necessary in order to achieve a satisfactory seal as the tape does

not completely stick to bare composite wood edges. Thus, the nominal emitting surfaces were typically 17.8-cm by 17.8 cm (0.0316 m^2). The thickness of particleboard, veneer and painted veneer are already summarized in Table D.1.

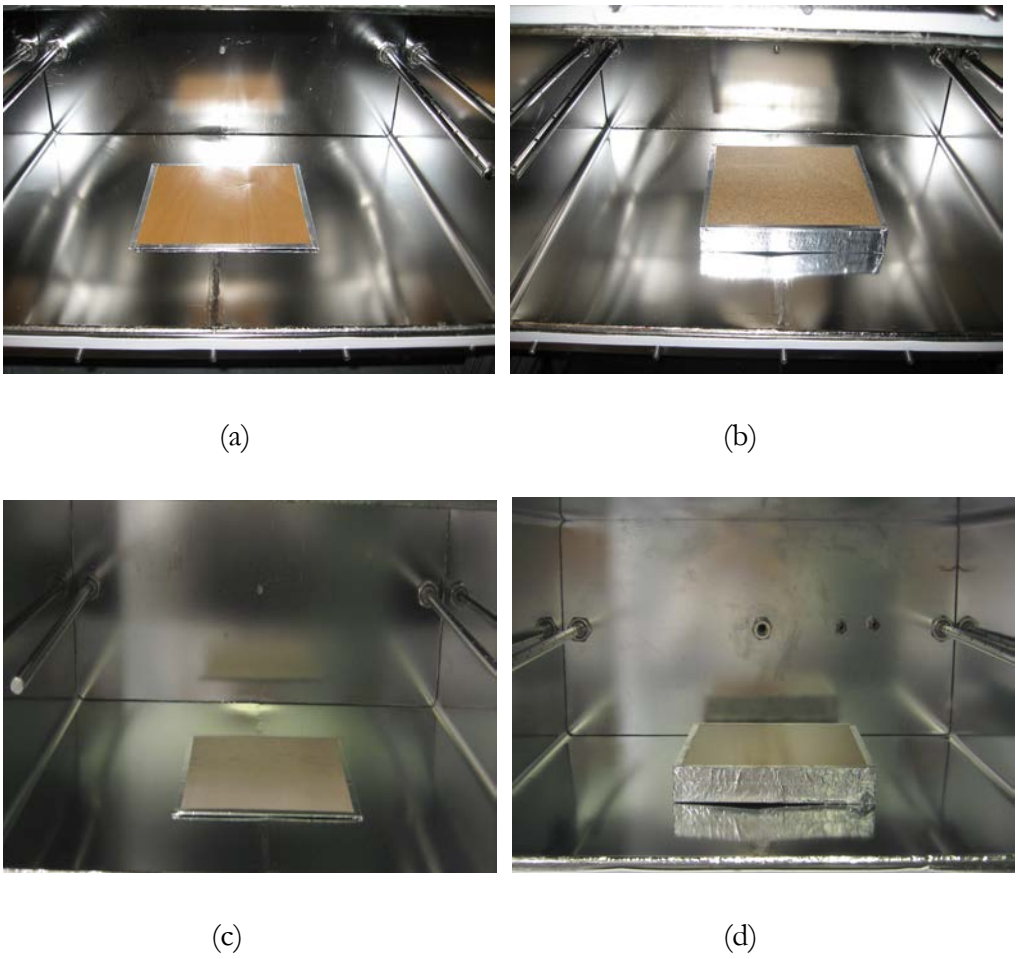

(a) (b)

(c) (d)

Figure D 3 Treatment of (a) Painted veneer (b) Particleboard (c) Veneer (d) Work surface

The tested specimens are shown in Fig. D 3(a) - (d). The worksurface consisted of painted veneer in the top layer, core particleboard in the middle layer and wood veneer in the bottom layer, and was illustrated sequentially from top to bottom in Fig. 5.3. Separate tests were conducted for worksurface, particleboard, wood veneer and painted veneer specimen, respectively.

D. 3 Determination of sampling intervals of each material

The sampling of each material was determined separately by virtue of different standards developed by BEESL. Duplicate samples of particleboard followed the same sampling intervals

developed in the BIFMA standard, i.e. 24hrs, 48hrs, 72hrs, 96hrs, 168hrs and 336hrs, and extended four more weeks with one week interval. One set of samples of worksurface were also taken with the same sampling intervals in BIFMA standard in the first two weeks, with the extention of two more weeks. Duplicate samples of painted veneer have only three sampling pointes, i.e. 72hrs, 168hrs and 336hrs because new sampling standard was developed in the report of Zhang et al 2008. It was found that the concentration level of VOCs from veneer was quite low compared to the concentration levels from other materials, so only 24hrs data were taken in the veneer sample.

D. 4 Test results

The results of identified VOCs in the small test were provided in Table D.2 with VOCs concentrations in descending order. Painted veneer had more kinds of VOCs than particleboard and veneer.

Table D. 2 Results of identified VOCs for individual layer

Material	Identified VOCs
Particleboard	Hexanal, acetaldehyde, formaldehyde, toluene
Veneer	Hexanal, n-butanol, formaldehyde
Painted veneer	n-butanol, 2-methyl-1-propanol,formaldehyde,hexanal, 1,2,3-trimethylbenzene, isobutyl acetate, 3-ethyltoluene, 1,2,4-trimethylbenzene, 1,3,5-trimethylbenzene, o-xylene, m/p-xylene, acetaldehyde

The VOCs studied are acetaldehyde and hexanal because those are among the major emitted VOCs from particleboard. Particleboard is the core of the worksurface.

The result of the individual layers and worksurface will be provided in the section of the experiment validation for the multilayer model in chapter 5.

References

An Y., Zhang J., Shaw C.Y. (1999) Measurements of VOC adsorption/desorption characteristics of typical interior building material surfaces, International Journal of HVAC & R Research, 5(4), 297-316.

ASTM C 1498-01 (2001) Standard test method for hygroscopic sorption isotherms of building materials.

ASTM E96/ E 96M-05 (2005) Standard Test Methods for Water Vapor Transmission of Materials.

ASHRAE (1997) ASHRAE Handbook of Fundamentals, Atlanta, GA, American Society of Heating, Refrigerating and Air Conditioning Engineers.

ASHRAE 189.1 (2009) Standard for the Design of High-Performance Green Buildings Except Low-Rise Residential Buildings.

ASTM D6670 Standard Practice for Full-Scale Chamber Determinations of Volatile Organic Emissions from Indoor Materials/Products.

ASTM D5116. Standard Guide for Small-Scale Environmental Chamber Determination of Organic Emissions From Indoor Materials/Products.

Baechler, M.C. et al. Sick Building Syndrome: Sources, Health Effects, Mitigation (Pollution Technology Review No. 205) (1993) William Andrew publisher.

Bear, J., Bachmat, Y. (1991). Introduction to modeling of transport phenomena in porous media Kluwer Academic Publishers, Dordrecht.

BIFMA M 7.1 (2005) Proposed Standard Method For Testing VOC Emissions For Office Furniture Systems, Components And Seating. BIFMA International, 2680 Horizon Drive Suite A1, Grand Rapids MI 49546.

Blondeau, P., Tiffonnet, A.L., Damian, A., Amiri, O.and Molina, J.L. (2003) Assessment of contaminant diffusivities in building materials from porosimetry tests. Indoor air 2003, 13, 302-310

Blondeau, P., Tiffonnet, A.L., Allard, F. and Highighat, F. (2008) Physically based modeling of the material and gaseous contaminant interactions in buildings: models, experimental data and future developments, Advances in building energy research*, 2*, 57-93

Bodaldal, A., Zhang J.S., Plett, E.G. (2000) A method for measuring internal diffusion and equilibrium partition coefficients of volatile organic compounds for building materials., Building and Environment, 35,101-110.

Bodalal A., Zhang J., Plett E., Zhu J. (2001) Correlations between the internal diffusion and equilibrium partition coefficients of volatile organic compounds (VOCs) in building materials and the VOC properties, ASHRAE Transactions, 107(1), 789-800.

Bodaldal, A. (1999) Funamental mass transfer modeling of emission of volatile organic compounds from building materials. Ph.D. thesis, Carleton University, Canada, 1999.

Boublik, T., Fried, V., and Hala, E. (1984) The vapour pressures of pure substances: selected values of the temperature dependence of the vapour pressures of some pure substances in the normal and low pressure region. Amsterdam: Elsevier

Bouilly, C.R., Allard, F., Blondeau, P., Collignan, B., Popescu, R. and Sjoberg, A. (2006) A physically-based analysis of the interactions between humidity and VOCs in building materials. In: Proceedings of Healthy Buildings, 89-94.

California. (2000) California Government Offices Purchase Criteria Environmental Specifications for Office Furniture Systems (http://www.dhs.ca.gov/ps/deodc/ehlb/iaq/VOCS/workstation.pdf)

California 1350 (2010) Standard Practice for the Testing of Volatile Organic Emissions from Various Sources Using Small-Scale Environmental Chambers (Supercedes previous versions

of small-scale environmental chamber testing portion of California Specification 01350), July 15, 2004. (http://www.dhs.ca.gov/ps/deodc/ehlb/iaq/VOCS/Practice.htm)

Clausen, P.A., Wolkoff, P., Holst, E., Nielsen, P.A. (1991) Long term emission of volatile organic compounds from waterborne paints-methods of comparison, Indoor Air, 4, 562-576.

Core, H.A., Cote, W.A. and Day, A.C. (1979) Wood Structure and Identification, Second edition. Syracuse University Press, Page 19.

Cox, S.S., Little, J.C., Hodgson, A.T. (2002) Predicting the emission rate of volatile organic compounds from vinyl flooring, Environmental science & technology, 36, 709-714.

Cox, S.S., Zhao, D., Little, J.C. (2001) Measuring partition and diffusion coefficients for volatile organic compounds in vinyl flooring, Atmospheric Environment, 35, 3823-3830.

Crank, J. (1975) The mathematics of diffusion. 2nd edition. Oxford University Press, New York, 44-49.

Deng, B. and Kim, C.N. (2004) An analytical model for VOCs emission from dry building materials, Atmospheric Environment, 38, 1173-1180.

Destaillats, Hugo, Lunden, Melissa M., Singer, Brett C., Coleman, Beverly K., Hodgson, Alfred T. Weschler, Charles J., and Nazaroff, William W. (2006) Indoor Secondary Pollutants from Household Product Emissions in the Presence of Ozone: A Bench-Scale Chamber Study. Environmental science and technology, 40(14), 4421-4428.

Do, D.D. (1998) Adsorption analysis: equilibria and kinetics. Imperial college press.

Dunn, J.E. (1987) Models and statistical methods for gaseous emission testing of finite source in well-mixed chambers, Atmospheric Environment, 21(2), 425-430.

EPA/RTI ETV (1999) Large Chamber Protocol for Measuring Emissions of VOCs and Aldehydes from Office Workstations (http://www.epa.gov/etv/test_plan.htm#prevention or http://etv.rti.org/iap/documents.cfm)

Fang L., Clausen G., Fanger P.O. (1999) Impact of temperature and humidity on chemical and sensory emissions from building materials, Indoor Air, 9, 193-201.

Farajollah, Y., Chen, Z., Haghighat, F. (2009) An experimental study for examining the effects of environmental conditions on diffusion coefficient of VOCs in building materials, Clean-Soil,Air,Water, 37, 436-443.

Grunewald, J., Nicolai, A., Li, H. and Zhang, J.S. (2007) Modelling of coupled numerical HAM and pollutant simulation—Implementation of VOC storage and transport equations. In: Proceedings of the 12. Symposium for Building Physics, Dresden, Germany, 2, 792-800

Gunnarsen, L., Nielsen, P.A. and Wolkoff, P. (1994) Design and characterization of the CLIMPAQ, chamber for laboratory investigations of materials, pollution and air quality, Indoor Air, 4, 56-62.

Guo, H., Murray, F., Lee, S. (2002) Emissions of total volatile organic compounds from pressed wood products in an environmental chamber, Building and Environment, 37, 1117-1126.

Guo, H., Murray, F., Lee, S.C., Wilkinson, S. (2004) Evaluation of emissions of total volatile organic compounds from carpets in an environmental chamber. Building and Environment, 39, 179-187.

Guo, Z. and Tichenor, B.A. (1992) Fundamental mass transfer models applied to evaluating the emissions of vapor-phase organics from interior architectural coatings. Proceedings of EPA/AWMA Symposium, Durham, NC.

Haghighat, F. and Zhang, Y. (1999) Modelling of emission of volatile organic compounds from building materials—estimation of gas-phase mass transfer coefficient, Building and Environment, 34, 377-389.

Haghighat, F., Lee, C.-., Ghaly, W.S. (2002) Measurement of diffusion coefficients of VOCs for building materials: Review and development of a calculation procedure, Indoor Air, 12, 81-91.

Haghighat, F. and Huang, H. (2003) Integrated IAQ model for prediction of VOC emissions from building material, Building and Environment, 38, 1007-1017.

Hazim Awbi (2002) Ventilation of buildings, second edition, pp.49

Haghighat, F., Lee, C. S. and Ghaly, W.S. (2002) Measurement of diffusion coefficients of VOCs for building materials: review and development of a calculation procedure. Indoor Air, 12, 81-91

Hu, H.P., Zhang, Y.P., Wang, X.K., Little, J.C. (2007) An analytical mass transfer model for predicting VOC emissions from multi-layered building materials with convective surfaces on both sides, International Journal of Heat and Mass Transfer, 50, 2069-2077.

Huang, H., Haghighat, F., Blondeau, P. (2006) Volatile organic compound (VOC) adsorption on material: Influence of gas phase concentration, relative humidity and VOC type, Indoor Air, 16, 236-247.

Järnström, H., Saarela, K., Kalliokoski, P., Pasanen, A.-. (2007) Reference values for structure emissions measured on site in new residential buildings in finland, Atmospheric Environment, 41, 2290-2302.

Koivula, M., Kymäläinen, H., Virta, J., Hakkarainen, H., Hussein, T., Komulainen, J., Koponen, H., Hautala, M., Hämeri, K., Kanerva, P., Pehkonen, A., Sjöberg, A. (2005) Emissions from thermal insulations—part 2: Evaluation of emissions from organic and inorganic insulations, Building and Environment, 40, 803-814.

Korea thermophysical properties data bank. Korean national chemical engineering research information center.
http://www.cheric.org/research/kdb/hcprop/showcoef.php?cmpid=1232&prop=PVP

Kline, S.J. (1985), The purpose of uncertainty analysis. ASME Journal of Fluids Engineering; 107: 153-160.

Kumar, D. and Little, J.C. (2003) Characterizing the source/sink behavior of double-layer building materials, Atmospheric Environment, 37, 5529-5537.

Li, H. (2007) A modeling and experimental investigation of coupled heat, air, moisture and pollutants transport in building envelop systems. Ph.D. thesis. Syracuse University, Syracuse, NY. U.S.A.

Lide, D.R. (2004) CRC handbook of chemisty and physics: a ready-reference book of chemical and physical data. Boca Raton, Fla.: CRC press

Little, J.C., Hodgson, A.T., Gadgil, A.J. (1994), Modeling emissions of volatile organic compounds from new carpets, Atmospheric Environment, 28, 227-234.

Magee, R.J., Zhu, J.P., Zhang, J.S., and et al. (1999) A small chamber test method for measuring volatile organic compound emissions from "dry" building materials, Consortium for material emissions and IAQ Modeling, Final report 1.2, National Research Council Canada

McQuiston, F.C., Parker, J.D. and Spitler, J.D. (2005) Heating, Ventilating and Air Conditioning: Analysis and design. Sixth edition. John Wiley&Sons, Inc. Appendix Table A -1a

Meininghaus, R., Knudsen, H.N. and Gunnarsen, L. (1998) Diffusion and sorption of volatile organic compounds in indoor surface materials, EPIC '98, Proceedings of the of the Second European Conference on Energy Performance and Indoor Climate in Buildings and the Third International Conference on Indoor Air Quality, Ventilation and Energy Conservation, Lyon, France, Vol. 1, 33-38.

Meininghaus, R., Gunnarsen, L. and Knudsen, H.N. (2000) Diffusion and sorption of volatile organic compounds in building materials-impact on indoor air quality. Environ. Sci. Technol. & Technoogy, 34, 3101-3108

Nelson, G.O. (1992) Gas Mixtures: Preparation and Control, 137-146, 243-249

Pazera, M. (2007) Development of experimental methods for characterizing water vapor transmission in building materials. Ph.D thesis. Syracuse University, Syracuse, NY. U.S.A.

Ruthven, D. M. (1984) Principles of adsorption and adsorption process. John Wiley &Sons.

Salonvaara, M., Zhang, J.S. and Yang, M. (2006) A study of air, water and VOC transport through building materials with the dual chamber system. In: Proceedings of International Specialty Conference: Indoor Environmental Quality - Problems, Research and Solutions, 2006, Durham, NC, Session 6A

Sander, R., Compilation of henry's law constants for inorganic and organic species of potential importance in environmental chemistry. http://www.mpch-mainz.mpg.de/~sander/res/henry.html ;1999

Shinohara, N., Kai, Y., Mizukoshi, A., Fujii, M., Kumagai, K., Okuizumi, Y., Jona, M., Yanagisawa, Y. (2009) On-site passive flux sampler measurement of emission rates of carbonyls and VOCs from multiple indoor sources, Building and Environment, 44, 859-863.

Smith, J., Gao, Z., Zhang, J.S. and Guo, B. (2009). A new experimental method for the determination of emittable initial VOC concentrations in building materials and sorption isotherms for IVOCs, Clean-Soil, Air, Water, 37(6), 454-458.

Taylor, J.R. (1982) An introduction to error analysis: the study of uncertainty in physical measurements. In: Anonymous University Science Books, Mill Valley, CA; p.71-74.

Tiffonnet, A.L., Blondeau, P., Amiri, O. and Allard, F. (2000) Assessment of contaminant diffusivities in building materials from porosity tests, Proc. Healthy building, Espoo, finland, Vol. 4, 199-203

U.S. Environmental Protection Agency (1989) Office of Air and Radiation. Report to Congress on Indoor Air Quality, Volume Ⅱ: Assessment and Control of Indoor Air Pollution, pp. Ⅰ, 4-14. EPA 400-1-89-001C

U.S. Environmental Protection Agency (1990) Reducing risk: setting priorities and strategies for environmental protection, Science Advisory Board, U.S. Environmental Protection Agency, Washington, DC.

Vargaftik, N. B. (1975) Tables on the thermophysical properties of liquids and gases, John Wiley & Sons, Inc.

Virta, J., Koivula, M., Hussein, T., Koponen, S., Hakkarainen, H., Kymäläinen, H., Hämeri, K., Kulmala, M., Hautala, M. (2005) Emissions from thermal insulations—part 1: Development and characteristics of the test apparatus, Building and Environment, 40, 797-802.

Weschler, C.J., Shields, H.C. (1999) Indoor ozone/terpene reactions as a source of indoor particles. Atmospheric Environment, 33, 2301-2312.

Weschler, C.J. (2009) Changes in indoor pollutants since the 1950s. Atmospheric environment. 43, 153-169.

Whitaker, S. (1969) Advances in the theory of fluid motion in porous media. Industrial and engineering chemistry, 61, 14-28.

Wolkoff P. (1998) Impact of air velocity, temperature, humidity, and air on long-term VOC emissions from building products, Atmospheric Environment, 32, 2659-2668.

Won D., Corsi R.L., Rynes M. (2001) Sorptive interactions between VOCs and indoor materials, Indoor Air 2001, 11, 246-256.

World Health Organization (1989) Indoor Air quality: organic pollutants, Copenhagen, WHO regional office for Europe (EURO report and studies No: 111)

Xiong, J., Zhang, Y., Wang, X., Chang, D. (2008) Macro–meso two-scale model for predicting the VOC diffusion coefficients and emission characteristics of porous building materials, Atmospheric Environment, 42, 5278-5290.

Xu, J., Grunewald, J., Zhang, J.S. and Guo, B. (2007) Modeling the formaldehyde emission from multi-layer work surfaces used in office workstation systems. In: proceedings of the 6th international conference on indoor air quality, ventilation & energy conservation in buildings. Oct 28-31, 2007. Sendai, Japan.

Xu., J., Zhang, J.S., Grunewald, J. et al. (2008). A dual-chamber experimental method for determining the transport properties of building materials. In: Proceedings of the 11th international conference on indoor air quality and climate. Aug 17-22, 2008. Copenhagen, Denmark. No. 232.

Xu, J., Zhang, J.S., Grunewald, J., Zhao, J., Plagge, R., Amiri, Q., Allard F. (2009) A study on analogy of water vapor and VOCs diffusion in porous media by dual chamber method. Clean-Soil,Air,Water, 37, 444-453.

Xu, Y. and Zhang, Y. (2003) An improved mass transfer based model for analyzing VOC emissions from building materials, Atmospheric Environment, 37, 2497-2505.

Xu, Y. and Zhang, Y. (2004) A general model for analyzing single surface VOC emission characteristics from building materials and its application, Atmospheric Environment, 38, 113-119.

Yang, X., Chen, Q., Zeng, J., Zhang, J.S., Shaw, C.Y. (2001) A mass transfer model for simulating volatile organic compound emissions from 'wet' coating materials applied to absorptive substrates. International journal of heat and mass transfer, 44(9), 1803-1815.

Yang, X., Chen, Q., Zhang, J.S., Magee, R., Zeng, J., Shaw, C.Y. (2001) Numerical simulation of VOC emissions from dry materials, Building and Environment, 36, 1099-1107.

Yuan, H., Little, J.C., Marand, E., Liu, Z. (2007) Using fugacity to predict volatile emissions from layered materials with a clay/polymer diffusion barrier, Atmospheric Environment, 41, 9300-9308.

Zhang, J.S. (2005) Combined heat, air, moisture, and pollutants transport in building environmental systems. JSME International Journal Series B, 48, 1-9.

Zhang J., Zhang J., Chen Q. (2002) Effects of environmental conditions on the VOC sorption by building materials-part I: Experimental results, ASHRAE Transactions, 108, 273-282.

Zhang, J., Nong, G., Shaw, C., Wang, J. (1996) Measurements of volatile organic compound (VOC) emissions from wood stains using an electronic balance, ASHRAE Transactions, 105, 279-288.

Zhu, J.P., Magee, R.J., Zhang, J.S. and et al.(1999) A small chamber test method for measuring volatile organic compound emissions from "wet" building materials, Consortium for material emissions and IAQ Modeling, Final report 1.3, National Research Council Canada

Curriculum Vitae

EDUCATION

- Ph.D. Mechanical Engineering, May 2012; Syracuse University, Syracuse, NY, U.S.A.
  Dissertation: Study of VOCs Transport and Storage in Porous Media and Assemblies.
  Advisor: Jianshun (Jensen) Zhang
- M.S. Heating, Ventilation and Air conditioning, September 2005 ; Tianjin University, Tianjin, China
  Thesis: CFD Simulation and Study on Airflow in Gymnasium
  Advisor: Huan Zhang Coadvisor: Shijun You
- B.S. Building Service Engineering, June 2003; Tianjin University, Tianjin, China
  Thesis: Design of Air Conditioning System for Sichuan Toyota Auto Co., Ltd
  Advisor: Shijun You

PROFESSIONAL EXPERIENCES

Graduate Teaching Assistant, August 2011-December 2011

Department of Mechanical and Aerospace Engineering, Syracuse University

- Instructed recitation twice every week for sixty undergraduate students in the class of Engineering Mechanics-statics
- Graded mid term exams every month for the professor of Engineering Mechanics-statics
- Answer questions from students in office hours twice every week for Engineering Mechanics-statics

Graduate Teaching Assistant and research assistant, January 2011-May 2011

Department of Mechanical and Aerospace Engineering, Syracuse University

- Taught four classes regarding Numerical methods in heat conduction and Engineering Equation Solver(EES); Instructed recitation three times every week for seventy two undergraduate students in Fundamental Heat and Mass transfer course
- Graded quizzes every two weeks for the professor of Fundamental Heat and Mass Transfer course; Supervised the grader in grading the homework every week
- Answer questions from students in office hours every week in Fundamental Heat and Mass transfer course

Graduate Research Assistant, August 2005 – December 2010

Building Energy and Environmental Systems (BEESL), Department of Mechanical and Aerospace Engineering, Syracuse University. As the lead researcher or key team member,

successfully completed several research projects mainly in the area of VOCs sorption and emission in building and furniture materials and in the field of air cleaning technologies, including:

- Project manager in preparation of the Quality Assurance Project Plan, Operating testing and Final Report in the project "Determination of partition and diffusion coefficients for formaldehyde and selected building materials" (sponsored by United States Environmental Protection Agency), Dec. 2009-Aug. 2010
- Testing in "A new experimental method for the determination of emittable initial VOC concentrations in building materials and sorption isotherms for IVOCs" (sponsored by United States Environmental Protection Agency), Apr. 2009- Dec. 2009
- Project manager in testing and modeling in "Similarity between Water Vapor and VOCs Diffusion through Porous Building/Furniture Material by Dual Chamber Test Method" (sponsored by United States Environmental Protection Agency), Aug. 2007-Dec. 2009
- Testing and modeling in "Proposed Standard Method For Testing VOC Emissions From Office Furniture Systems, Components and Seating" (sponsored by The Business and Institutional Furniture Manufactuer's Association (BIFMA®International)), Aug. 2005-March. 2008
- Testing in "Evaluation of Gaseous and Particulate Emissions from a Room Air Cleaner" (sponsored by S.C.Johnson & Son, Inc.), Feb. 2006-Jun. 2006
- Tutoring in graduate level classes Building Environmental Modeling (MAE 658) and HVAC System Analysis/Design (MAE 553) regarding the software Coupled Heat Air Moisture and Pollutant Simulation in Building Envelope Systems(CHAMPS-BES), Spring 2010 and Fall 2010

PUBLICATIONS

- **Peer Reviewed Journal or Transactions**

1. **Jing Xu**, Jianshun Zhang. A Method for Estimating the Effect of Relative Humidity on VOC Partition Coefficient and Diffusion Coefficient in a Porous Media. (In preparation)
2. **Jing Xu**, Jianshun Zhang. Modeling the VOCs Emissions from a Multilayer Material Assembly. (In preparation)
3. **Jing Xu**, Jianshun Zhang, Hui Li and Beverly Guo. Emissions from Office Workstation Systems, Chairs, and Their Components and Materials. (in preparation)
4. Zhi Gao, Jianshun Zhang, Beverly Guo, **Jing Xu** and James Smith. Characterization of VOC emission from an oriented strand board by conventional chamber method and a VOC

extraction method. (Manuscript in revision, to be submitted to Chemosphere)

5. Zhi Gao, Jianshun Zhang and **Jing Xu**. Experimental evaluation of formaldehyde, methyl vinyl ketone and particulate emissions from room air cleaners. (Submitted to Indoor Air)
6. **Jing Xu**, Jianshun Zhang, Xiaoyu Liu and Zhi Gao. Determination of Partition and Diffusion Coefficient for Formaldehyde and Selected Building Materials and Impact of Humidity. (Accepted by Journal of the Air & Waste Management Association).
7. **Jing Xu,** Jianshun Zhang. An Experimental Study of Relative Humidity Effect on VOCs' Effective Diffusion Coefficient and Partition Coefficient in a Porous Medium. (Building and Environment: Vol 46, Iss. 9, 2011, P1785-1796)
8. **Jing Xu**, Jianshun Zhang, John Grunewald, Jianhua Zhao, Rudolf Plagge, Amiri Ouali and Francis Allard. A Study on Analogy of Water Vapour and VOCs Diffusion in Porous Media by Dual Chamber Method. Clean-Soil, Air, Water: Vol. 37 Iss. 6, 2009. P444-453
9. Wenqian Yuan, Junjie Liu, Neng Zhu and **Jing Xu**. Effect on Coal Gaugue Porous Brich on Building Energy Consumption. Gas& Heat. Vol. 26 No.12 December 2006 (in Chinese)
10. Bin Wang, Huan Zhang, Shijun You and **Jing Xu**. The study on Photo Catalysis and Discharge Plasma Treating VOCs and Bacterium. Journal of Hebei Institute of Architectural Science and Technology，December 2004 (in Chinese)

- **Refereed Conference Proceedings**

1. **Jing Xu**, Jianshun (Jensen) Zhang. Modeling Emissions from a Multi-Layer Furniture Material Assembly. Healthy Building 2012 10th International Conference, July 8-12, Brisbane, Queensland, Australia (Accepted with changes)
2. **Jing Xu**, Jianshun (Jensen) Zhang and Xiaoyu Liu. Determination of Partition and Diffusion Coefficient of Formaldehyde in Selected Building Materials and Impact of Relative Humidity. The 12th International Conference on Indoor Air Quality and Climate. Paper ID 635. June 5-10, 2011, Austin, Texas, U.S.A.
3. **Jing Xu** and Jianshun（Jensen） Zhang. An Experimental Study of Relative Humidity Effect on VOCs' Effective Diffusion Coefficient and Partition Coefficient in a Porous Material (Extended abstract). The 7th international conference on indoor air quality, ventilation & energy conservation in buildings. Paper ID 200-196. August 15-18, 2010, Syracuse, New York, U.S.A.
4. Jianshun (Jensen) Zhang, Wenhao Chen, Zhi Gao and **Jing Xu**. A Pilot Study on Effect of Relative Humidity on Emittable Formaldehyde Concentration in Particleboard and

Discussion on the Role of Hydrolysis. The 7th international conference on indoor air quality, ventilation & energy conservation in buildings. Paper ID 1-187. August 15-18, 2010, Syracuse, New York, U.S.A.

5. Alfred T Hodgson, Jianshun (Jensen) Zhang, Beverly Guo and **Jing Xu**. Development and Validation of a Scaling Method for Environmental Chamber Determination of VOC Emissions from Office Furniture. Healthy Building, Paper ID 444, September 13-17, 2009, Syracuse, U.S.A.
6. Jianhua Zhao, **Jing Xu**, Jianshun (Jensen) Zhang and Rudolf Plagge. Determination of the Heterogeneous Properties of a Work Surface Assembly and their Impact on Moisture and VOC Transport. Healthy Building, Paper ID 416, September 13-17, 2009, Syracuse, U.S.A.
7. **Jing Xu**, Jianshun (Jensen) Zhang, John Grunewald, Jianhua Zhao and Rudi Plagge. A Dual-Chamber Experimental Method for Determining the Transport Properties of Building Materials. The 11th International Conference on Indoor Air Quality and Climate, Paper ID 232, August 17-22, 2008, Copenhagen, Denmark
8. James F. Smith, Jianshun (Jensen) Zhang, Bing Guo, and **Jing Xu**. Determination of Emittable Initial VOC Concentrations in Building Materials and Sorption Isotherm for IVOCs. The 11th International Conference on Indoor Air Quality and Climate, Paper ID 70. August 17-22, 2008, Copenhagen, Denmark
9. **Jing Xu**, John Grunewald, Jianshun (Jensen) Zhang, Hui Li and Bing Guo. Modeling the Formaldehyde Emission from Multi-layer Work Surfaces used in Office Workstation Systems. The 6th international conference on indoor air quality, ventilation & energy conservation in buildings. October 28-31, 2007. Sendai, Japan. Part II, Page: 161-168
10. Hui Li, Jianshun Zhang, **Jing Xu** and H.M. Salonvaara, From Component Testing to System Prediction of VOC Emissions from Office Furniture. October 14-17 – ASHRAE IAQ 2007: Healthy & Sustainable Buildings. Baltimore's Inner Harbor, Maryland
11. **Jing Xu**, Huan Zhang and Shijun You. The Assessment and Function Research of Plasma Air Cleaner. The 10th International Conference on Indoor Air Quality and Climate, September 4-9, 2005, Beijing, China. Volume IV. Paper ID: 4.1-06. Page: 2920-2924
12. **Jing Xu**, Huan Zhang and Shijun You. CFD Simulation of Two types of Indoor Air Supply. The 2th International Conference on Built Environment and Public Health, Shenzhen, China, December, 2004
13. Hui Yang, Huan Zhang, Shijun You, Peiwen Wang and **Jing Xu**, CFD simulation and Study on Office Thermal Environment. The 2th International Conference on Built Environment and Public Health. December 2004, Shenzhen, China

CONFERENCE PRESENTATIONS

1. Oral presentation on "Determination of Partition and Diffusion Coefficient of Formaldehyde in Selected Building Materials and Impact of Relative Humidity". The 12th International Conference on Indoor Air Quality and Climate. Paper ID 635. June 5-10, 2011, Austin, Texas, U.S.A.
2. Poster presentation on "Experimental Study of Relative Humidity Effect on VOCs' Effective Diffusion Coefficient and Partition Coefficient in Porous Building Material". The 7th international conference on indoor air quality, ventilation & energy conservation in buildings. No 200-196. August 15-18, 2010, Syracuse, New York, U.S.A.
3. Oral presentation on "Determination of the Heterogeneous Properties of a Work Surface Assembly and their Impact on Moisture and VOC Transport". Healthy Building, September 13-17, 2009, Syracuse, U.S.A.
4. Oral presentation on "Dual-Chamber Experimental Method for Determining the Transport Properties of Building Material" The 11th International Conference on Indoor Air Quality and Climate, August 17-22, 2008, Copenhagen, Denmark
5. Oral presentation on "From Component Testing to System Prediction of VOC Emissions from Office Furniture." 2007 October 14-17 - IAQ 2007: Healthy & Sustainable Buildings. Baltimore's Inner Harbor, Maryland

RESEARCH REPORT INVOLVED

1. **Jing Xu**, Beverly Guo and Jianshun (Jensen) Zhang. September 2010. Determination of Partition and Diffusion Coefficient for Formaldehyde and Selected Building Materials. Final Report. Submitted to Indoor Environment Management Branch, United States Environmental Protection Agency, National Risk Management Research Laboratory, Air Pollution Prevention and Control Division, Research Triangle Park, NC 27711. 81 Pages.
2. Jianshun (Jensen) Zhang, Beverly Guo and **Jing Xu**/BEESL and Alfred T Hodgson, Berkley Analytical Associates (BAA), LLC Richmond, CA. April 2008. Validation of Emission Test Method ANSI/BIFMA M7.1 and Development of a Method for Component Material to System Prediction of VOC Emissions. Final Report Part 3: Scaling Method Development and Validation. Submitted to BIFMA® International, 2680 Horizon Drive Suite A1, Grand Rapids MI. 62 pages.
3. Hui Li, Jianshun (Jensen) Zhang, Bing Guo and **Jing Xu**. February 2007. Validation of the Proposed BIFMA Emission Test Method (BIFMA M7.1) and Development of a Method for

Component to System Prediction of VOC Emissions. Final Report Part 1: Emissions from Office Workstation Systems, Chairs, and Their Components and Materials. Submitted to BIFMA® International, 2680 Horizon Drive Suite A1, Grand Rapids MI. 309 pages. Building Energy and Environmental System Laboratory. Syracuse University, Syracuse, NY

4. Zhi Gao, Jianshun (Jensen) Zhang, Wenhao Chen and **Jing Xu**. June 2006. Evaluation of Gaseous and Particulate Emissions from a Room Air Cleaner. Final Report. Submitted to S.C. Johnson & Son, Inc. 49 pages. Building energy and environmental system laboratory. Syracuse University, Syracuse, NY

AWARDS/HONOURS

Graduate

1. ASHRAE Grant-in-Aid Fellowship, 2008-2009
2. China Part Graduate Mathematical Contest in Modeling, Third Place in National Contest. September, 2005
3. Honeywell Scholarship, October, 2004
4. First session of Innovation Prize(organized by School of Environment Science &Technology, Tianjin University), November, 2003

Undergraduate

1. The Fourth 'Tiancai' Cup students' academic works competition, Second Place, May, 2003
2. Third session of Outstanding Student of Science and Technology in Tianjin University, December, 2002
3. Three A's Student of Tianjin University, December, 2002
4. Scholarship of the 11th Nationwide Artificial Environment Engineering(sponsored by Tsinghua Tongfang Co., Ltd), Second Place, August, 2002
5. Model of Three A's Student of Tianjin University, December, 2001
6. Wang Ke Chang Scholarship(awarded by Tianjin Education Committee), First Place, November, 2000